คุณลักษณะและสมบัติการเป็นตัวเร่งปฏิกิริยาของโคบอลต์บนตัวรองรับออกไซด์ผสมของนาโนแกมมาอะลูมินาในปฏิกิริยาไฮโดรจิเนชันของคาร์บอนมอนอกไซด์

นายธนัชนันท์ บุรกรณ์

วิทยานิพนธ์นี้เป็นส่วนหนึ่งของการศึกษาตามหลักสูตรปริญญาวิศวกรรมศาสตรมหาบัณฑิต

สาขาวิชาวิศวกรรมเคมี ภาควิชาวิศวกรรมเคมี

คณะวิศวกรรมศาสตร์ จุฬาลงกรณ์มหาวิทยาลัย

ปีการศึกษา 2548

ISBN: 974-53-2772-7

CHARACTERISTICS AND CATALYTIC PROPERTIES OF MIXED NANO-γ-Al_2O_3 BASED-SUPPORTED COBALT CATALYST DURING CARBON MONOXIDE HYDROGENATION

Mr. Tanuchnun Burakorn

A Thesis Submitted in Partial Fulfillment of the Requirements
for the Degree of Master of Engineering Program in Chemical Engineering
Department of Chemical Engineering
Faculty of Engineering
Chulalongkorn University
Academic Year 2005

ISBN: 974-53-2772-7

Thesis Title	CHARACTERISTICS AND CATALYTIC PROPERTIES OF MIXED NANO-γ-Al_2O_3 BASED-SUPPORTED COBALT CATALYST DURING CARBON MONOXIDE HYDROGENATION
By	Mr. Tanuchnun Burakorn
Field of Study	Chemical Engineering
Thesis Advisor	Assistant Professor Bunjerd Jongsomjit, Ph.D.

Accepted by the Faculty of Engineering, Chulalongkorn University in Partial Fulfillment of the Requirements for the Master's Degree

..... Dean of the Faculty of Engineering
(Professor Direk Lavansiri, Ph.D.)

THESIS COMMITTEE

..... Chairman
(Professor Piyasan Praserthdam, Dr.Ing..)

..... Thesis Advisor
(Assistant Professor Bunjerd Jongsomjit, Ph.D.)

..... Member
(Assistant Professor Muenduen Phisalaphong, Ph.D.)

..... Member
(Assistant Professor Joongjai Panpranot, Ph.D.)

ธนัชนันท์ บุรกรณ์: คุณลักษณะและสมบัติการเป็นตัวเร่งปฏิกิริยาของโคบอลต์บนตัวรองรับออกไซด์ผสมของนาโนแกมมาอะลูมินาในปฏิกิริยาไฮโดรจิเนชันของคาร์บอนมอนอกไซด์ (CHARACTERISTICS AND CATALYTIC PROPERTIES OF MIXED NANO-γ-Al_2O_3 BASED-SUPPORTED COBALT CATALYST DURING CARBON MONOXIDE HYDROGENATION) อาจารย์ที่ปรึกษา: ผศ.ดร. บรรเจิด จงสมจิต, 93 หน้า. ISBN : 974-533-2772-7

วิทยานิพนธ์นี้ศึกษาคุณสมบัติทางกายภาพและทางเคมีของโคบอลต์ออกไซด์ที่กระจายตัวบนตัวรองรับผสมของอะลูมินาและเซอร์โคเนียที่มีขนาดไมโครเมตรและนาโนเมตร ตัวอย่างได้ถูกเตรียมโดยวิธีการฝังเคลือบของสารละลายโคบอลต์บนตัวรองรับผสมของอะลูมินาและเซอร์โคเนียที่มีอัตราส่วนต่างกัน หลังจากการเผาในอากาศ ตัวอย่างจะถูกนำไปตรวจสอบคุณลักษณะด้วยวิธีการต่างๆ การวิเคราะห์ด้วยกล้องจุลทรรศน์อิเล็กตรอนแบบส่องกราด แสดงให้เห็นว่า ขนาดของโคบอลต์ออกไซด์ขึ้นอยู่กับขนาดของตัวรองรับที่ใช้ในการทดลอง สำหรับตัวรองรับอะลูมินาที่มีขนาดไมโครเมตรและนาโนเมตรถูกพบว่า ความว่องไวในการเกิดปฏิกิริยาและการเลือกเกิดผลิตภัณฑ์มีค่าเท่ากัน อย่างไรก็ตาม ความว่องไวในการเกิดปฏิกิริยาของตัวรองรับเซอร์โคเนียขนาดนาโนเมตรมีค่ามากเมื่อเทียบกับเซอร์โคเนียขนาดไมโครเมตร เมื่อพิจารณาตัวรองรับผสมของอะลูมินาและเซอร์โคเนีย สำหรับตัวเร่งปฏิกิริยาบนตัวรองรับขนาดไมโครเมตรได้บ่งชี้ว่า การผสมเซอร์โคเนียไม่มีผลต่อความว่องไวในการเกิดปฏิกิริยาและการเลือกเกิดผลิตภัณฑ์ในปฏิกิริยาไฮโดรจิเนชันของคาร์บอนมอนนอกไซด์ อย่างไรก็ตามผลการศึกษาตัวเร่งปฏิกิริยาบนตัวรองรับผสมของอะลูมินาและเซอร์โคเนียขนาดนาโนเมตรได้พบว่า ความว่องไวในการเกิดปฏิกิริยาลดลงแต่การเลือกเกิดผลิตภัณฑ์ไฮโดรคาร์บอน 2 อะตอมถึง คาร์บอน 4 อะตอมมีค่าเพิ่มขึ้น ภาวะที่แตกต่างของความว่องไวในการเกิดปกิกิริยาและการลือกเกิดผลิตภัณฑ์สามารถบอกลักษณะของอันตรกิริยาของตัวรองรับและขนาดอนุภาคของโคบอลต์ออกไซด์ โดยขึ้นกับชนิดของตัวรองรับนั้นได้

ภาควิชา .....วิศวกรรมเคมี..... ลายมือชื่อนิสิต.....ธนัชนันท์ บุรกรณ์.....

สาขาวิชา .....วิศวกรรมเคมี..... ลายมือชื่ออาจารย์ที่ปรึกษา.....

ปีการศึกษา .....2548.....

#4770634121 : MAJOR CHEMICAL ENGINEERING
KEY WORD : ALUMINA/ ZRICONIA/ COBALT/ CO HYDROGENATION

TANUCHNUN BURAKORN: CHARACTERISTICS AND CATALYTIC PROPERTIES OF MIXED NANO-γ-Al_2O_3 BASED-SUPPORTED COBALT CATALYST DURING CARBON MONOXIDE HYDROGENATION THESIS ADVISOR: ASSISTANT PROFESSOR BUNJERD JONGSOMJIT, Ph.D., 93 pp. ISBN : 974-53-2772-7

In the present study, the physicochemical properties of Co oxide species dispersed on different micron- and nanoscale mixed Al_2O_3-ZrO_2 supports were investigated. The samples were prepared by impregnation of the cobalt precursor onto the various mixed Al_2O_3-ZrO_2 supports. After calcination, the samples were characterized with different techniques. TEM revealed that the size of Co_3O_4 species depended on the size of supports used. For pure micron- and nanoscale Al_2O_3 supports, it was found that the catalysts exhibited the similar activities and selectivity. However, increased activity was observed when the nanoscale ZrO_2 support was used compared with the micronscale one. Considering the mixed Al_2O_3-ZrO_2 supports, for the micronscale ones it indicated that the presence of ZrO_2 had no effect on both activity and selectivity during CO hydrogenation. However, the presence of the nanoscale ZrO_2 in nanoscale Al_2O_3 apparently resulted in decreased activities, but somehow increased selectivity to C_2-C_4 products. Differences in activity and selectivity can be attributed to the support interaction and the particle size of Co oxide species along with the nature of support itself.

Department ...Chemical Engineering..... Student's signature.....Tanuchnun Burakorn

Field of study...Chemical Engineering... Advisor's signature.....Bunjerd Jongsomjit.....

Academic year.....2005.....

ACKNOWLEDGEMENTS

The author would like to express his sincere gratitude and appreciation to his advisor, Dr. Bunjerd jongsomjit, for his invaluable suggestions, stimulating, useful discussions throughout this research and devotion to revise this thesis otherwise it can not be completed in a short time. In addition, the author would also be grateful to Professor Dr. Piyasan Praserthdam, as the chairman, and Dr. Muenduen Phisalaphong, Dr. Joongjai Panpranot, as the members of the thesis committee. The financial supports from the National Research Council of Thailand (NRCT), Thailand Research Fund (TRF) and Thailand Japan Technology Transfer Project (TJTTP-JBIC) are also gratefully acknowledged.

Most of all, the author would like to express his highest gratitude to his parents who always pay attention to his all the times for suggestions and have provided his support and encouragement. The most success of graduation is devoted to his parents.

Finally, the author wishes to thank the members of the Center of Excellence on Catalysis and Catalytic Reaction Engineering, Department of Chemical Engineering, Faculty of Engineering, Chulalongkorn University for their assistance especially Miss Pramrutai Kruachot.

CONTENTS

Page

Page

LIST OF TABLES

TABLE **Page**

LIST OF FIGURES

FIGURE **Page**

FIGURE **Page**

CHAPTER I

INTRODUCTION

In general, a catalyst usually consists of three components; (i) a catalytic phase, (ii) a promoter, and (iii) a support or carrier. As known, the catalytic properties apparently depend upon the components as mentioned above. The catalytic phase can be metal, metal oxide, metal carbide and etc. The active form of the catalytic phase definitely depends on the specific reaction within the catalyst is applied. It is known that the performance of catalysts could be improved using a promoter such as noble metals. However, besides the consideration only in a catalytic phase and a promoter, it should be noted that a support could play a crucial role, especially as a dispersing medium for the catalytic phase. Hence, the nature of support can affect the catalytic properties based on the fact that the dispersion and interaction between a support and a catalytic phase can be altered with different supports.

It was reported that many inorganic supports such as SiO_2 [1-4], Al_2O_3 [5-9], TiO_2 [10-15], ZrO_2 [16], and zeolites [17] have been extensively studied for many years. In particular, the use of mixed oxide support was also mentioned [18-20] as one of the promising ways to obtain a suitable support due to its synergetic effect arising from the mixing property. In the recent years, a significant development in nanoscience and nanotechnology has been tremendous. Therefore, many inorganic nanoscale materials have brought much attention to the research in this field [21]. However, only few studies have been done on using a nanoscale material as a support for a catalytic phase. In addition, it would be of great benefits to understand different physicochemical properties of catalytic phase dispersed on the nanoscale support and the traditional micronscale support. This will lead to a significant development in a catalyst design.

In the present study, the properties of cobalt (Co) catalysts dispersed on various mixed nano-Al_2O_3-ZrO_2 supports for carbon monoxide (CO) hydrogenation reaction were investigated and compared with those on the traditional mixed micron-Al_2O_3-ZrO_2 supports. The samples were prepared and analyzed by means of X-ray

diffraction (XRD), transmission electron spectroscopy (TEM), and temperature-programmed reduction (TPR). The reaction study was performed in order to measure activity and product selectivity toward CO hydrogenation at 220°C and 1 atm.

CHAPTER II

THEORY

2.1 Fischer-Tropsch synthesis (FTS)

Fischer-Tropsch synthesis (FTS) or CO hydrogenation reaction, the production of liquid hydrocarbons from synthesis gases (CO and H_2) is a promising, developing route for environmentally sound production of chemicals and fuels from coal and natural gas. During the past decades, FTS has been developed continuously by many researchers, although the rise and fall in research intensity on this process has been highly related to the demands for liquid fuels and relative economics. This synthesis is basically the reductive polymerization (oligomerization) of carbon monoxide by hydrogen to form organic products containing mainly hydrocarbons and some oxygenated products in lesser amounts. The main reactions of FTS are:

$$CO + 3H_2 \rightarrow CH_4 + H_2O \tag{1}$$

$$CO + 2H_2 \rightarrow (\frac{1}{n})(C_nH_{2n}) + H_2O \tag{2}$$

$$CO + H_2O \rightarrow CO_2 + H_2 \tag{3}$$

$$2CO \rightarrow C + CO_2 \tag{4}$$

Equations (1) is the formation of methane, the equation (2) is the synthesis of hydrocarbons higher than methane, the equation (3) is the water-gas shift reaction, and the equation (4) is the Boudouard reaction resulting in which results in deposition of carbon.

The reaction mechanism of methanation can be described by the following set of mechanism:

(1) $CO + * = CO*$

(2) $CO* + * = C* + O*$

(3) $H_2 + 2* = 2H*$

(4) $C* + H* = CH* + *$

(5) $CH* + H* = CH_2* + *$

(6) $CH_2* + H* = CH_3* + *$

(7) $CH_3* + H* = CH_4(g) + 2*$

(8) $O* + H* = OH* + *$

(9) $OH* + H* = H_2O(g) + 2*$

Normally, catalysts used for FTS are group VIII metals. By nature, the hydrogenation activity increases in order of Fe < Co < Ni < Ru. Ru is the most active. Ni forms predominantly methane, while Co yields much higher ratios of paraffins to olefins and much less oxygenated products such as alcohols and aldehydes than Fe does.

Commercially, Entrained bed reactors or slurry bubble column reactors are used in FTS since they can remove heat from this exothermic synthesis, allowing better temperature control.

The current main goal in FTS is to obtain high molecular weight, straight chain hydrocarbons. However, methane and other light hydrocarbons are always present as less desirable products from the synthesis. According to the Anderson-Schulz-Flory (ASF) product distribution, typically 10 to 20% of products from the synthesis are usually light hydrocarbon (C_1-C_4). These light alkanes have low boiling points and exist in the gas phase at room temperature, which is inconvenient for transportation. Many attempts have been made to minimize these by-products and increase the yield of long chain liquid hydrocarbons by improving chain growth probability. It would be more efficient to be able to convert these less desirable products into more useful forms, rather than re-reforming them into syngas and recycling them [22]. Depending upon the type of catalyst used, promoters, reaction conditions (pressure, temperature and H_2/CO ratios), and type of reactors, the

distribution of the molecular weight of the hydrocarbon products can be noticeably varied.

2.2 Cobalt [23, 24]

2.2.1 General

Cobalt, a transition series metallic element having atomic number 27, is similar to silver in appearance.

Cobalt and cobalt compounds have expended from use colorants in glasses and ground coat frits for pottery to drying agents in paints and lacquers, animal and human nutrients, electroplating materials, high temperature alloys, hard facing alloys, high speed tools, magnetic alloys, alloys used for prosthetics, and used in radiology. Cobalt is also as a catalyst for hydrocarbon refining from crude oil for the synthesis of heating fuel.

2.2.2 Physical Properties

The electronic structure of cobalt is [Ar] $3d^7 4s^2$. At room temperature the crystalline structure of the α (or ε) form, is close-packed hexagonal (cph) and lattice parameters are a = 0.2501 nm and c = 0.4066 nm. Above approximately 417°C, a face-centered cubic (fcc) allotrope, the γ (or β) form, having a lattice parameter a = 0.3544 nm, becomes the stable crystalline form. Physical properties of cobalt are listed in Table 2.1.

The scale formed on unalloyed cobalt during exposure to air or oxygen at high temperature is double-layered. In the range of 300 to 900°C, the scale consists of a thin layer of mixed cobalt oxide, Co_3O_4, on the outside and cobalt (II) oxide, CoO, layer next to metal. Cobalt (III) oxide, Co_2O_3, may be formed at temperatures below 300°C. Above 900°C, Co_3O_4 decomposes and both layers, although of different appearance, are composed of CoO only. Scales formed below 600°C and above

750°C appear to be stable to cracking on cooling, whereas those produced at 600-750°C crack and flake off the surface.

Cobalt forms numerous compounds and complexes of industrial importance. Cobalt, atomic weight 58.933, is one of the three members of the first transition series of Group 9 (VIIIB). There are thirteen know isotopes, but only three are significant: ^{59}Co is the only stable and naturally occurring isotope; ^{60}Co has a half-life of 5.3 years and is a common source of γ-radioactivity; and ^{57}Co has a 270-d half-life and provides the γ-source for Mössbauer spectroscopy.

Cobalt exists in the +2 or +3 valance states for the major of its compounds and complexes. A multitude of complexes of the cobalt (III) ion exists, but few stable simple salt are known. Octahedral stereochemistries are the most common for cobalt (II) ion as well as for cobalt (III). Cobalt (II) forms numerous simple compounds and complexes, most of which are octahedral or tetrahedral in nature; cobalt (II) forms more tetrahedral complex than other transition-metal ions. Because of the small stability difference between octahedral and tetrahedral complexes of cobalt (II), both can be found equilibrium for a number of complexes. Typically, octahedral cobalt (II) salts and complexes are pink to brownish red; most of the tetrahedral Co (II) species are blue.

Table 2.1 Physical Properties of Cobalt [24]

Property	Value
atomic number	27
atomic weight	58.93
transformation temperature, ^{o}C	417
heat of transformation, J/g[a]	251
melting point, ^{o}C	1493
latent heat of fusion, ΔH_{fus} J/g[a]	395
boiling point, , ^{o}C	3100
latent heat of vaporization at bp, ΔH_{vap} kJ/g[a]	6276
specific heat, J/(g·^{o}C)[a]	
15-100°C	0.442
molten metal	0.560
coefficient of thermalexpansion, $^{o}C^{-1}$	
cph at room temperature	12.5
fcc at 417°C	14.2
thermal conductivity at 25 ^{o}C, W/(m·K)	69.16
thermal neutron absorption, Bohr atom	34.8
resistivity, at 20 ^{o}C[b], $10^{-8}\Omega\cdot m$	6.24
Curie temperature, ^{o}C	1121
saturation induction, $4\pi I_s$, T[c]	1.870
permeability, μ	
initial	68
max	245
residual induction, T[c]	0.490
coercive force, A/m	708
Young's modulus, Gpac	211
Poisson's ratio	0.32

Table 2.1 Physical Properties of Cobalt (cont.)

Property	Value		
Hardness[f], diamond pyramid, of %Co		99.9	99.98[e]
At 20 ^{o}C		225	253
At 300 ^{o}C		141	145
At 600 ^{o}C		62	43
At 900 ^{o}C		22	17
strength of 99.99 %cobalt, MPa[g]	as cast	annealed	sintered
tensile	237	588	679
tensile yield	138	193	302
compressive	841	808	
compressive yield	291	387	

[a] To convert J to cal, divided by 4.184.

[b] conductivity = 27.6 % of International Annealed Copper Standard.

[c] To convert T to gauss, multiply by 10^4.

[d] To convert GPa to psi , multiply by 145,000.

[e] Zone refined.

[f] Vickers.

[g] To convert MPa to psi , multiply by 145.

2.2.3 Cobalt Oxides

Cobalt has three well-known oxides:

Cobalt (II) oxide, CoO, is an olive green, cubic crystalline material. Cobalt (II) oxide is the final product formed when the carbonate or the other oxides are calcined to a sufficiently high temperature, preferably in a neutral or slightly reducing atmosphere. Pure cobalt (II) oxide is a difficult substance to prepare, since it readily takes up oxygen even at room temperature to re-form a higher oxide. Above about 850°C, cobalt (II) oxide form is the stable oxide. The product of commerce is usually dark gray and contains 75-78 wt % cobalt. Cobalt (II) oxide is soluble in water, ammonia solution, and organic solvents, but dissolves in strong mineral acids. It is used in glass decorating and coloring and is a precursor for the production of cobalt chemical.

Cobalt (III) oxide, Co_2O_3, is form when cobalt compounds are heated at a low temperature in the presence of an excess of air. Some authorities told that cobalt (III) oxide exists only in the hydrate form. The lower hydrate may be made as a black power by oxidizing neutral cobalt solutions with substances like sodium hypochlorite. H_2O is completely converted to Co_3O_4 at temperatures above 265°C. Co_3O_4 will absorb oxygen in a sufficient quantity to correspond to the higher oxide Co_2O_3.

Cobalt oxide, Co_3O_4, is formed when cobalt compounds, such as the cabonate or the hydrated sesquioxide, are heated in air at temperatures above approximately 265°C and not exceeding 800°C.

2.3 Co-based Catalysts

Supported cobalt (Co) catalysts are the preferred catalysts for the synthesis of heavy hydrocarbons from natural gas based syngas (CO and H_2) because of their high Fischer-Tropsch activity, high selectivity for linear hydrocarbons and low activity for the water-gas shift reaction. It is known that reduced cobalt metal, rather than its oxides or carbides, is the most active phase for CO hydrogenation in such catalysts. Investigations have been done to determine the nature of cobalt species on various supports such as alumina, silica, titania, magnesia, carbon, and zeolites. The influence of various types of cobalt precursors used was also investigated. It was found that the used of organic precursors such as Co (III) acetyl acetate resulting in an increase of CO conversion compared to that of cobalt nitrate.

2.4 General feature of alumina

The extensive historic research of the individual crystallographic phases of alumina has been traced by many researchers. A very detailed description of the crystallography of sapphire single crystals was given by Kronberg et al [25]. The structure of alumina consists of close packed planes of the large oxygen ions stacking in the sequence of A-B-A-B, forming hexagonal close packed array of anions. The aluminium cations are placed on the octahedral sites of this anionic array and form another type of close packed planes which are inserted between the oxygen layers. To maintain charge neutrality, however, only two third of the octahedral sites available are filled with cations. Figure 2.1 illustrates the packing of Al and O in the basal plane. Since the vacant octahedral sites also form regular hexahedral array, three different types of cation layers can be defined, depending on the position of the vacant cation site within the layer. They may be named a, b, c and stacked in the sequence a-b-c-a-b-c.

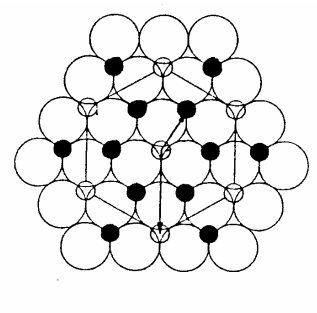

Figure 2.1 Illustrates the Packing of Al and O ions in the basal plane.[25]

Alumina (Al_2O_3) can exist in many metastable phases before transformating to the stable α-alumina (corundum form). Differences in the phase transformation sequence are result from the difference in the precursor structure[26, 27]. The temperature ranges of stability given for the transition alumina are only approximate and depend upon the degree of crystallinity, impurities in the starting materials, and the subsequent thermal history. All the phases of transition aluminas are reproducible and stable at room temperature. However, the transformation sequence is irreversible. There are six principal phases designated by the Greek letters chi (χ), kappa (κ), eta (η), theta (θ), delta (δ), and gamma (γ), respectively. The nature of the product obtained by calcination depends on the starting hydroxide and on the calcination condition.

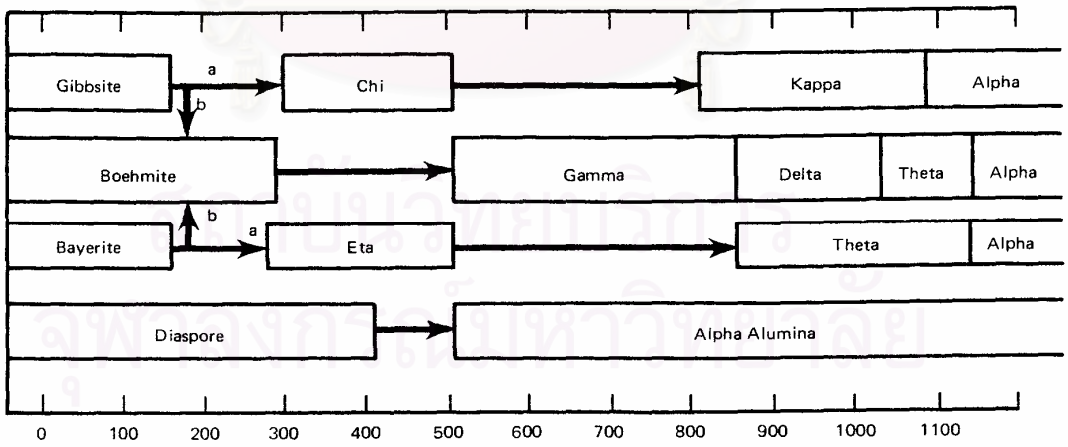

Figure 2.2 Decomposition sequence of aluminum hydroxides[28].

2.5 General feature of zirconia

Zirconia exhibits three polymorphs, the monoclinic, tetragonal, and cubic phases. Figure 2.3 shows the typical systems: cubic, tetragonal and monoclinic onses. Crystal structure of cubic, tetragonal and monoclinic zirconia are shown in Figure 2.4 The monoclinic is stable up to ~1170°C, at which temperature it transforms into the tetragonal phase, which is stable up to 2370°C [29]. The stabilization of the tetragonal phase below 1100°C is important in the use of zirconia as a catalyst in some reaction. Above 2370°C, the cubic phase is stable and it exists up to the melting point of 2680°C. Due to the martensitic nature of the transformations, neither the high temperature tetragonal nor cubic phase can be quenched in rapid cooling to room temperature. However, at low temperature, a metastable tetragonal zirconia phase is usually observed when zirconia is prepared by certain methods, for example by precipitation from aqueous salt solution or by thermal decomposition of zirconium salts. This is not the expected behavior according to the phase diagram of zirconia (i.e., monoclinic phase is the stable phase at low temperatures). The presence of the tetragonal phase at low temperatures can be attributed to several factors such as chemical effects, (the presence of anionic impurities) [30, 31] structural similarities between the tetragonal phase and the precursor amorphous phase [31-33] as well as particle size effects based on the lower surface energy in the tetragonal phase compared to the monoclinic phase[34]. The transformation of the metastable tetragonal form into the monoclinic form is generally complete by 650-700°C.

Table 2.2 The unit cells of the crystal systems[34].

Crystal system	Unit cell shape
Cubic	$a = b = c$, $\alpha = \beta = \gamma = 90^{o}$
Tetragonal	$a = b \neq c$, $\alpha = \beta = \gamma = 90^{o}$
Monoclinic	$a \neq b \neq c$, $\alpha = \gamma = 90^{o}$, $\beta \neq 90^{o}$

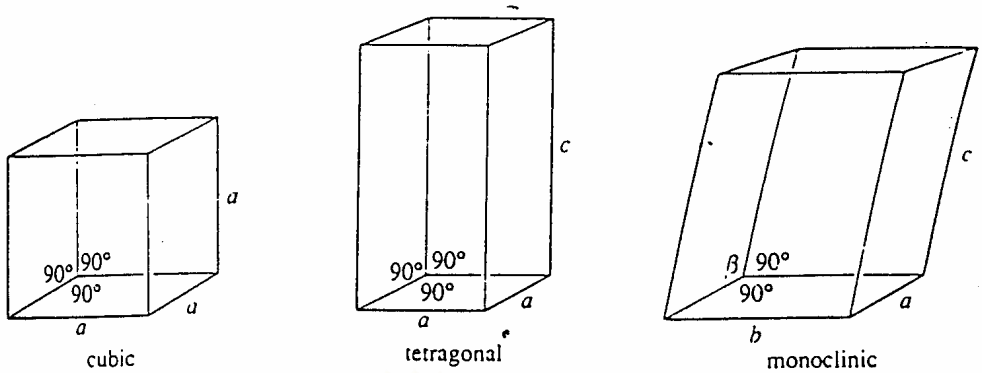

Figure 2.3 The unit cells of the crystal systems[34].

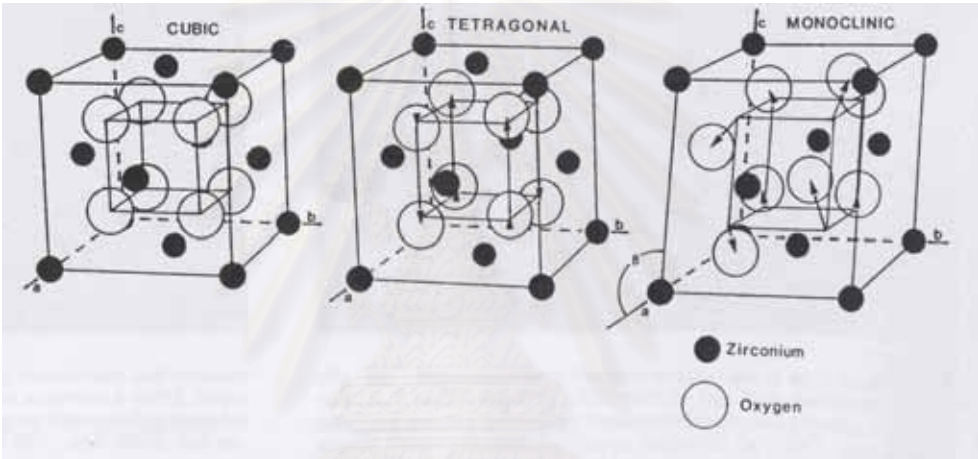

Figure 2.4 Crystal structure of cubic, tetragonal and monoclinic zirconia[35].

CHAPTER III

LITERATURE REVIEWS

There have been a number of researchers studying alumina and other oxide supports catalysts in Fischer-Tropsch synthesis. Many researchers have been found better knowledge about alumina and other oxide supports especially supported cobalt catalyst. These reports are very useful and will use to develop works for the future.

3.1 Alumina supported cobalt catalysts

Rafeh Bechara et al[36]. studied the Co/Al_2O_3 catalysts, prepared from four commercial alumina, with different cobalt loading have been studied for the carbon monoxide hydrogenation. The activity of the powder catalyst at 15 wt.% cobalt on alumina follows a logarithmic decrease with the time on stream, as for the paraffin/olefin ratio. This behaviour can be explained by the evolution of the catalyst surface (partial re-oxidation, site blocking). On the other hand, the product distribution does not significantly change with the time on stream. The selectivity follows the Schulz-Flory model; secondary reactions, are not significant. An increase in the reduction temperature generally improves the CO transformation rate and favours the production of higher hydrocarbons. The activity and selectivity on heavy product improvements result from the increases, respectively in the number of active sites and in the coordination number of metallic cobalt atoms. It seems that the increase of cobalt loading affect the specific rate of reaction or/and the selectivity only through its influence on the reducibility of the active phase. For higher cobalt loading, high site density leads to secondary, which modifies the product distribution. The study of the influence of the support has shown the importance of the porosity of pellet catalysts after impregnation on the activity and the selectivity. The evolution of the chain growth probability α is closely related to the degree of reduction. The more reduced the cobalt is. Nevertheless, the chain growth probability α seems to be limited at a maximum value, which is around 0.89 in our conditions.

Junling Zhang et al[37]. studied the cobalt supported on different γ-alumina carries prepared by incipient wetness impregnation are used to investigate the effect of support on the performance of cobalt catalysts for FTS. It is found that the acidity of support has a great influence on the interaction between metallic cobalt and then the reducibility of cobalt. The support with low acidity leads to the higher active FTS catalysts. Furthermor, the high reducibility and more bridged type Co which is favored by γ-alumina with low acidity appears to be responsible for high C_{5+} hydrocarbon selectivity and low methane selectivity.

B. Jongsomjit and J.G. Goodwin, Jr[8]. investigated the effect of the addition of CO during H_2 reduction on Co-support compound formation in a Co/Al_2O_3 catalyst. They have reported that the addition of CO during H_2 reduction of a 20% Co/Al_2O_3 catalyst produced specific activities about four times greater than when the catalyst reduced without CO addition. Most of this increase appears to have been due to increases in Co reducibility and dispersion. They also suggested that the effect of CO addition may be due to one or more of possibly three reasons: (i) CO may help to prevent the formation of Co species strongly interacting with the support, thereby facilitating its reduction, (ii) CO may decrease sintering of the Co may block Co "aluminate" formation by minimizing the impact of water vapor even at low partial pressures.

H. Xiong et al[38]. studied Al_2O_3 was calcined at different temperature to get the support with different pore size. Co/Al_2O_3 catalysts with different pore size were prepared by incipient wetness impregnation technique. The pore size of support Al_2O_3 was found to have a significant effect on Co_3O_4 crystallite diameter, catalyst reducibility and FTS activity. The larger pore size enhanced the formation of bigger crystallite diameter Co_3O_4 on the catalyst and the occurrence of larger pore size catalyst decreased the number of cobalt active sites on the surface of the catalyst and the reducibility of the catalyst, resulting in the decrease in FTS activity.

3.2 Zirconia supported cobalt catalysts

M. Kraum et al[39]. studied the dependence of the activity of cobalt-based catalysts for Fischer–Tropsch synthesis on the type of cobalt precursor and support material. All catalysts were characterised by XRD, XPS, TPR and CO pulse experiments. The catalytic performance of the catalysts was examined at a total pressure of 20 bar, a temperature of 200°C, a space velocity (GHSV) of 1200 $h^{-1}$and using a syngas having a H_2 to CO ratio equal to 2.

For catalysts prepared by incipient wetness impregnation, titania, ceria and zirconia were additionally used as supports. The activity changed in the following order: $ZrO_2 < TiO_2 < CeO_2$.

K. Maruya et al[40]. investigated the selective formation of isobutene from CO and H_2 over ZrO_2. ZrO_2 catalysts having different fraction of monoclinic phase were prepared by changing pH value in the mother solution at the precipitation of zirconium hydroxide. The rate of isobutene formation increased with an increase in the volumetric fraction of monoclinic phase in ZrO_2, while those of C_1, C_2, C_3, and C_{5+} were independent of the fraction. The amounts of adsorbed methoxy and formate species during the reaction and also of the surface sites with strong basicity increased with an increase in the fraction of monoclinic phase. Chemical trapping experiment showed that the amount of surface methoxy species is comparable to that of site with the strong basicity. These findings were explained by both coordinate unsaturation and stronger basicity based on the configuration of ZrO_2 group in the monoclinic structure.

D.I. Enache et al[41]. reported the thermal treatment, which leads to the best catalytic results, is the direct reduction of the nitrate precursor in the reactor. The effect of the pretreatment is higher in the case of zirconia supported catalyst. The direct reduction of nitrate precursors is even more effective when using a slow-temperature ramping protocol. This phenomenon is explained by the exothermicity of the nitrate reduction. The slower the temperature ramps, the better the heat evacuation, avoiding any increase in cobalt-support interactions or particle agglomeration. The reduction of Co_3O_4 oxide is difficult and leads to an increase of

the cubic crystallised cobalt at the expense of amorphous cobalt or hexagonal cobalt with stacking faults. The direct reduction of nitrate precursor increases the quantity of amorphous cobalt or hexagonal cobalt with crystallographic defects, which are active phases in this reaction. At the same time, the direct reduction leads to weaker metal-support interactions than does precalcination of catalysts. The nitrogen-flow calcination conducts to an intermediate situation. The quantity of crystallised Co_3O_4 is less important than in the case of airflow calcination and it is more reducible.

D.I. Enache et al[42]. studied the activity and the selectivity of cobalt catalysts supported on a crystallised and on an amorphous zirconia were compared with cobalt supported on a γ-alumina catalyst. The catalysts supported on zirconium dioxide were found to present a better reducibility of the active phase and also to be capable of hydrogen adsorption via a spillover mechanism. It is proposed that these properties could account for a better catalytic activity and an increase of the chain growth probability (α). At the same time, the estimated quantity of crystallised Co_3O_4 obtained after airflow calcination (for the same total cobalt loading) is related with the surface area of the support.

M. Shinoda et al[43]. investigated the Co/SiO_2 catalysts derived from silica bimodal supports in slurry phase FTS. The catalysts showed high activities and favorable selectivities due to high dispersion of supported cobalt crystallite by bimodal structure, as proved by XRD and TEM, and fastened diffusion efficiency inside catalyst pellet with bimodal structure. Furthermore, besides the spatial effect from bimodal structure as shown in silica–silica bimodal catalyst, significantly enhanced activity was realized using ZrO_2-silica bimodal support, as ZrO_2 inside the large pores of SiO_2 not only formed small pores but also intrinsically promoted FTS.

J. Panpranot et al[16]. investigated the nanocrystalline zirconia prepared by the glycothermal method in two different glycons (1,4-butanediol and 1,5-pentanediol) and employed as the support for cobalt catalysts. Commercial zirconia supported cobalt catalyst was also prepared and used as a reference material. The glycothermal-derived zirconia possesses large surface areas with crystallite sizes of 3-4 nm. The catalytic activities for CO hydrogenation of the glycothermal-derived zirconia supported cobalt catalysts were found to be much higher than of the

commercial zirconia supported one. However, the cobalt catalysts supported on zirconia prepared in 1,4-butanediol with lower amount of Zr content in the starting solution exhibited higher activities than the ones supported on zirconia prepared in 1,5-pentanediol. The results suggest that the different crystallization mechanism occurred in the two glycols may affect the amount of crystal defects produced in the corresponding zirconia. As shown by TPR profiles, lower metal-support interaction was observed for the catalysts supported on the ziconia formed via solid-state reaction in 1,4-butanediol (more defects). Consequently, higher active surface cobalt was available for H_2 chemisorption and CO hydrogenation reaction.

3.3 Effect of Al_2O_3 with other oxide supported of cobalt catalysts

F. Rohr et al[44]. studied effect of adding zirconia to the alumina support on supported cobalt Fischer–Tropsch catalysts. They also showed that at 5 bar with H_2:CO ratio 9:1 zirconia addition to the support leads to a significant increase in both activity and selectivity to higher hydrocarbons as compared to the unmodified catalysts. This effect has been studied with SSITKA, and can be attributed to changes in the surface coverage of reactive intermediates, not to a change in the intrinsic activity. The SSITKA experiments also revealed unexpectedly an increase in the surface coverage of reactive intermediates with increasing temperature.

B. Jongsomjit et al[5]. synthesized the Zirconia (Zr)-modified alumina-supported Co catalysts by the sequential impregnation method. They have studied the impact of Zr loading on the reducibility of Co in the absence and presence of water vapor. They reported that Zr modification of the alumina support had a significant impact on the catalyst properties: the overall activity during FT synthesis increased significantly upon Zr modification due to an increase in reducibility during standard reduction. Furthermore, the increase in reducibility appeared to have been caused by a decrease in the amount of Co-SCF. They also suggested that Zr modification may have caused: (i) a stabilization of the alumina support by blocking Co "aluminate" formation and/or (ii) a minimization of the impact of water vapor in modifying the surface properties of alumina, thereby decreasing the ease of Co reaction with the alumina.

3.4 Other oxide supported cobalt catalysts

R.C. Reuel and C.H. Bartholomew[45] studied the effect of support and dispersion on the CO hydrogenation activity/selectivity properties of cobalt. They found that the specific activity and selectivity of cobalt in CO hydrogenation is a function of support, dispersion, metal loading and preparation. The order of decreasing CO hydrogenation activity at 1 atm and 225°C for catalysts containing 3wt% cobalt is Co/TiO_2 > Co/SiO_2 > Co/Al_2O_3 > Co/C > Co/ MgO. The specific activity of cobalt best correlated with dispersion and extent of reduction. In the Co/Al_2O_3 system, activity and selectivity for high molecular weight hydrocarbons increase very significantly with increasing cobalt loading.

J. Choi [46] investigated the reduction of cobalt catalysts supported on Al_2O_3, SiO_2 and TiO_2 and the effect of metal loading on the reduction. He reported that the activation energy of reduction increased in the following order: Co/SiO_2 > Co/Al_2O_3 > Co/TiO_2. For different metal loading, the catalyst with the higher loading is more readily reducible than with the lower metal loading.

G. Jacobs et al[47]. investigated the effect of support, loading and promoter on the reducibility of cobalt catalysts. They have reported that significant support interactions on the reduction of cobalt oxide species were observed in the order Al_2O_3 > TiO_2> SiO_2. Addition of Ru and Pt exhibited a similar catalytic effect by decreasing the reduction temperature of cobalt oxide species, and for Co species where a significant surface interaction with the support was present, while Re impacted mainly the reduction of Co species interaction with the support. They also suggested that, for catalysts prepared with a noble metal promoter and reduced at the same temperature, the increase in the number of active sites was due mainly to improvements in the percentage reduction rather than the actual dispersion (cluster size). Increasing the cobalt loading, and therefore the average Co cluster size, was found to exhibit improved reducibility by decreasing interactions with the support.

M. Vob et al[48]. investigated the structural, chemical and electronic properties of Co and Co/Mn catalysts supported on Al_2O_3, SiO_2 and TiO_2 by a

combination of different methods such as TEM, XRD, XPS, TPR and TPO. They reported that temperature-programmed reduction and oxidation reveal the formation of various oxides in dependence on temperature. In case of the alumina- and titania-supported cobalt catalysts, the formation of high-temperature compounds $CoAl_2O_4$ and $CoTiO_3$, respectively. Moreover, these compounds are not reducible under the applied conditions, the degrees of reduction are only 18-20% (Co/Al_2O_3) and 77% (Co/TiO_2).

CHAPTER IV

EXPERIMENTAL

This chapter consists of experimental systems and procedures used in this study. The chapter is divided into three parts; (4.1) catalyst preparation (4.2) catalyst characterization and (4.3) reaction study. The first part (section 4.1) presents catalyst preparation including materials used, preparation of Al_2O_3-ZrO_2 mixed oxide supports, cobalt loading and catalyst nomenclature. The second part (section 4.2) shows the details of characterization techniques such as XRD, TPR, H_2 chemisorption, SEM, and TEM. And the last part (section 4.3) illustrates the reaction study in CO hydrogenation.

4.1 Catalyst Preparation

4.1.1 Chemicals

All chemicals using in this experiment are as following :

1. Nano-γ-Al_2O_3 supports from Aldrich
2. Nano-ZrO_2 supports prepared by Flame spray pyrolysis
3. Micro-Al_2O_3 supports from Sumitomo Aluminum Smelting Co., Ltd., Japan
4. Micro-ZrO_2 supports from Aldrich
5. Cobalt (II) nitrate hexahydrate available from Aldrich
6. Toluene from Fisher Scientific

4.1.2 Preparation of Al_2O_3 – ZrO_2 mixed oxide support

The Al_2O_3-ZrO_2 mixed oxide supports consisting of various weight ratios [0-100 wt% of ZrO_2 in Al_2O_3] for Al_2O_3-ZrO_2 were prepared by the solution mixing. The desired amounts containing 1 g of mixture of Al_2O_3-ZrO_2 were mixed and stirred in toluene (20 ml) with a magnetic stirrer continuously for 30 min. The solvent was

removed and the mixture was dried at 110°C for 12 h and, then calcined in air at 350°C for 2 h.

4.1.3 Cobalt loading

A 20 wt% of cobalt dispersed on the mixed Al_2O_3-ZrO_2 support was prepared by the incipient wetness impregnation. A desired amount of cobalt nitrate [$Co(NO_3)_2$.$6H_2O$] was dissolved in deionized water and then impregnated onto the support obtained from 4.1.2 The sample was dried at 110°C for 12 h and calcined in air at 500°C for 4 h.

4.1.4 Catalyst Nomenclature

The nomenclature used for the samples in this study is following:

Al-a-Zr-b (M or N) refers to the mixed Al_2O_3-ZrO_2 support where

a is the weight percents of Al_2O_3

b is the weight percent of ZrO_2

M refers to the micronscale

N refers to the nanoscale

Co/Al-a-Zr-b refers to the mixed Al_2O_3-ZrO_2-supported cobalt catalyst

4.2. Catalyst Characterization

4.2.1 X-ray Diffraction (XRD)

The X-ray diffraction (XRD) patterns of powder were performed by a X-ray diffractometer SIEMENS D5000 connected with a computer with Diffract ZT version 3.3 program for fully control of the XRD analyzer. The experiments were carried out by using Ni-filtered CuK_{α} radiation. Scans were performed over the 2θ ranges from 10° to 80°. The crystallite size was estimated from line broadening according to the Scherrer equation and α-Al_2O_3 was used as standard.

4.2.2 Temperature Programmed Reduction (TPR)

TPR was used to determine the reducibility of catalysts. The catalyst sample 100 mg used in the operation and temperature ramping from 35°C to 800°C at 10°C/min. The carrier gas will be 5 % H_2 in Ar. During reduction, a cold trap will be placed to before the detector to remove water produced. A thermal conductivity detector (TCD) will be measure the amount of hydrogen consumption. The calibration of hydrogen consumption was performed with bulk cobalt oxide (Co_3O_4) at the same conditions.

4.2.3 Hydrogen Chemisorption

Static H_2 chemisorption at 100°C on the reduce catalysts was used to determine the number of reduce surface cobalt metal atoms and overall cobalt dispersion. The total hydrogen chemisorption was calculated from the number of injection of a known volume. H_2 chemisorption was carried out following the procedure discribed by Reuel and Bartholomew[46] using a Micrometritics Pulse Chemisorb 2700 instrument at the Analysis Center of Department of Chemical Engineering, Faculty of Engineering, Chulalongkorn University. Prior to chemisorption, the catalysts were reduced at 35°C for 3 hours after ramping up at a rate of 1°C/min.

4.2.4 Scanning Electron Microscopy (SEM) and Energy Dispersive X-ray Spectroscopy (EDX)

Catalyst granule morphology of the samples were observed by JSM-5410LV scanning electron microscopy at the Scientific and Technological Research Equipment Center, Chulalongkorn University (STREC).

4.2.5 Transmission Electron Microscopy (TEM)

The dispersion of cobalt oxide supports was determined using JEOL-TEM 200CX transmission electron spectroscopy operated at 50-100 kV with 100 k magnification. The sample was dispersed in ethanol.

4.3 Reaction Study in CO Hydrogenation

4.3.1 Materials

The reactant gas mixture used for the reaction study was composed of 9.73 vol% carbon monoxide in hydrogen and supplied by Thai Industrial Gas Limited (TIG). The total flow rate was 30 ml/min. Ultra high purity hydrogen and high purity argon manufactured by Thai Industrial Gas Limited (TIG) were used for reduction and balanced flowrate.

4.3.2 Equipment

The CO hydrogenation system is schematically shown in Figure 4.1. The system is consisted of a reactor, an automatic temperature controller, an electrical furnace and a gas controlling system.

4.3.2.1 Reactor

The reactor was made from a stainless steel tube (O.D. 3/8”). Two sampling points were provided above and below the catalyst bed. Catalyst was placed in the middle of the reactor and held by two quartz wool layers.

4.3.2.2 Automation Temperature Controller

This unit is consisted of a magnetic switch connected to a variable voltage transformer and a solid state relay temperature controller model no. SS2425DZ connected to a thermocouple. Reactor temperature was measured at the bottom of the catalyst bed in the reactor. The temperature control set point is adjustable within the range of 0-800°C at the maximum voltage output of 220 volt.

4.3.2.3 Electrical Furnace

The electrical furnace was used to supply heat to the reactor for CO hydrogenation. The reactor could be operated from room temperature up to 800°C at the maximum voltage of 220 volt.

4.3.2.4 Gas Controlling System

The flowrate of each gas used in this study was controlled by a gas controlling system which consisted of a pressure regulator, an on-off valve and the gas flow rates were adjusted by using metering valves.

4.3.2.5 Gas Chromatograph

The composition of hydrocarbons in the product stream was analyzed by a Shimadzu GC14B gas chromatograph equipped with a flame ionization detector. A Shimadzu GC8A (molecular sieve 5A) gas chromatograph equipped with a thermal conductivity detector was used to analyze CO and H_2 in the feed and product streams. The operating conditions for each instrument are shown in the Table 4.1.

4.3.3 CO Hydrogenation Procedure

CO hydrogenation was performed using 0.2 g of catalyst was packed in the middle of the stainless steel microrector, which located in the electrical furnace. The total flow rate was 60 ml/min with the H_2/CO ratio of 10/1. The catalyst sample was reduced *in situ* in flowing H_2 at 350°C for 10 h prior to CO hydrogenation. CO hydrogenation was carried out at 220°C and 1 atm total pressure. The streams were analyzed by gas chromatography technique.

Table 4.1 Operating Condition for Gas Chromatograph

Gas chromatograph	Shimadzu GC8A	Shimadzu GC14B
Detector	TCD	FID
Column	Molecular Sieve 5A	VZ10
Carrier gas	He (99.999%)	N_2 (99.999%)
Carrier gas flow	30 ml./min.	30 ml./min.
Column temperature		
- Initial	60^oC	70^oC
- Final	60^oC	70^oC
Detector temperature	100^oC	100^oC
Injector temperature	100^oC	150^oC
Analyzed gas	Ar, CO, H_2	Hydrocarbon C_1-C_4

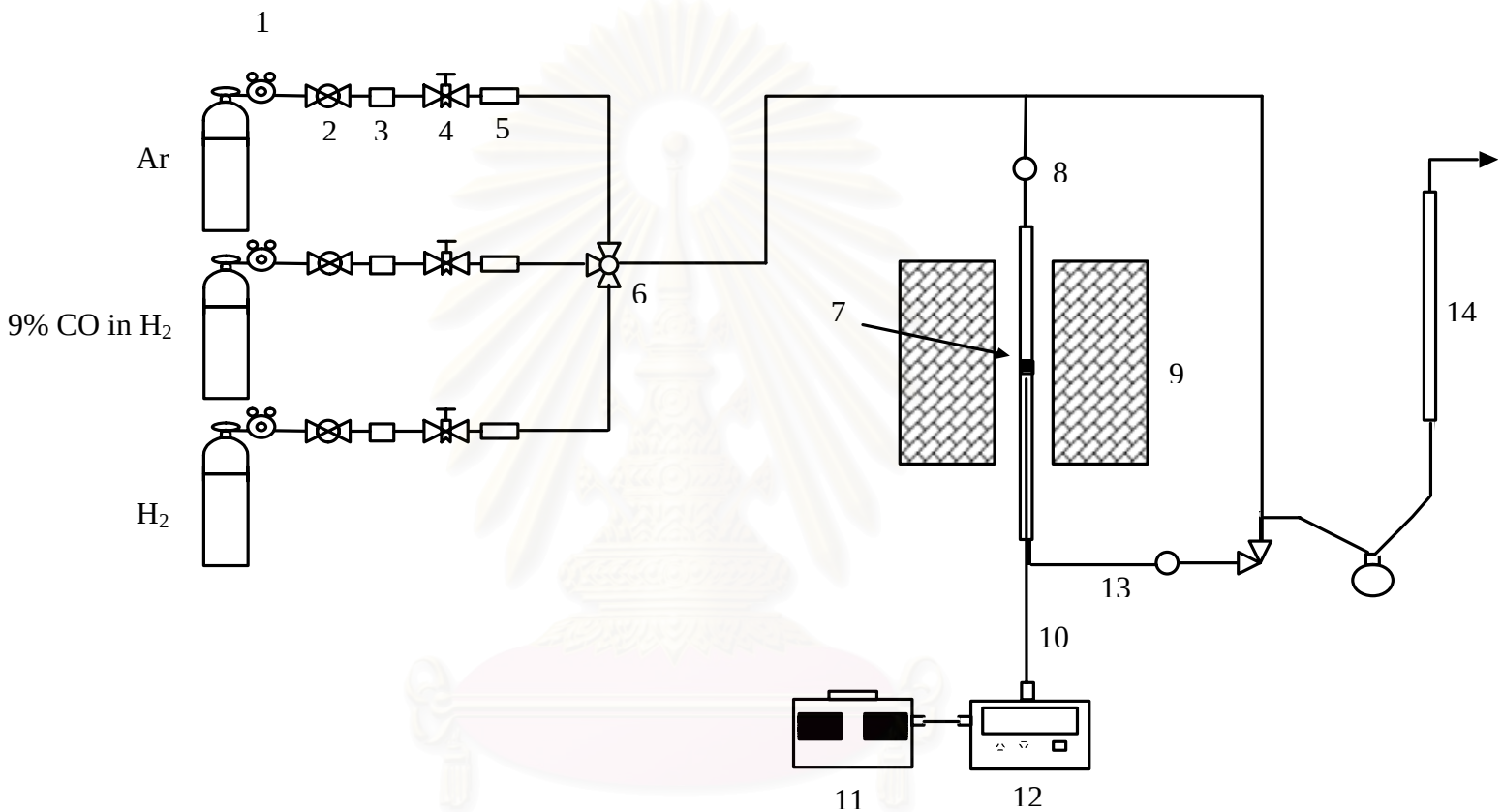

1. Pressure Regulator 2. On-Off Value 3. Gas Filter 4. Metering Valve
5. Back Pressure 6. 3-way Valve 7.Catalyst Bed 8. Sampling point
9. Furnace 10. Thermocouple 11. Variable Voltage Transformer 12. Temperature Controller
13. Heating Line 14. Bubble Flow Meter

Figure 4.1 Flow diagram of CO hydrogenation system

RESEACH METHODOLOGY

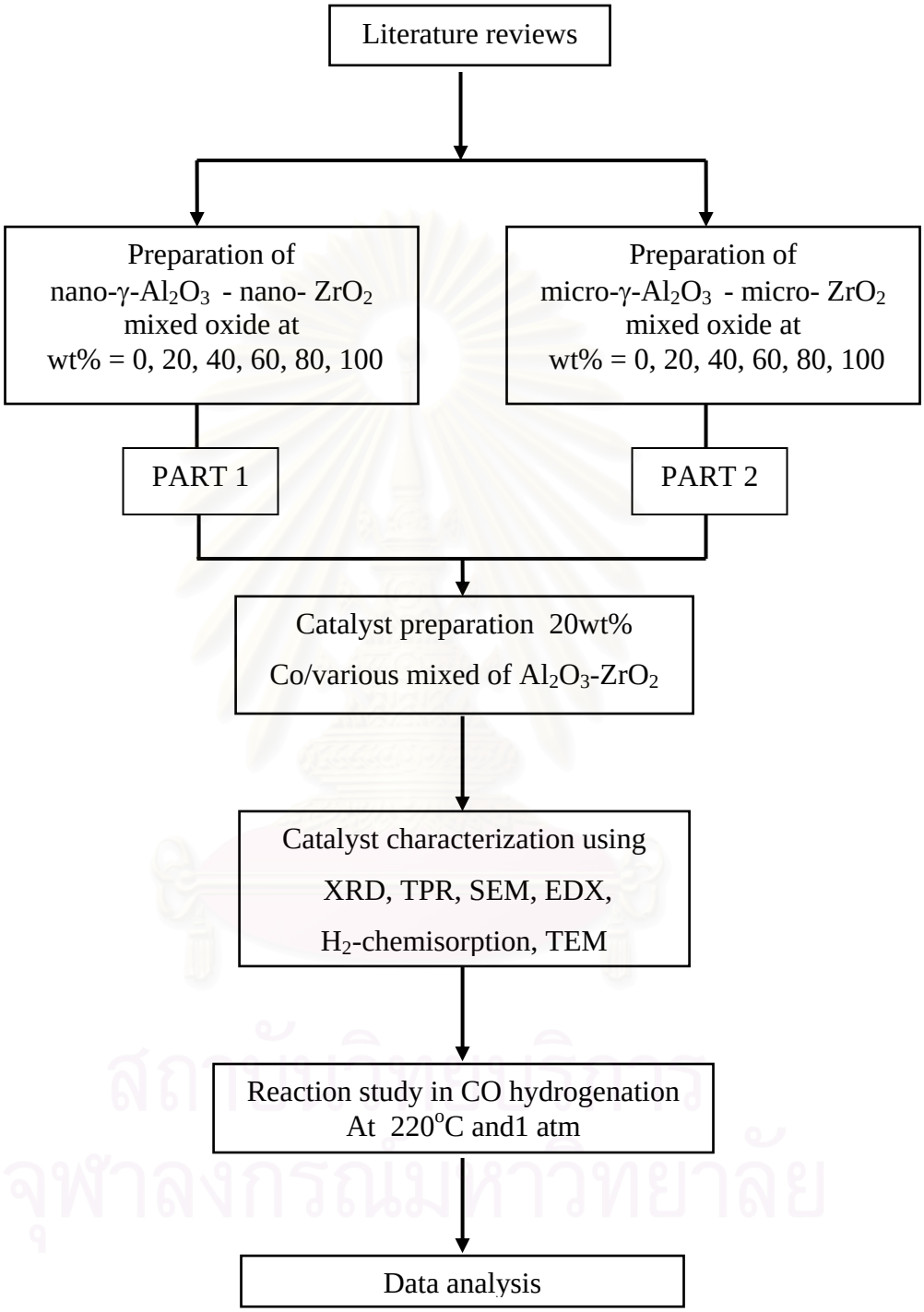

CHAPTER V

RESULTS AND DISCUSSION

The results and discussion in this chapter are divided into three sections. Section 5.1 is described characteristics and catalytic properties of Co oxide species dispersed on nanoscale mixed Al_2O_3-ZrO_2 supports. Section 5.2 is explained the physicochemical properties of Co oxide species dispersed on different micron- and nanoscale mixed Al_2O_3-ZrO_2 supports. Section 5.3 presents a comparative study of cobalt catalysts supported on micron- and nanoscale mixed Al_2O_3-ZrO_2 in CO hydrogenation reaction.

5.1 The physicochemical properties of nano-Al_2O_3-ZrO_2 supported Cobalt catalyst

5.1.1 Scanning Electron Microscopy (SEM) and Energy Dispersive X-ray Spectroscopy (EDX)

SEM and EDX were also conducted in order to study the morphologies and elemental distribution of the samples, respectively. In general, there was no significant change in morphologies and elemental distribution of all samples after calcination. A typical SEM micrograph and EDX mapping (for Co, Al, Zr, and O) for Co/nano-Al_2O_3-ZrO_2 sample are illustrated in Figure 5.1-5.6. Apparently, the Co oxide species showed well distributed on the surface of the support.

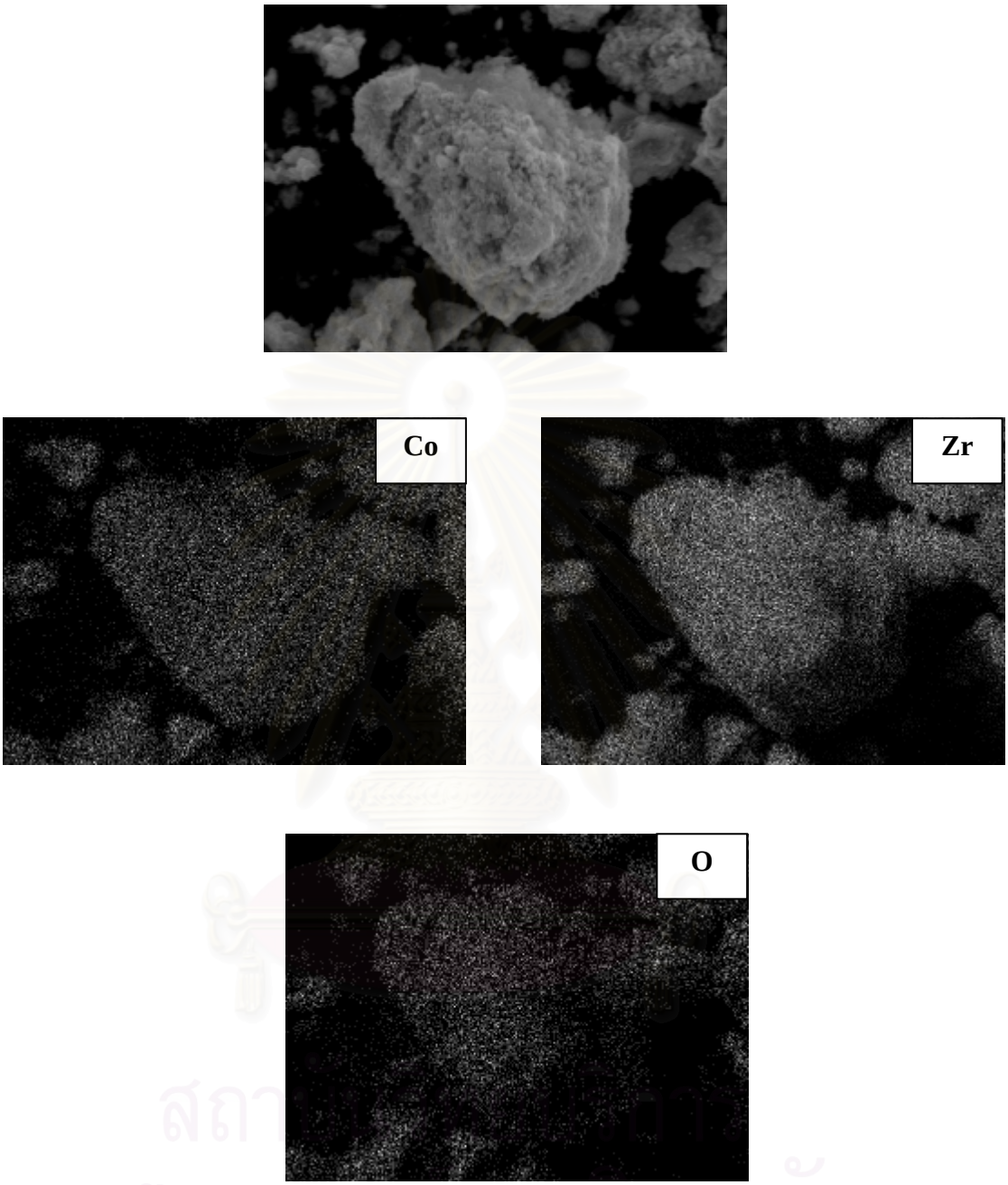

Figure 5.1 SEM micrograph and EDX mapping of Co/Al-0-Zr-100(N)

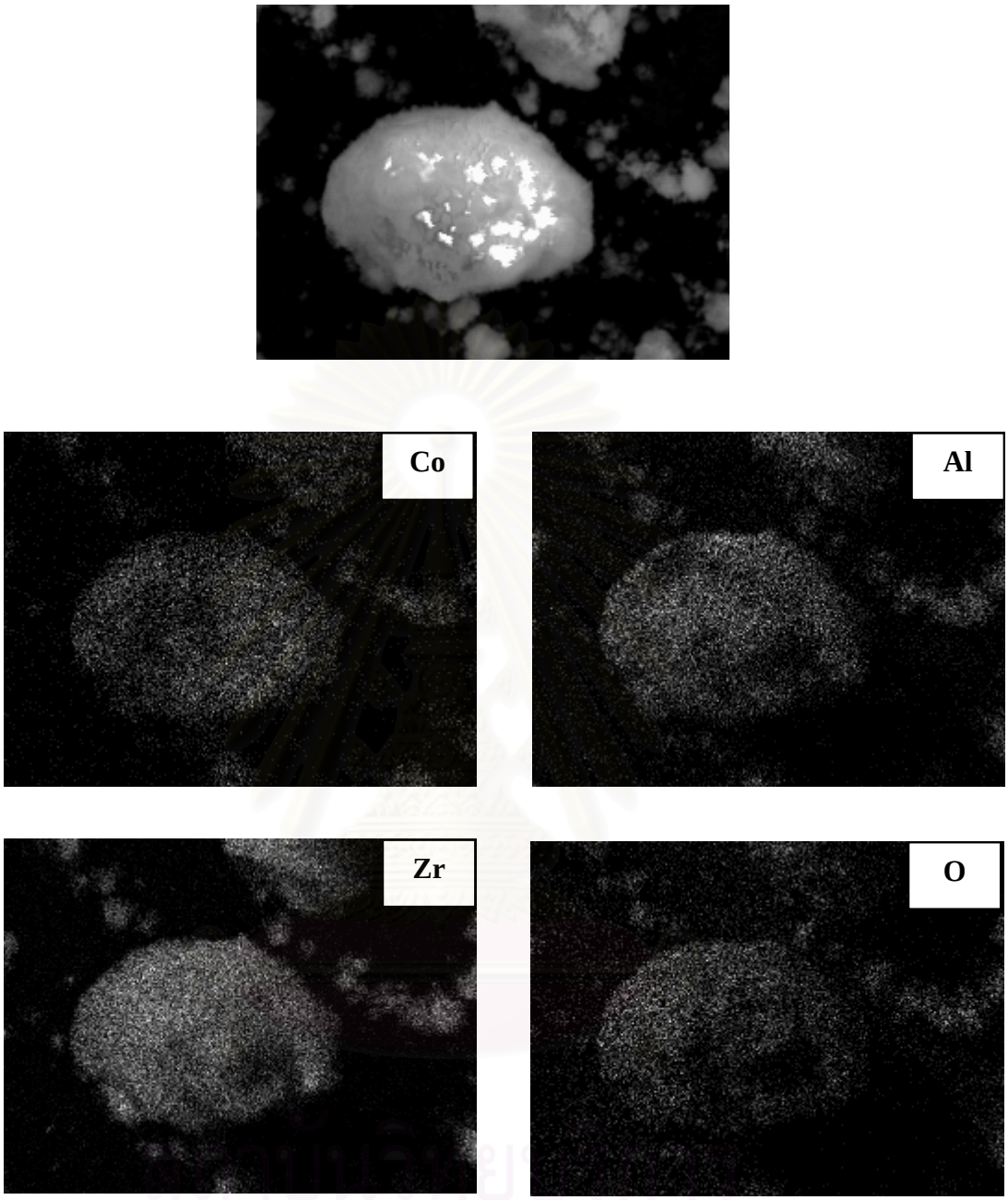

Figure 5.2 SEM micrograph and EDX mapping of Co/Al-20-Zr-80(N)

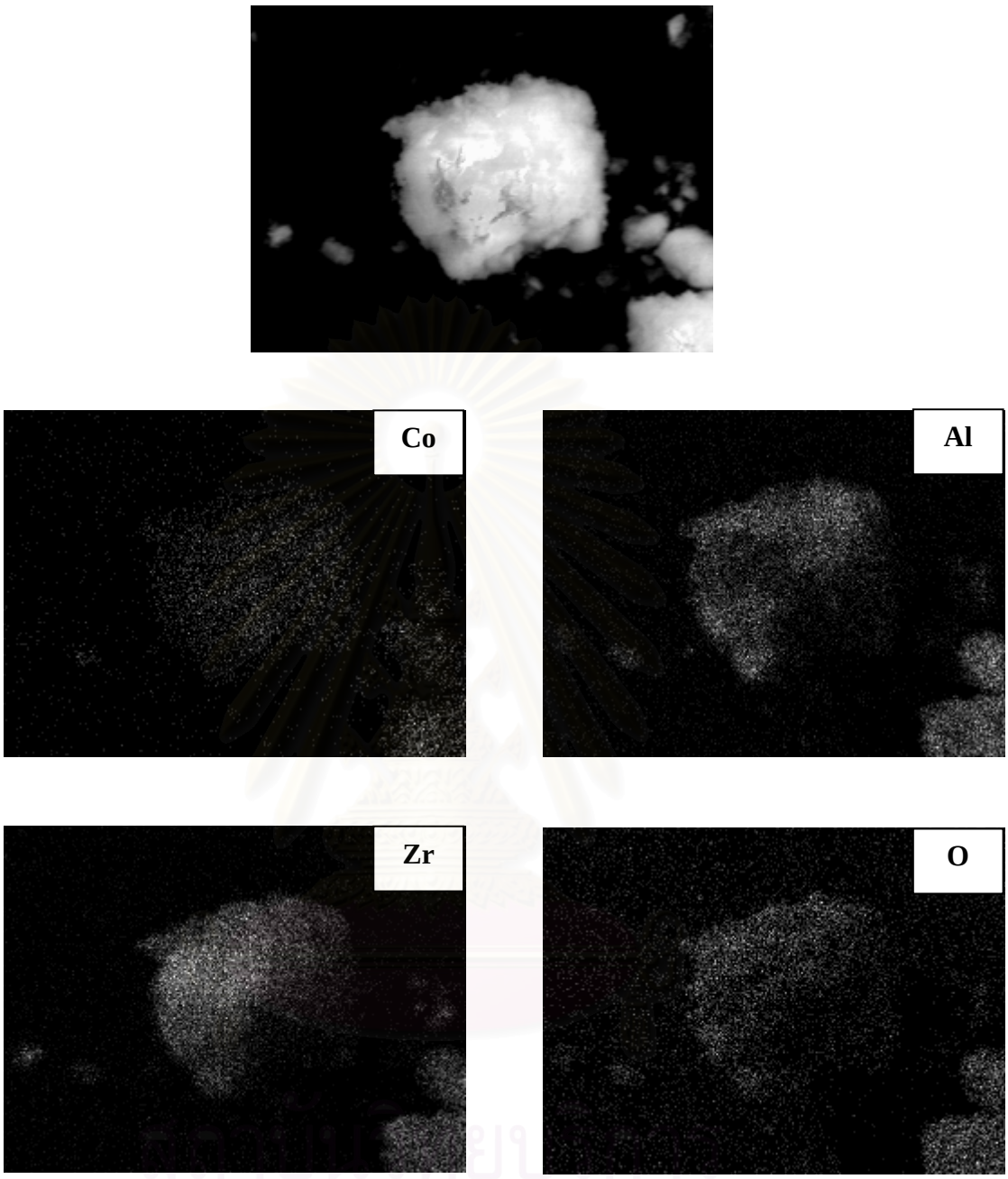

Figure 5.3 SEM micrograph and EDX mapping of Co/Al-40-Zr-60(N)

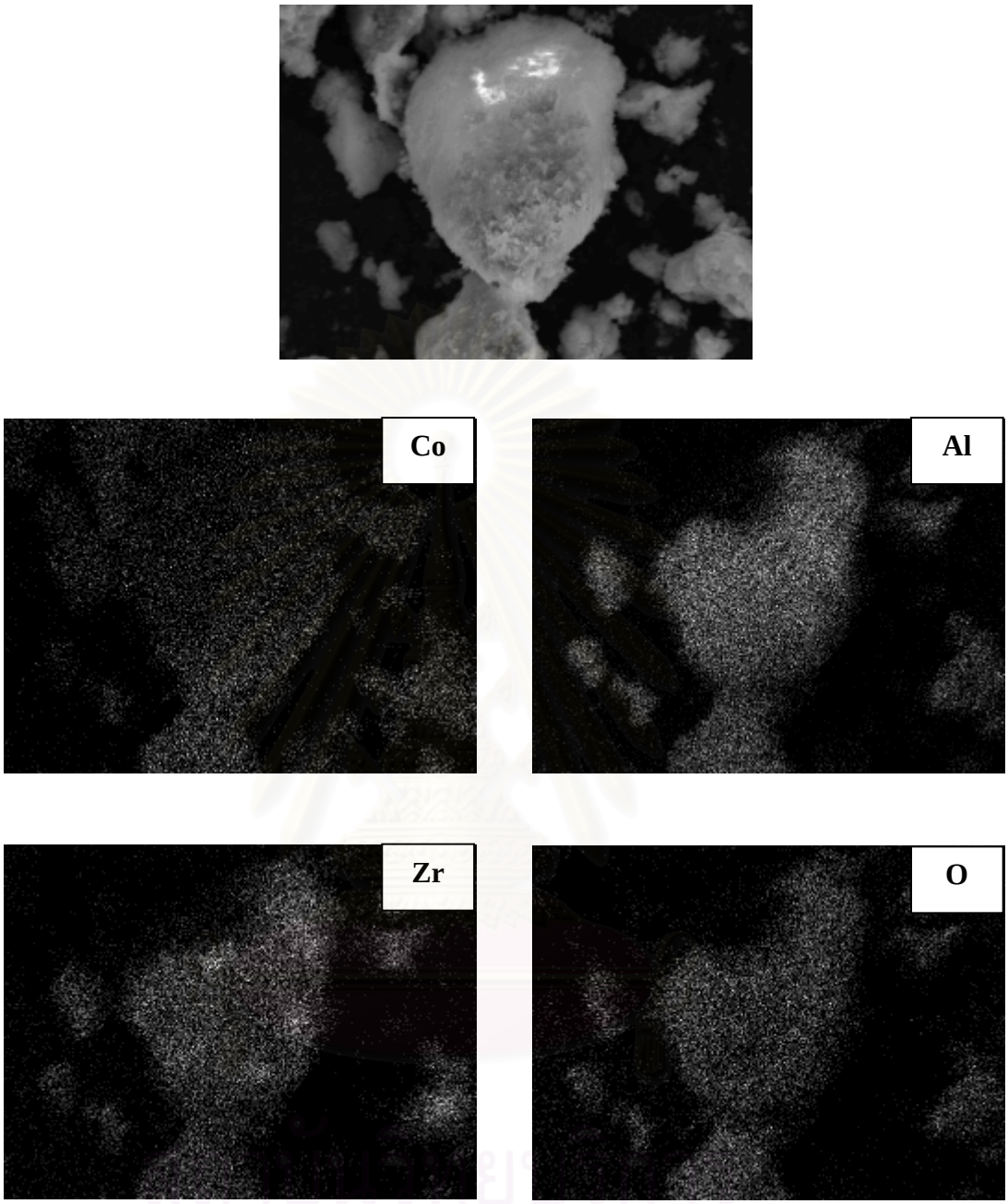

Figure 5.4 SEM micrograph and EDX mapping of Co/Al-60-Zr-40(N)

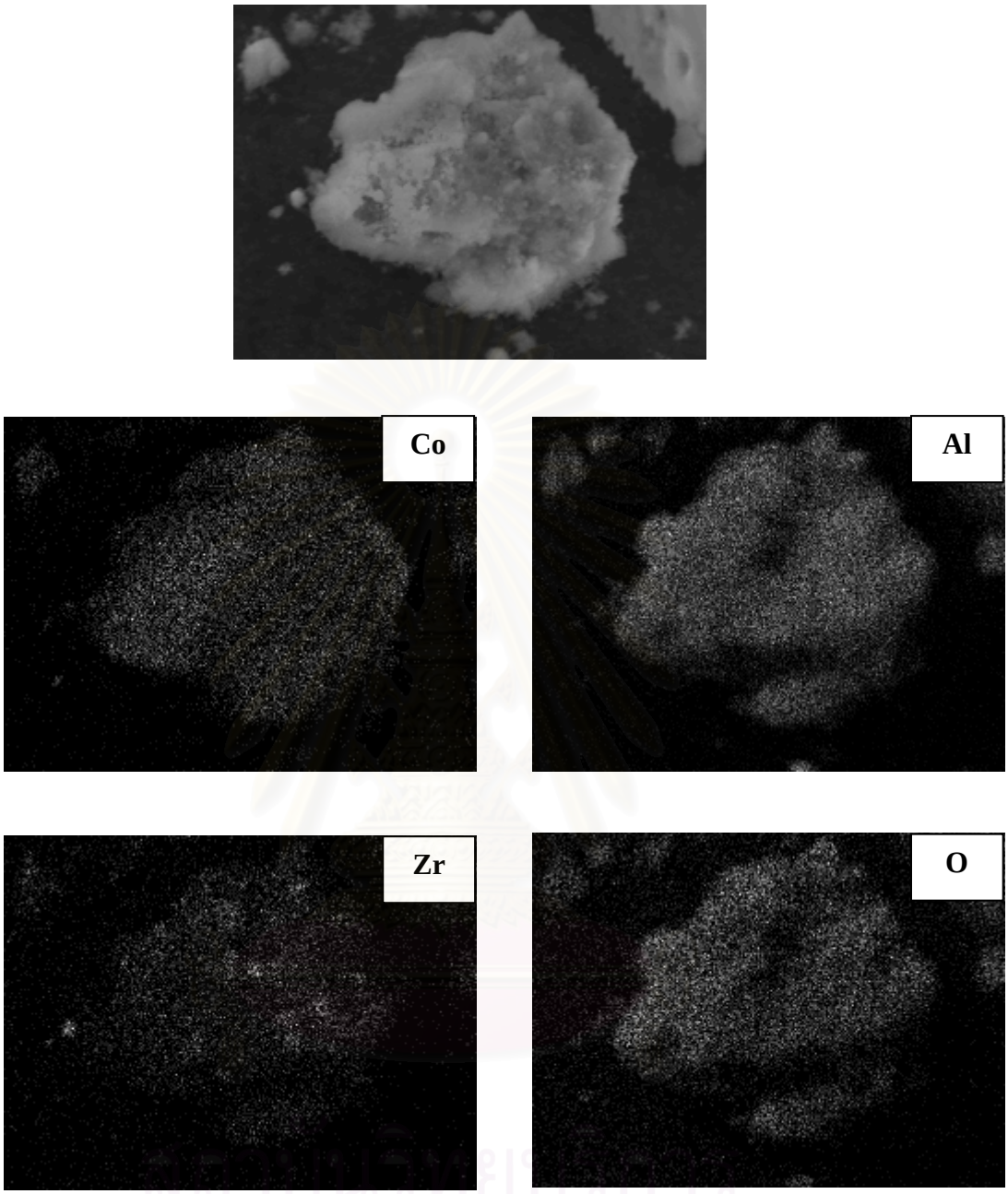

Figure 5.5 SEM micrograph and EDX mapping of Co/Al-80-Zr-20(N)

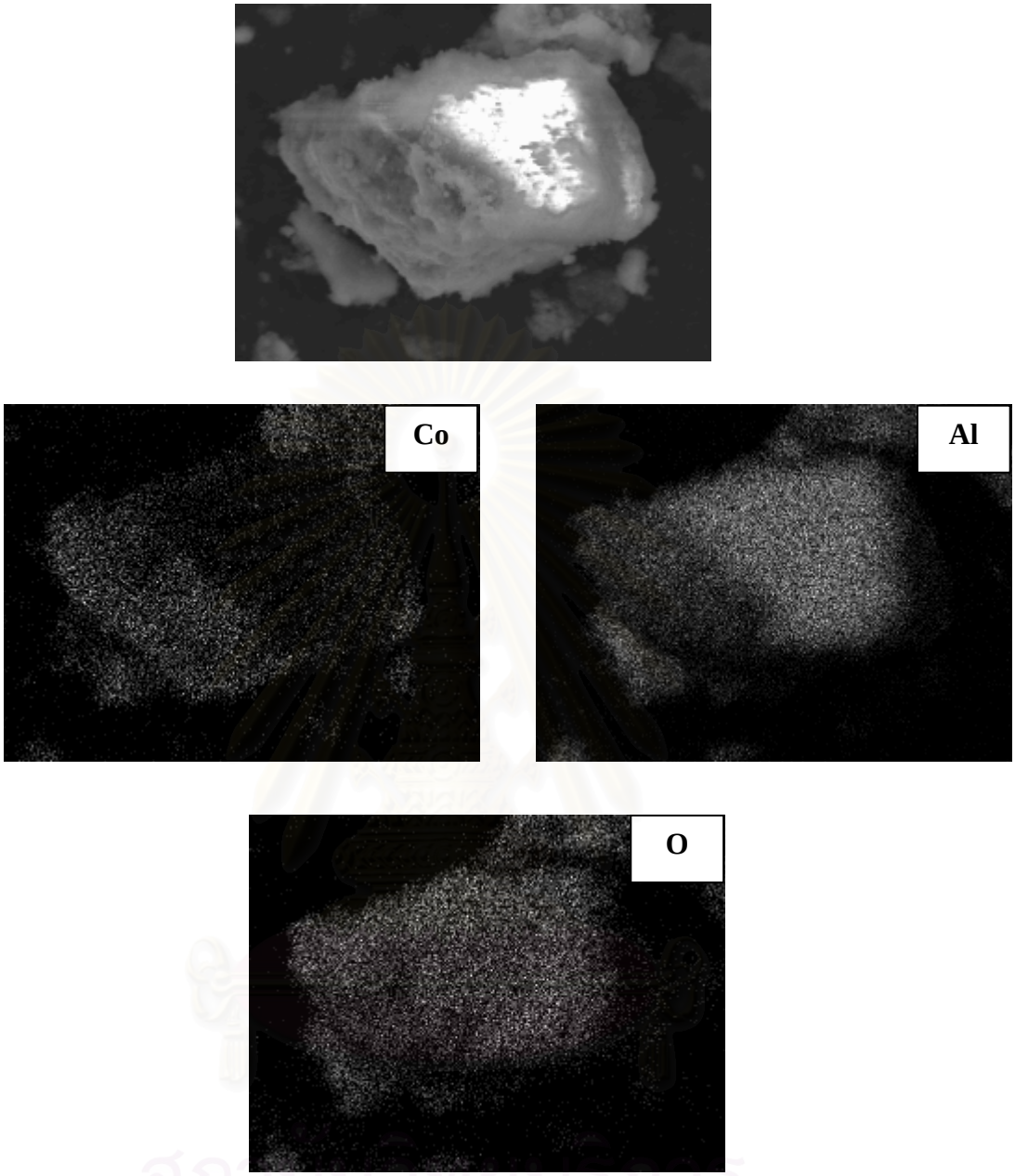

Figure 5.6 SEM micrograph and EDX mapping of Co/Al-100-Zr-0(N)

5.1.2 X-ray Diffraction (XRD)

The XRD patterns of the mixed nano-Al_2O_3-ZrO_2 supports consisting of various weight ratios of nano-Al_2O_3-ZrO_2 prior to impregnation are shown in Figure 5.7. Apparently, the pure nano-Al_2O_3 support (Al-100-Zr-0(N)) exhibited the XRD peaks at 32.5^o, 37°, 46° and 67.5^o indicating alumina in the gamma (γ) form. It was observed that the pure nano-ZrO_2 support (Al-0-Zr-100(N)) exhibited XRD peaks at 29.8^o, 34.2^o, 49.6^o, and 59.5^o assigning to the ZrO_2 in tetragonal phase. Besides the XRD peaks of tetragonal phase, the peaks at 24°, 28.2^o, 31.5^o, 41°, 45° and 55.8^o were also detected indicating the ZrO_2 in monoclinic phase. The XRD patterns for the mixed nano-Al_2O_3-ZrO_2 supports consisting of various weight ratios of the nano-Al_2O_3-ZrO_2 revealed the combination of Al_2O_3-ZrO_2 supports based on their contents. After impregnation with the cobalt onto the support, the samples were dried and calcined.

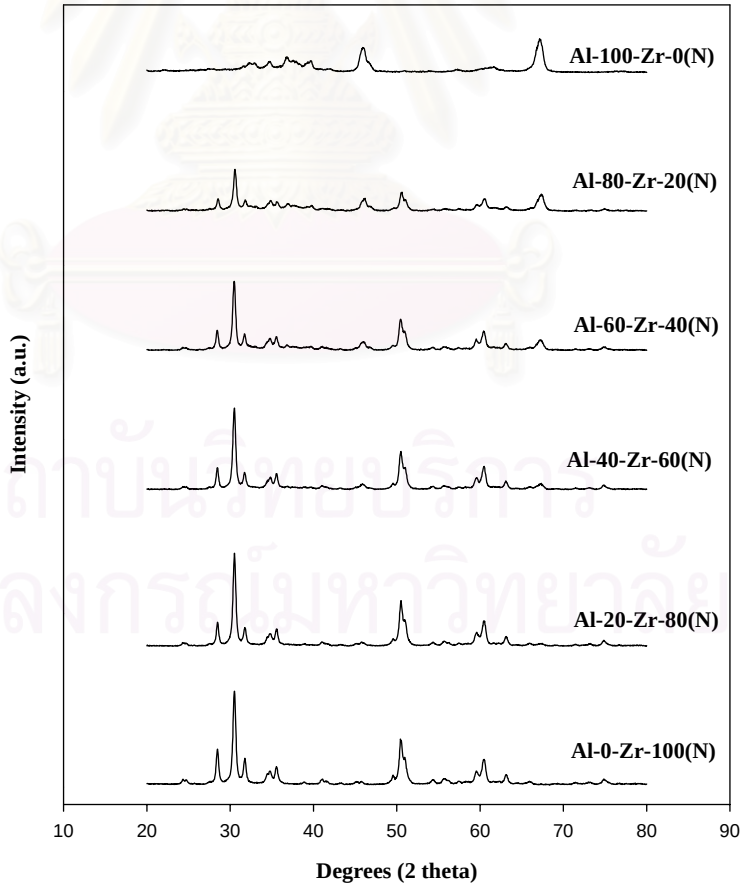

Figure 5.7 XRD patterns of various mixed nano-Al_2O_3-ZrO_2 supports

The XRD patterns for cobalt dispersed on various supports are shown in Figure 5.8. Besides the observation of the characteristic peaks of the supports as shown in Figure 5.7 as mentioned before, all calcined samples exhibited XRD peaks at 31° (weak), 36° (strong), and 65° (weak), which were assigned to the presence of Co_3O_4 after calcination of samples. This indicated that the Co_3O_4 formed was highly dispersed on the supports used.

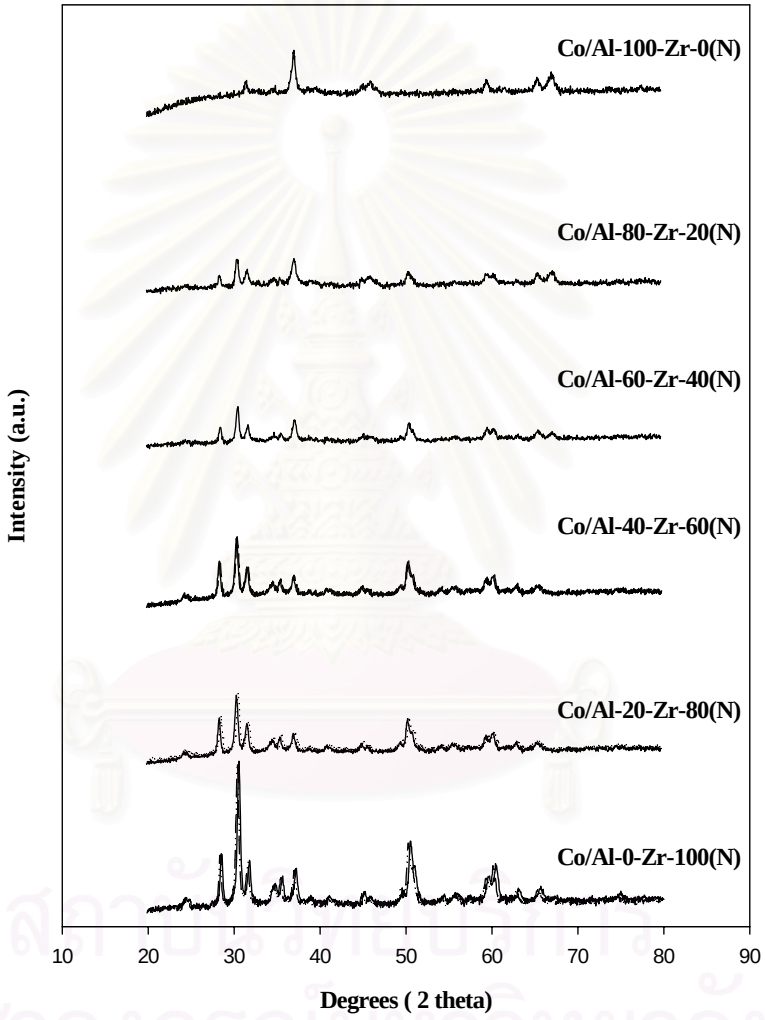

Figure 5.8 XRD patterns of cobalt oxide species dispersed on various mixed nano-Al_2O_3-ZrO_2 supports

5.13 Transmission Electron Microscopy (TEM)

TEM micrographs of the supports were collected and the typical TEM micrographs of the nano-ZrO_2, the nano-Al_2O_3 and the mixed Al_2O_3-ZrO_2 (Al-40-Zr-60(N)) supports are shown in Figure 5.9-5.11. As expected it indicated that the nano-ZrO_2 appeared in smaller particle compared to the nano-Al_2O_3. The mixed supports exhibited the combination between both supports present.

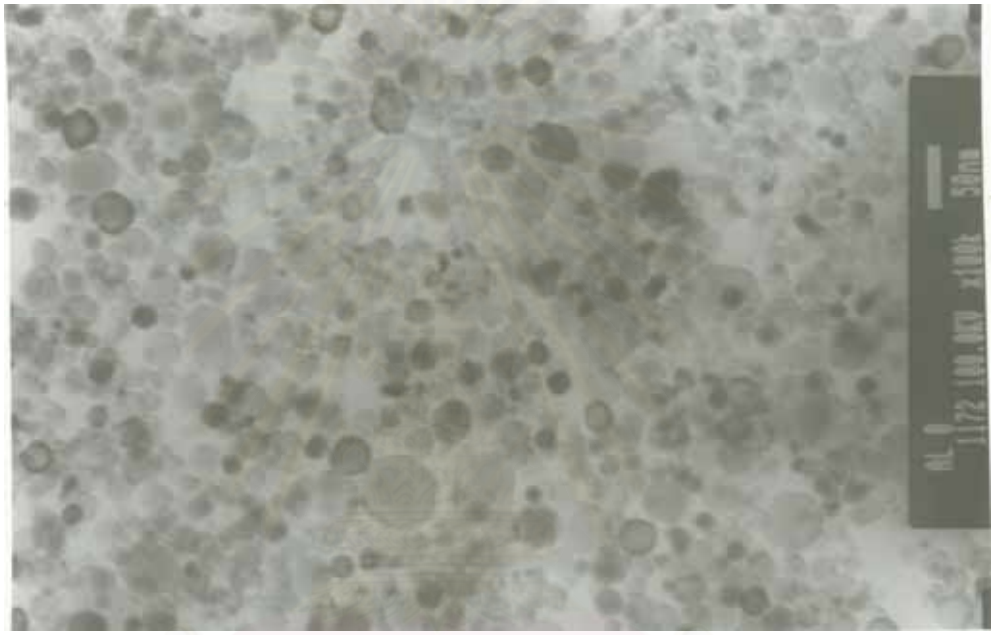

Figure 5.9 TEM micrographs of nano-ZrO_2 support

Figure 5.10 TEM micrographs of nano-Al_2O_3 support

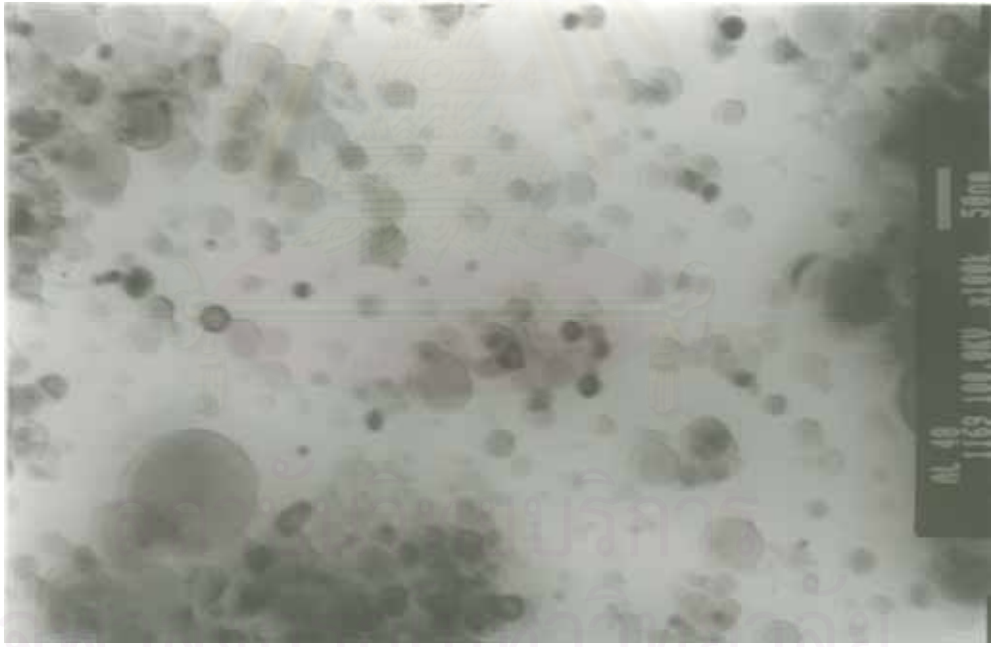

Figure 5.11 TEM micrographs of mixed nano-Al_2O_3-ZrO_2 (Al-40-Zr-60(N)) support

TEM micrographs for all cobalt dispersed on the various supports are shown in Figure 5.12-5.17 However, considering the morphologies for the cobalt oxide species dispersed on the support, they could not be differentiated between those and the supports. It was suggested that the morphologies of cobalt oxide species were essentially similar with those of the various supports indicating the more uniform dispersion on the supports. On the other hand, it revealed that the nano-size of cobalt oxide species could be achieved with the nano-sized support. In addition, the cobalt oxide species were also located and distributed side by side with the supports showing good distribution of the species. There was also no significant change based on different compositions of the support. It should be noted that the highly dispersed form of cobalt oxide species could not guarantee the large number of reduced cobalt metal surface atoms, which is related to the overall activity of the catalysts [14]. In addition, with the highly dispersed form of cobalt oxide species, the interaction of those with the specified supports has to be essentially considered. Therefore, the temperature-programmed reduction on the calcined samples needs to be performed in order to give a better understanding according to such a reduction behavior.

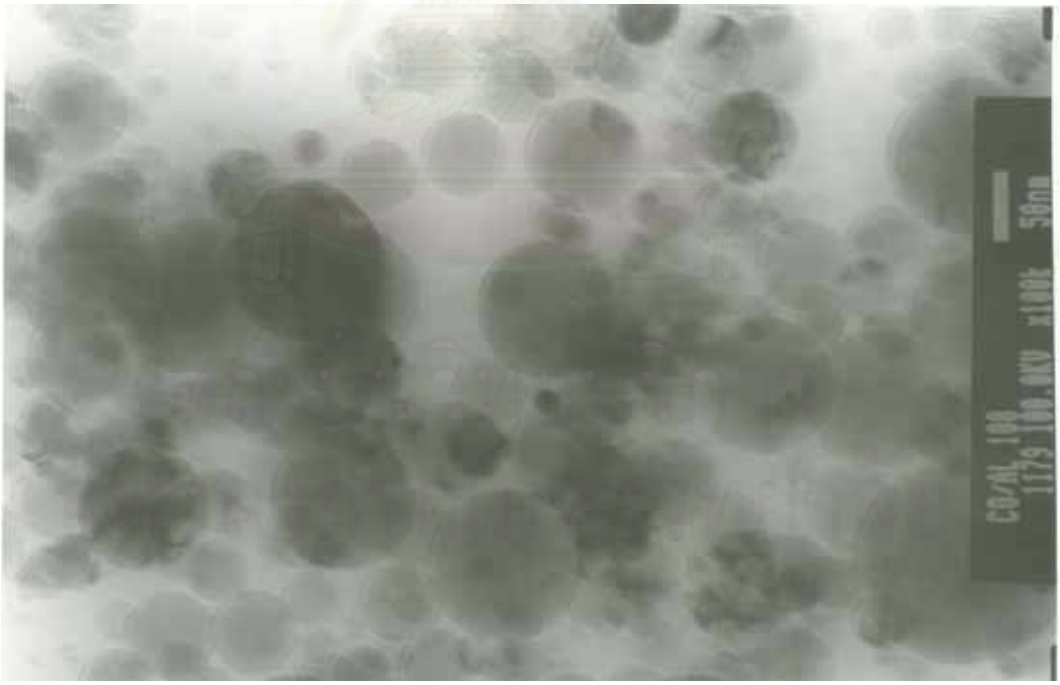

Figure 5.12 TEM micrograph of Co/Al-100-Zr-0(N)

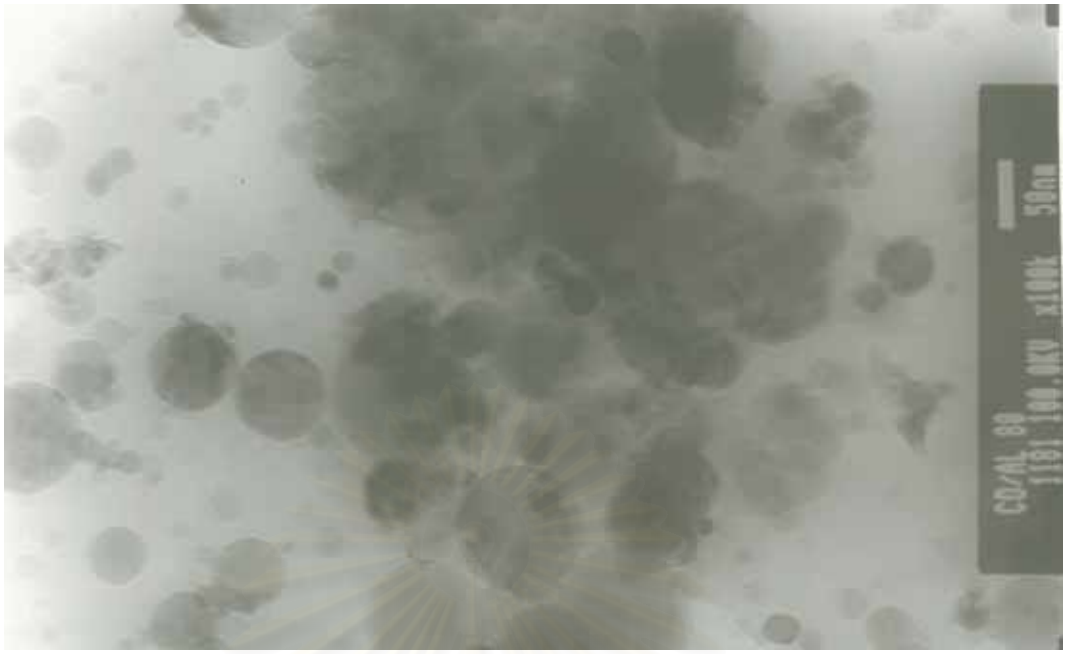

Figure 5.13 TEM micrograph of Co/Al-80-Zr-20(N)

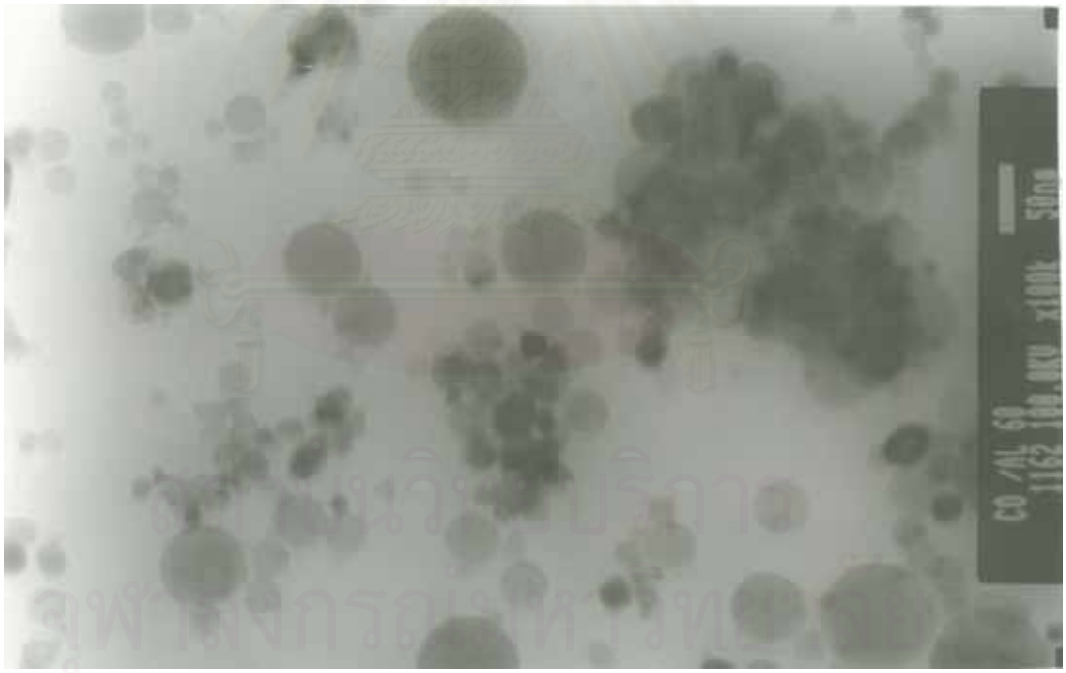

Figure 5.14 TEM micrograph of Co/Al-60-Zr-40(N)

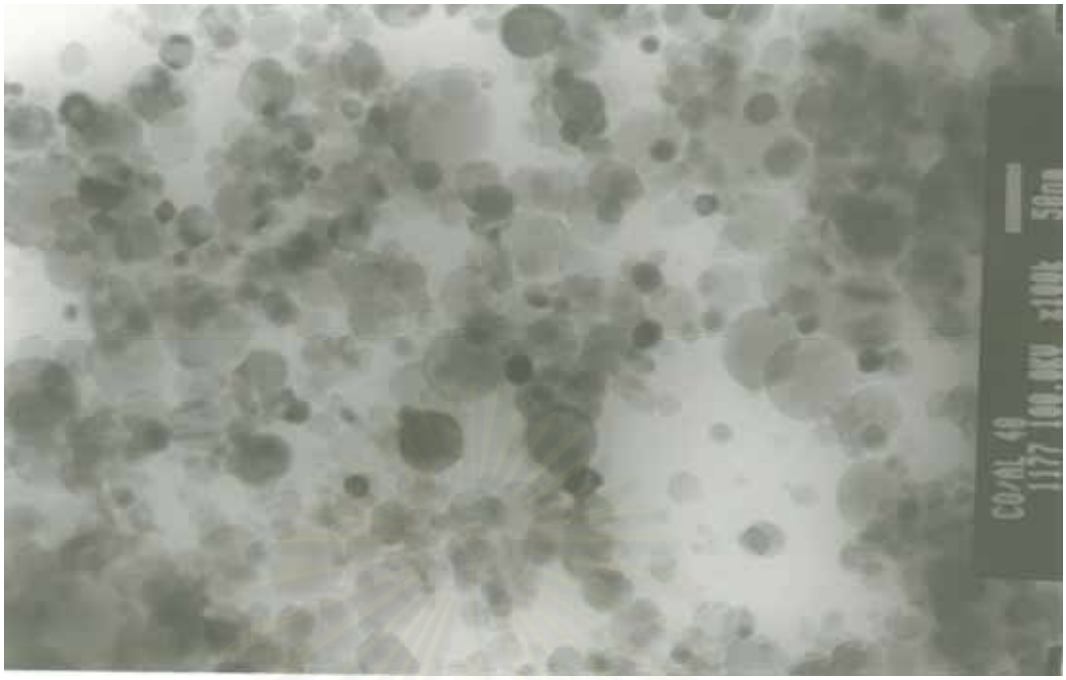

Figure 5.15 TEM micrograph of Co/Al-40-Zr-60(N)

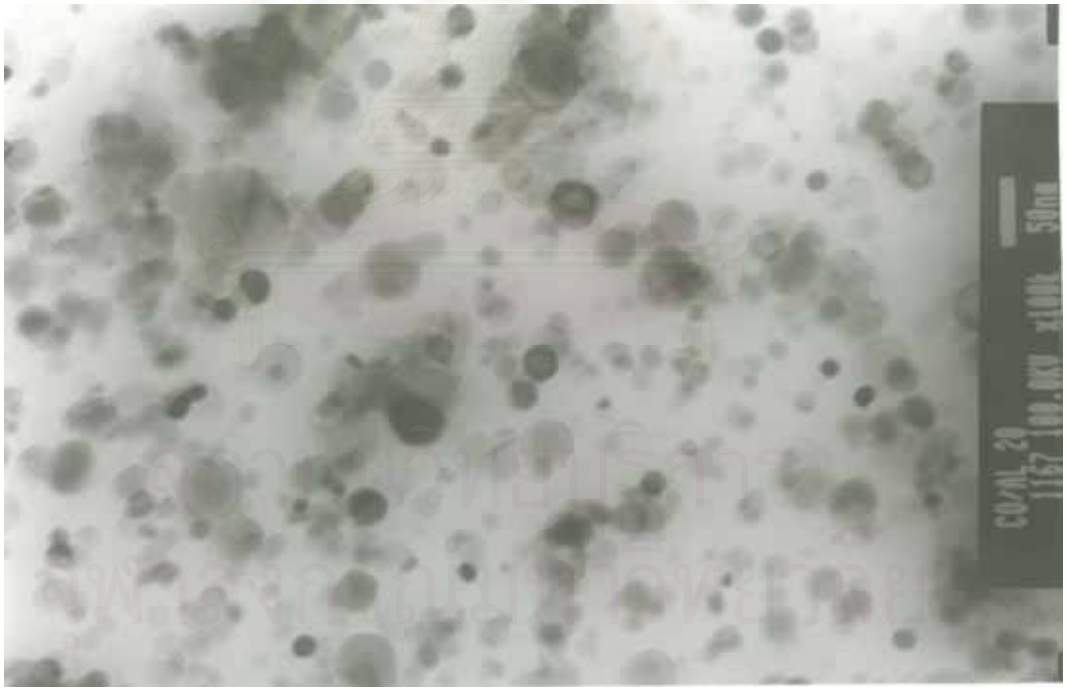

Figure 5.16 TEM micrograph of Co/Al-20-Zr-80(N)

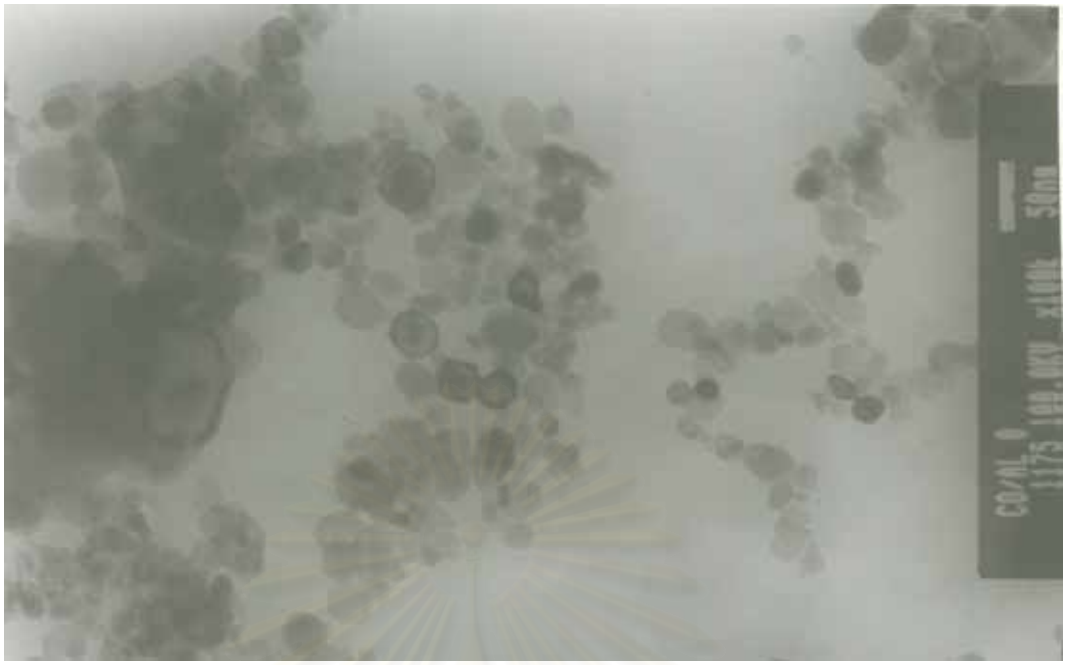

Figure 5.17 TEM micrograph of Co/Al-0-Zr-100(N)

5.1.4 Temperature Programmed Reduction (TPR)

TPR was performed in order to determine the reduction behaviors of samples. The TPR profiles for all samples are shown in Figure 5.18. It was found that there was only one reduction peak, however, at different reduction temperatures for all calcined samples. The one reduction peak can be assigned to the overlap of two-step reduction of Co_3O_4 to CoO and then to Co metal [5, 13]. Upon the TPR conditions, the two-step reduction may or may not be observed. Based on the TPR profiles, it indicated that Co oxides dispersed on the pure nano-Al_2O_3 exhibited the lowest maximum reduction temperature than those on the mixed nano-Al_2O_3-ZrO_2 supports. It was suggested that using the mixed nano-Al_2O_3-ZrO_2 supports resulted in increasing the reduction temperature of Co oxides due to the stronger metal-support interaction.

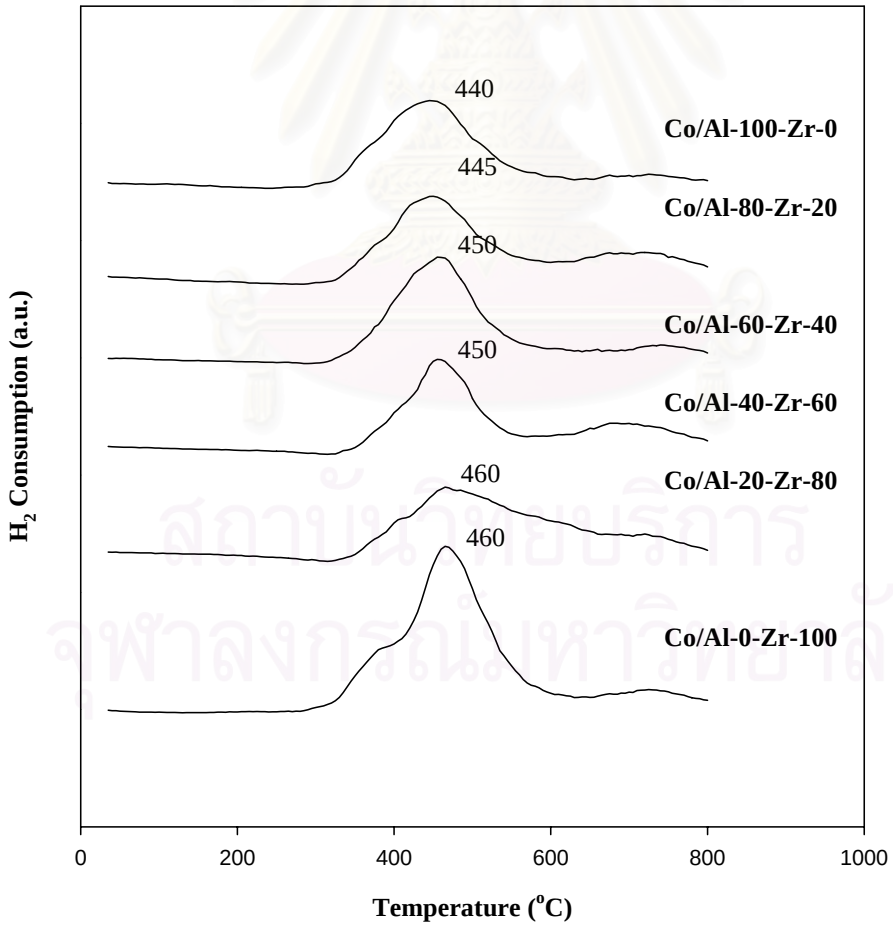

Figure 5.18 TPR profiles of cobalt oxide species dispersed on various mixed nano-Al_2O_3-ZrO_2 supports

5.2 The physicochemical properties of micron-Al_2O_3-ZrO_2 supported Cobalt catalyst

5.2.1 Scanning Electron Microscopy (SEM) and Energy Dispersive X-ray Spectroscopy (EDX)

SEM and EDX were also conducted in order to study the morphologies and elemental distribution of the samples, respectively. In general, there was no significant change in morphologies and elemental distribution of all samples after calcination. A typical SEM micrograph and EDX mapping (for Co, Al, Zr, and O) for Co/micron-Al_2O_3-ZrO_2 sample are illustrated in Figure 5.19 - 5.24. Apparently, the Co oxide species showed well distributed on the surface of the support.

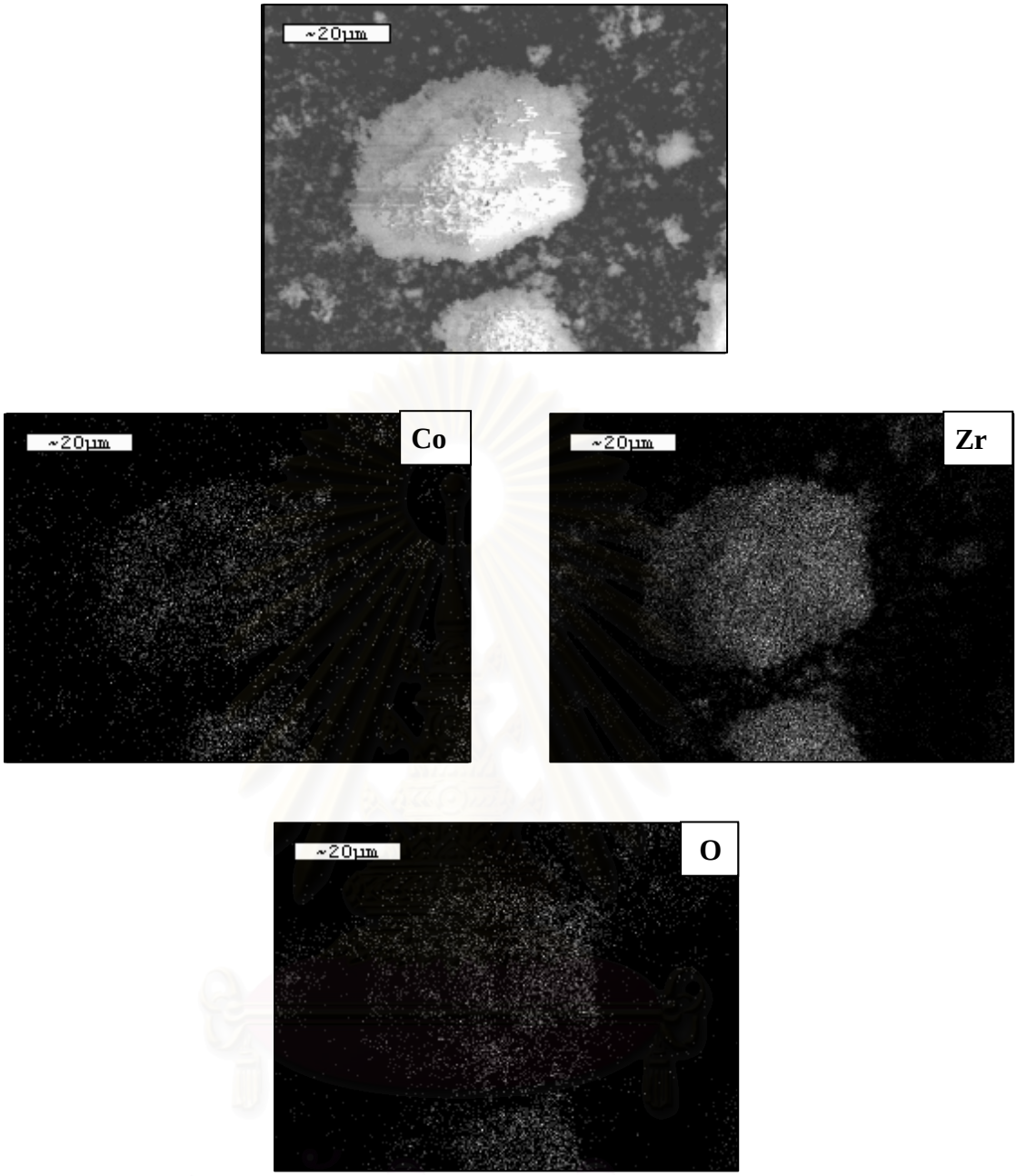

Figure 5.19 SEM micrograph and EDX mapping of Co/Al-0-Zr-100(M)

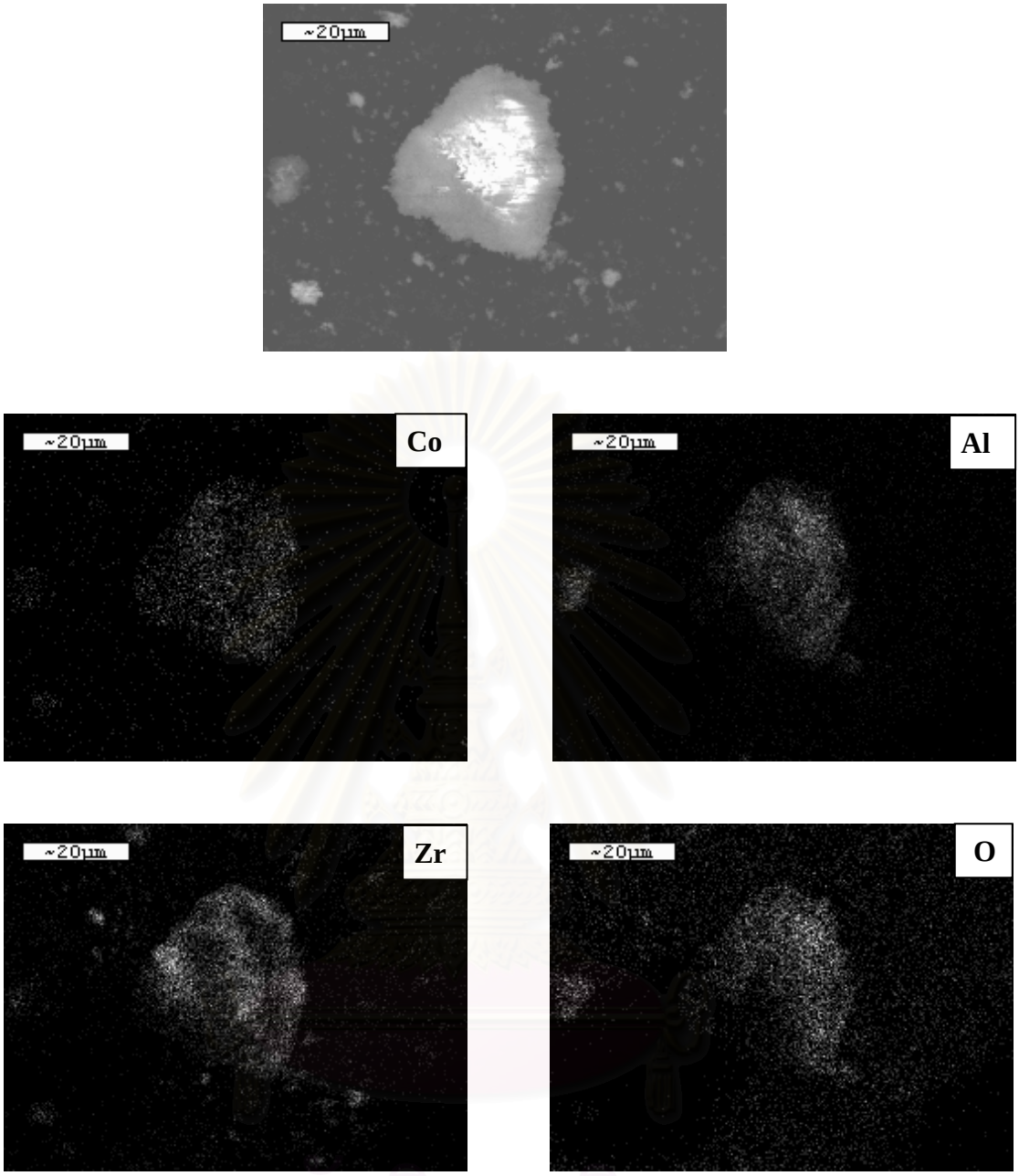

Figure 5.20 SEM micrograph and EDX mapping of Co/Al-20-Zr-80(M)

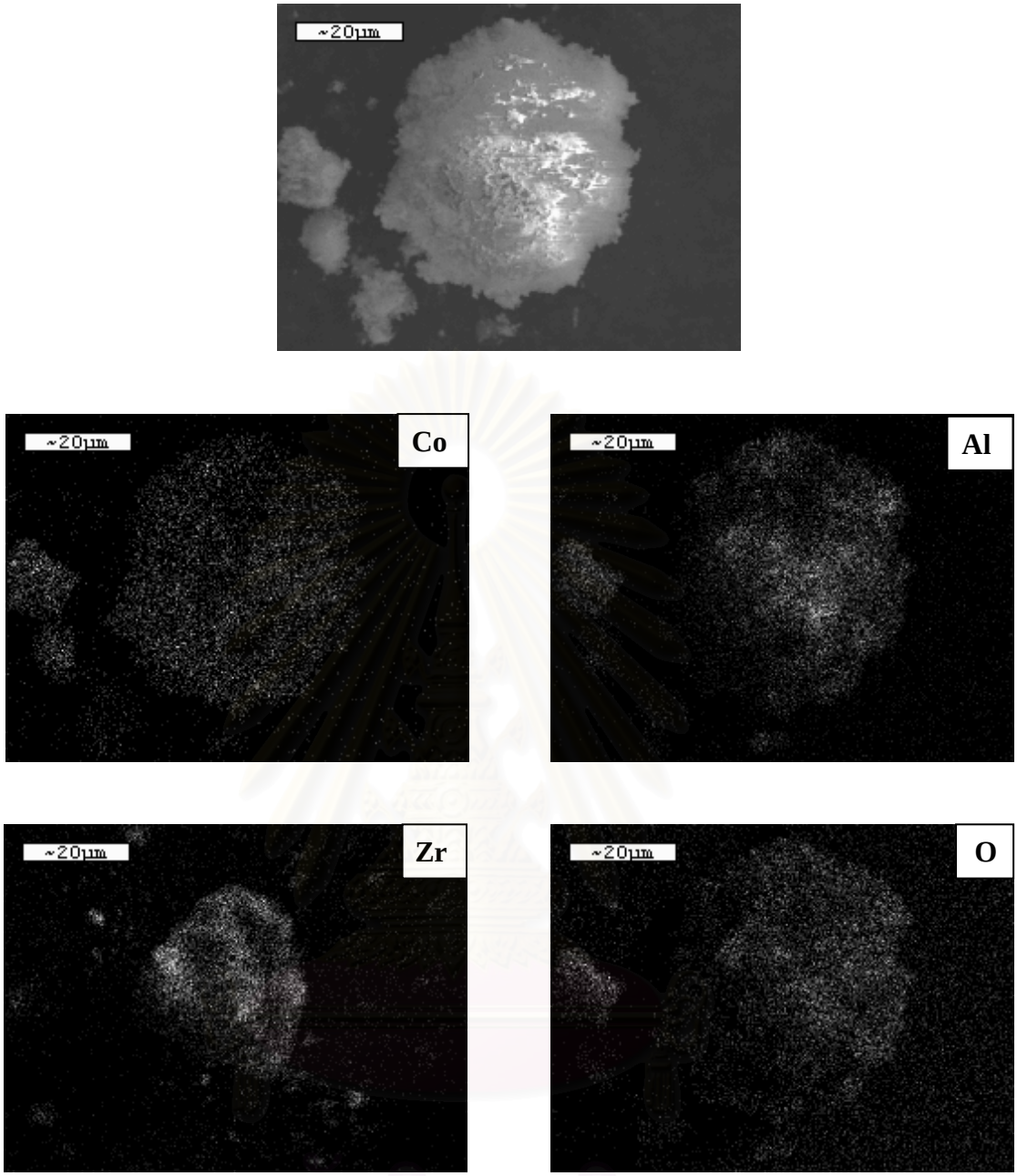

Figure 5.21 SEM micrograph and EDX mapping of Co/Al-40-Zr-60(M)

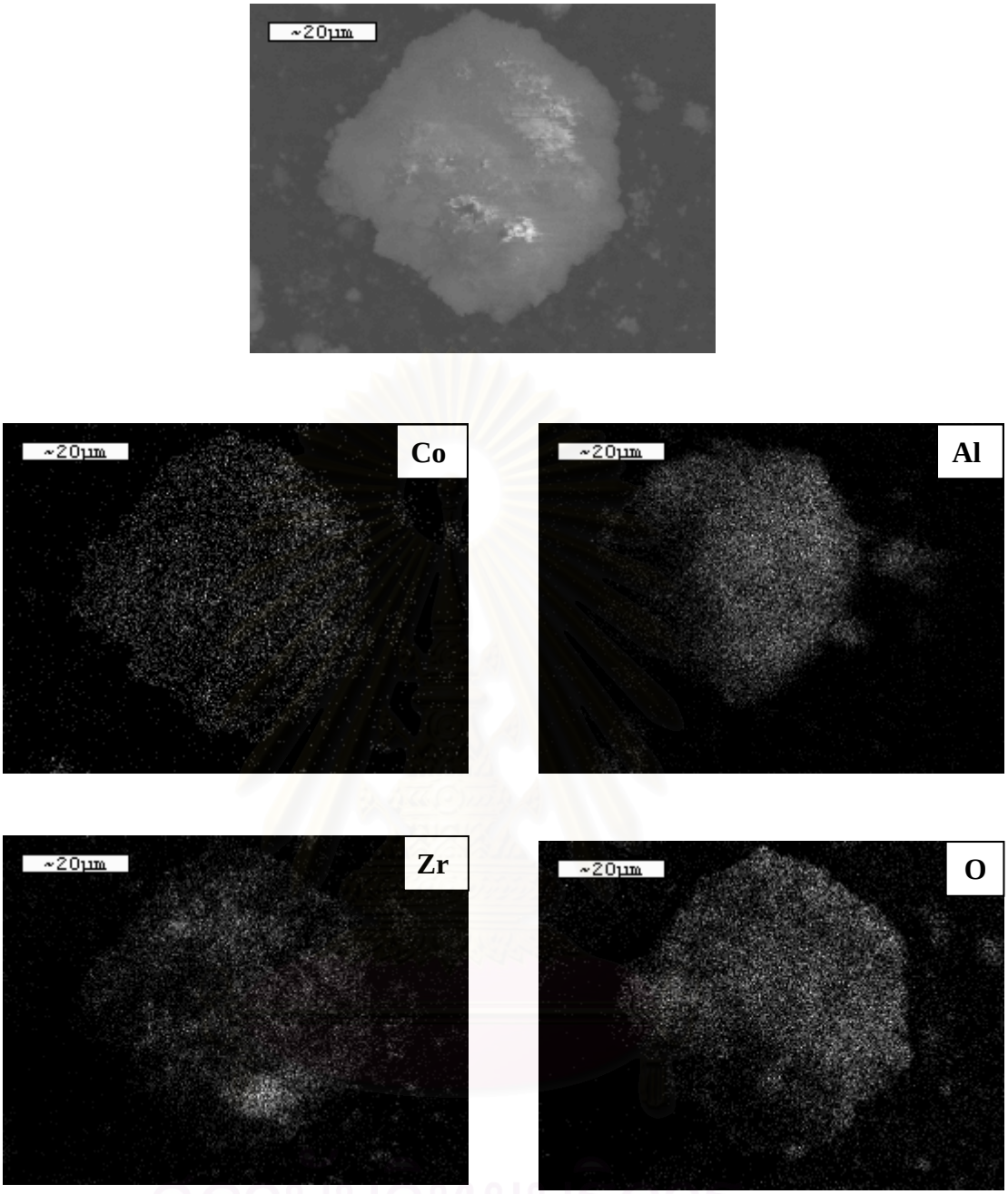

Figure 5.22 SEM micrograph and EDX mapping of Co/Al-60-Zr-40(M)

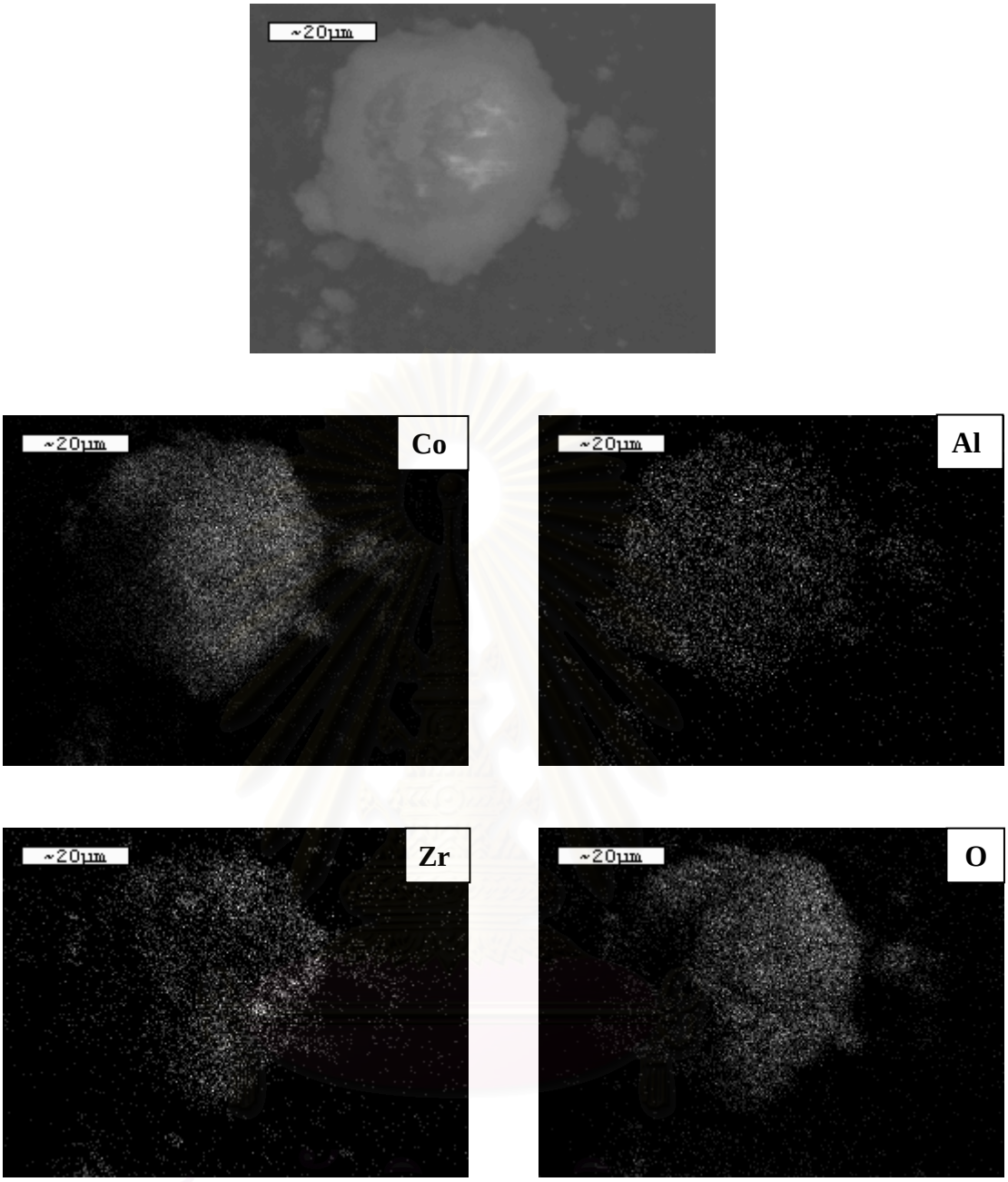

Figure 5.23 SEM micrograph and EDX mapping of Co/Al-80-Zr-20(M)

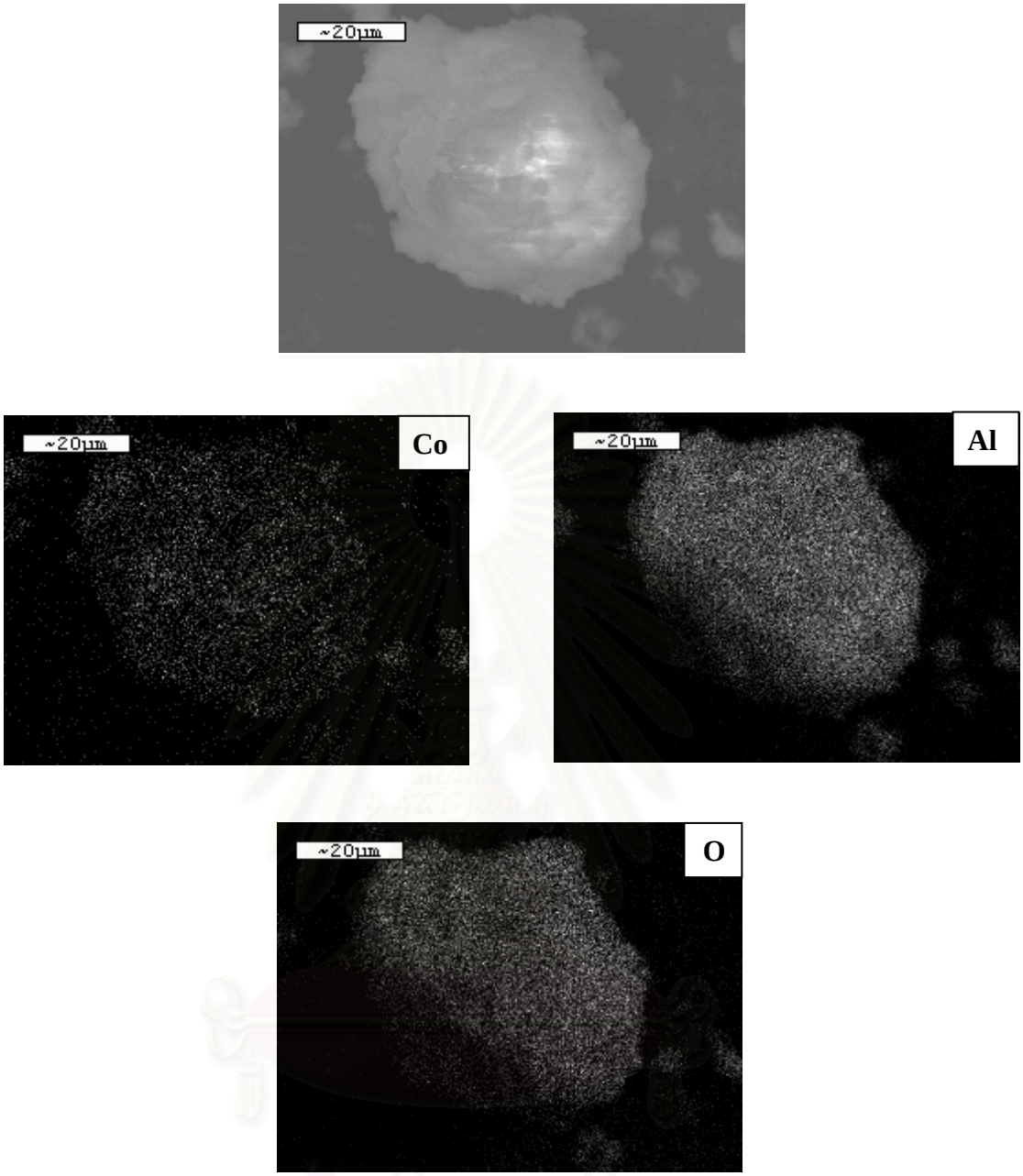

Figure 5.24 SEM micrograph and EDX mapping of Co/Al-100-Zr-0(M)

5.2.2 X-ray Diffraction (XRD)

The XRD patterns of the mixed micron-Al_2O_3-ZrO_2 supports consisting of various weight ratios of micron-Al_2O_3-ZrO_2 prior to impregnation are shown in Figure 5.25. Apparently, the pure micron-Al_2O_3 support (Al-100-Zr-0(M)) exhibited the XRD peaks at 32.5^o, 37°, 46° and 67.5^o indicating alumina in the gamma (γ) form. It was observed that the pure micron-ZrO_2 support (Al-0-Zr-100(M)) exhibited XRD peaks at 34.2^o, 49.6^o, and 59.5^o assigning to the ZrO_2 in tetragonal phase. Besides the XRD peaks of tetragonal phase, the peaks at 24°, 28.2^o, 31.5^o, 41°, 45° and 55.8^o were also detected indicating the ZrO_2 in monoclinic phase. The XRD patterns for the mixed micron-Al_2O_3-ZrO_2 supports consisting of various weight ratios of the micron-Al_2O_3-ZrO_2 revealed the combination of Al_2O_3-ZrO_2 supports based on their contents. After impregnation with the cobalt onto the support, the samples were dried and calcined.

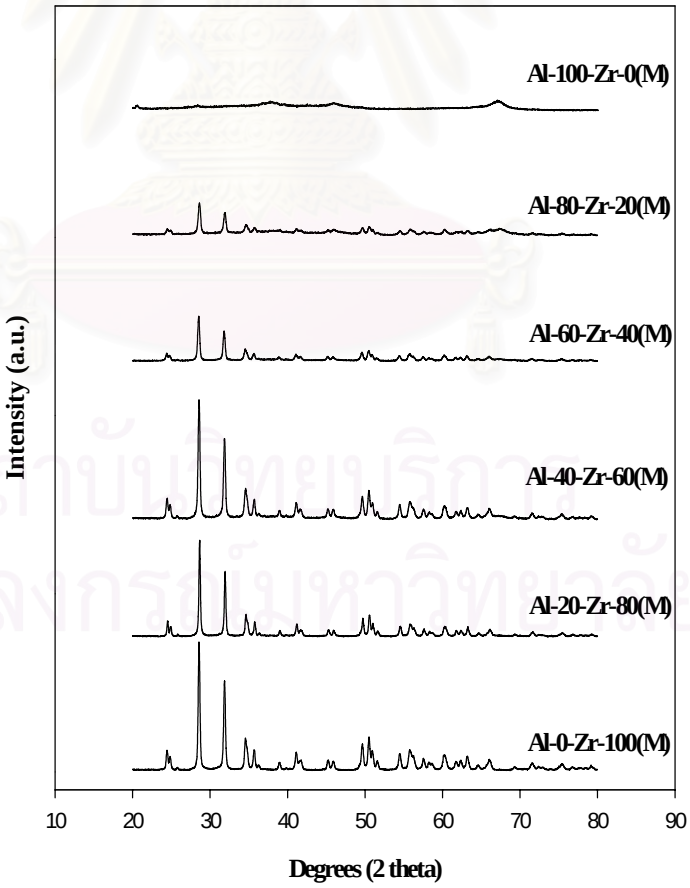

Figure 5.25 XRD patterns of various mixed micron-Al_2O_3-ZrO_2 supports

The XRD patterns for cobalt dispersed on various supports are shown in Figure 5.26. Besides the observation of the characteristic peaks of the supports as shown in Figure 5.25 as mentioned before, all calcined samples exhibited XRD peaks at 31° (weak), 36° (strong), and 65° (weak), which were assigned to the presence of Co_3O_4 after calcination of samples. This indicated that the Co_3O_4 formed was highly dispersed on the supports used.

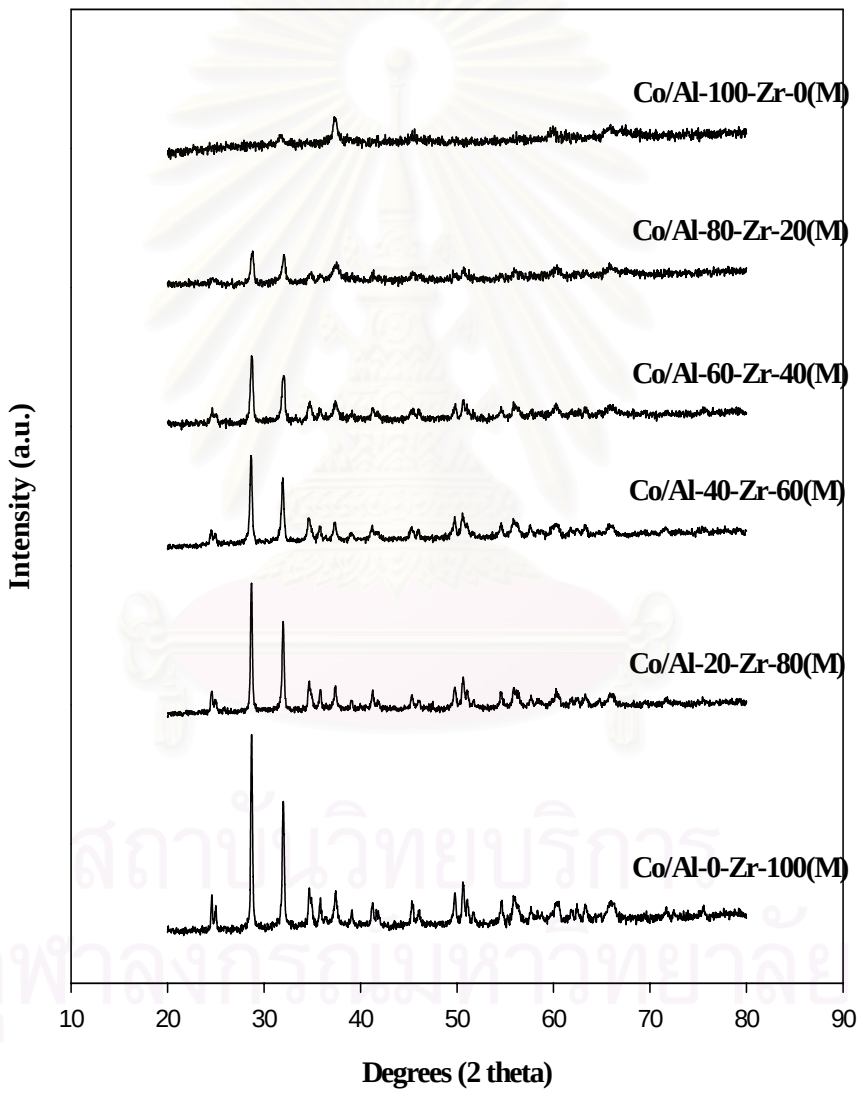

Figure 5.26 XRD patterns of cobalt oxide species dispersed on various mixed micron-Al_2O_3-ZrO_2 supports

5.2.3 Transmission Electron Microscopy (TEM)

TEM micrographs of the supports were collected and the typical TEM micrographs of the micron-ZrO_2, the micron-Al_2O_3 and the mixed Al_2O_3-ZrO_2 (Al-40-Zr-60(M)) supports are shown in Figure 5.27-5.29. The dispersion of Co oxide species on the various micronscale supports is shown in Figure 5.30 – 5.35. In fact, it revealed the similar dispersion of Co for all various supports here. Although it can not differentiate the Co oxide species and ZrO_2, it indicated that Co oxide species dispersed on the micronscale supports were apparently in the micronscale species as well. Considering the TEM micrographs for the nanoscale supports and the Co oxide dispersed on the various nanoscale supports, they are illustrated as seen in Figures 5.9 -5.11 and Figures 5.12 – 5.17, respectively. However, the differences in TEM micrographs for the micron- and nanoscale Al_2O_3 and ZrO_2 were evident. Obviously, the nanoscale Al_2O_3 and ZrO_2 appeared in the smaller crystal in the nano size (~30-40 nm). TEM micrographs of the mixed nanoscale supports also exhibited the similar appearance with those from the nanoscale ZrO_2. The typical TEM micrograph [Al-40-Zr-60 (N)] for the mixed nanoscale supports is also shown in Figure 5.11. The TEM micrographs for Co oxide species dispersed on the various nanoscale supports (Figure 5.12 – 5.17) showed very interesting results where good dispersion of Co oxide species can be achieved onto the nanoscale supports. This was suggested that the dispersion of Co oxide species could be altered with the size of the support used. On the other hand, the Co oxide species dispersing on the micronscale support were in the micron size whereas those were in the nano size on the nanoscale one.

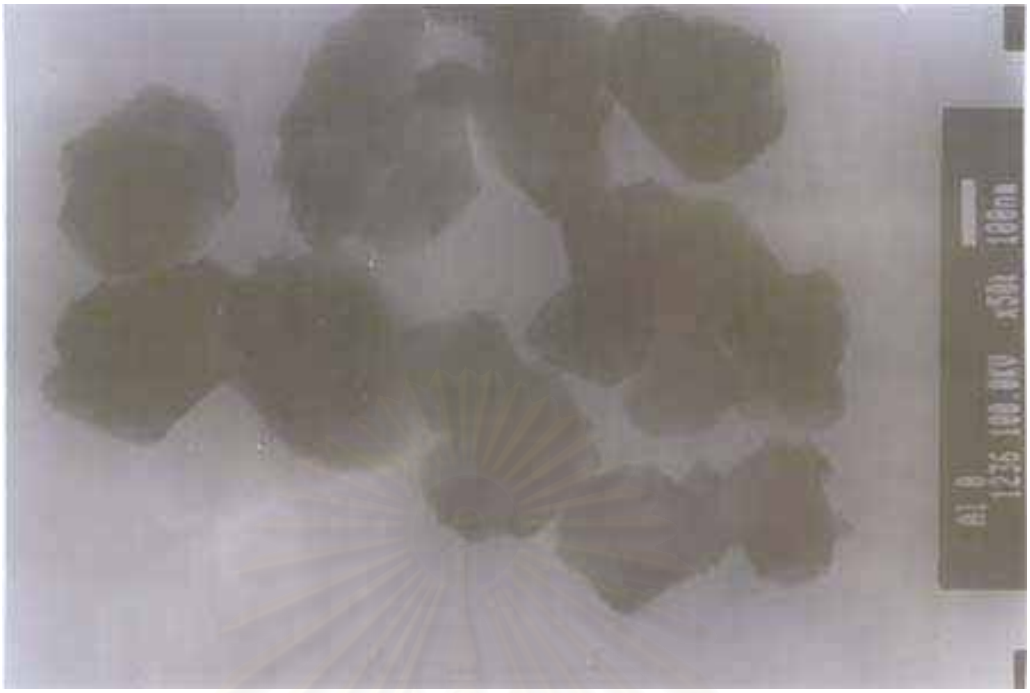

Figure 5.27 TEM micrographs of micron-ZrO_2 support

Figure 5.28 TEM micrographs of micron-Al_2O_3 support

Figure 5.29 TEM micrographs of mixed micron-Al_2O_3-ZrO_2 (Al-40-Zr-60(M)) support

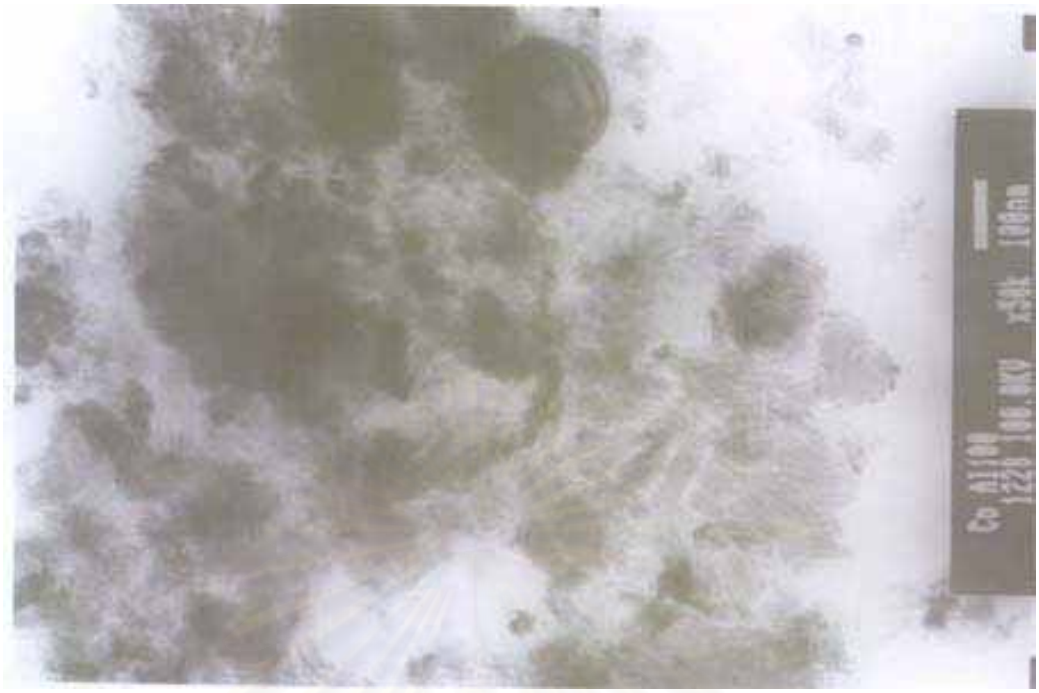

Figure 5.30 TEM micrograph of Co/Al-100-Zr-0(M)

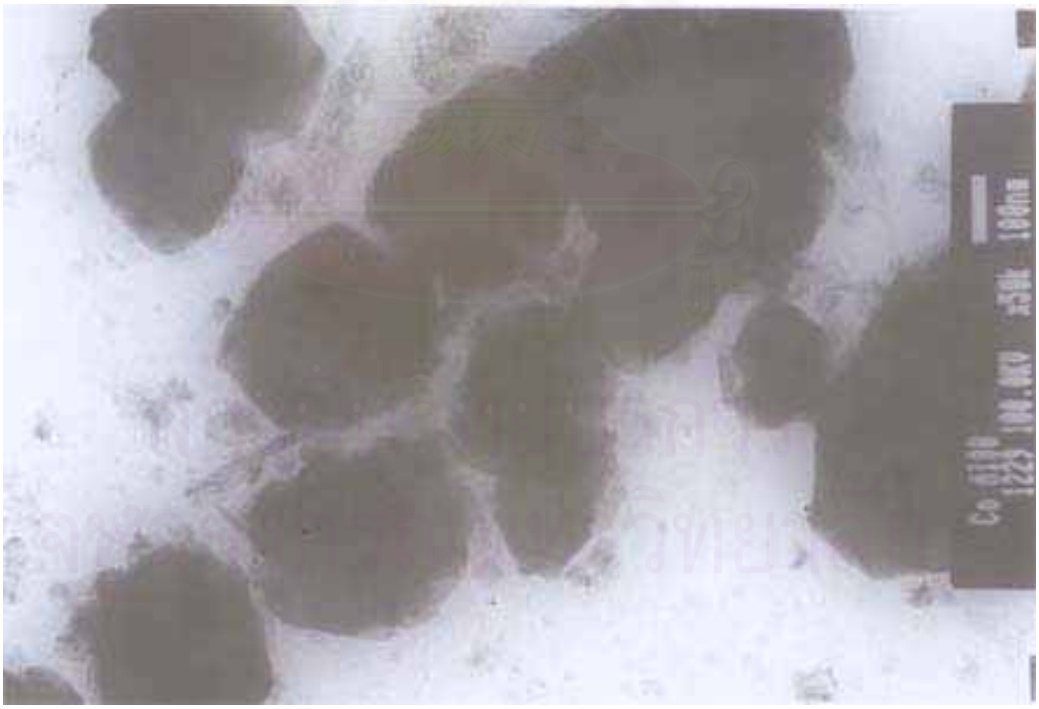

Figure 5.31 TEM micrograph of Co/Al-100-Zr-0(M)

Figure 5.32 TEM micrograph of Co/Al-100-Zr-0(M)

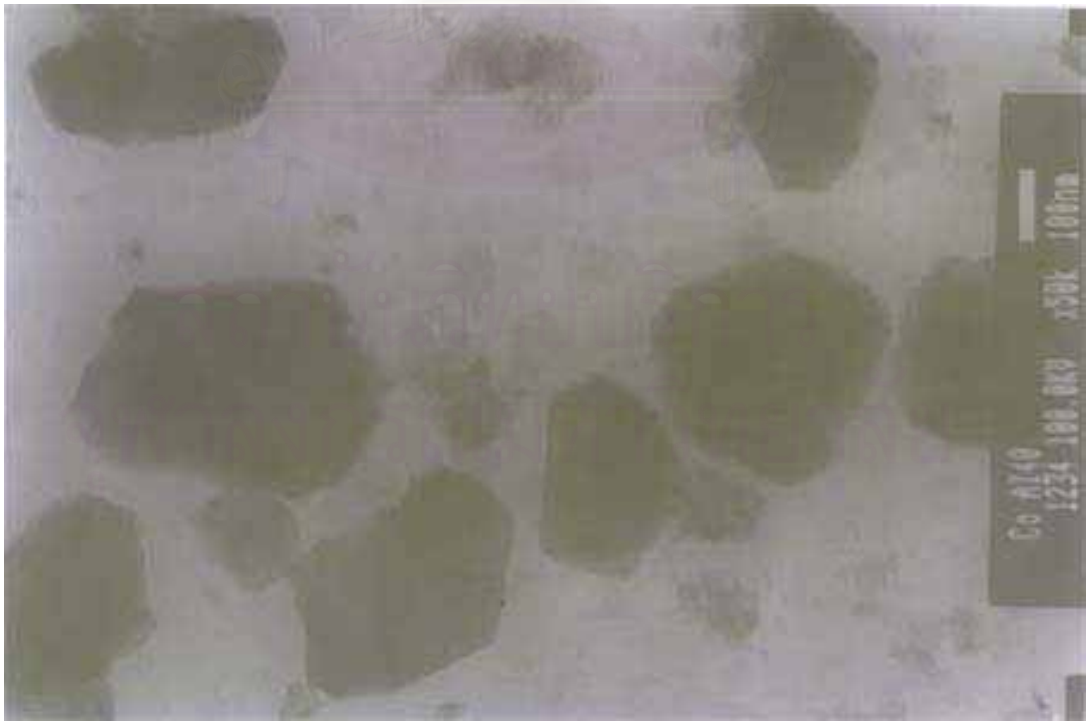

Figure 5.33 TEM micrograph of Co/Al-100-Zr-0(M)

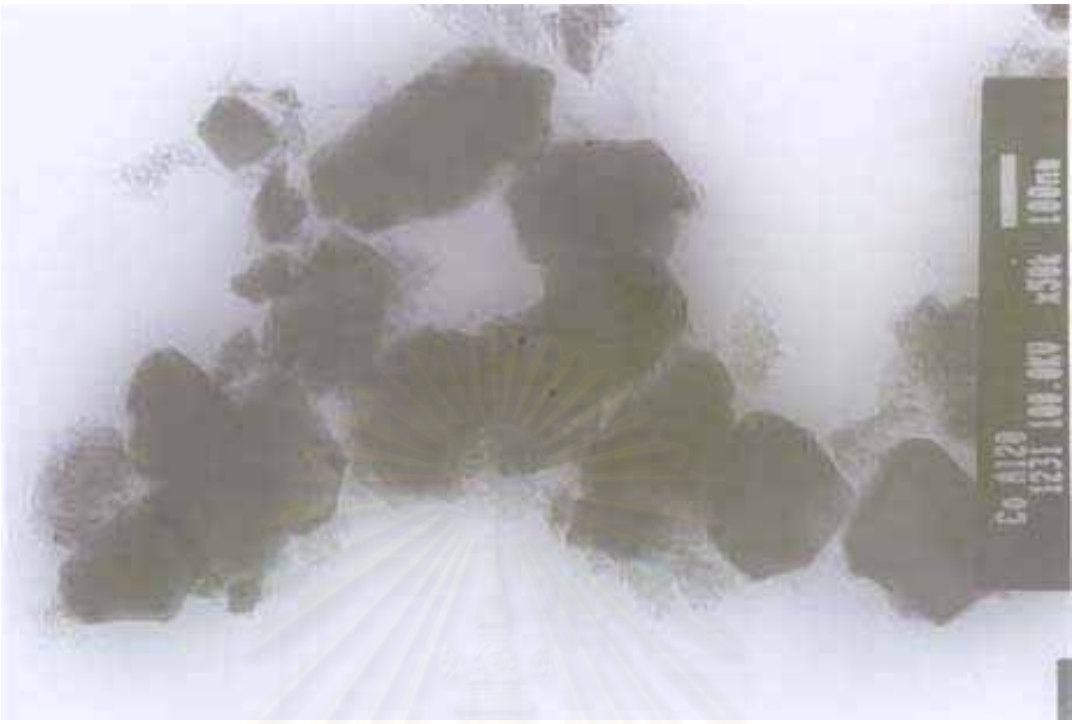

Figure 5.34 TEM micrograph of Co/Al-100-Zr-0(M)

Figure 5.35 TEM micrograph of Co/Al-100-Zr-0(M)

5.2.5 Temperature Programmed Reduction (TPR)

TPR profiles of the Co catalysts on the various micron supports are shown in Figures 5.36. There were two major reduction peaks located at ca. 300-450°C and 600-660°C for the micronscale Al_2O_3 and Al_2O_3-ZrO_2 supports. These peaks were related to the following step: Co_3O_4 to CoO, CoO to Co metal, and Co_XO_Y-support to Co metal, where Co_XO_Y-support was represented the Co oxide species strongly interacted with the support. However, there was only one reduction peak (ca. 320-420°C) for Co oxide species dispersed on the micron ZrO_2. In some cases, the peak of the decomposition of cobalt nitrates (as the precursor) during TPR of supported Co catalysts can be observed at temperatures between 200° to 300°C, especially with silica and alumina supports [8-9]. Prolonged calcination or reduction and recalcination resulted in completed decomposition of any cobalt nitrates present [9]. However, there was no observation of the decomposition peak of cobalt nitrate in this present study.

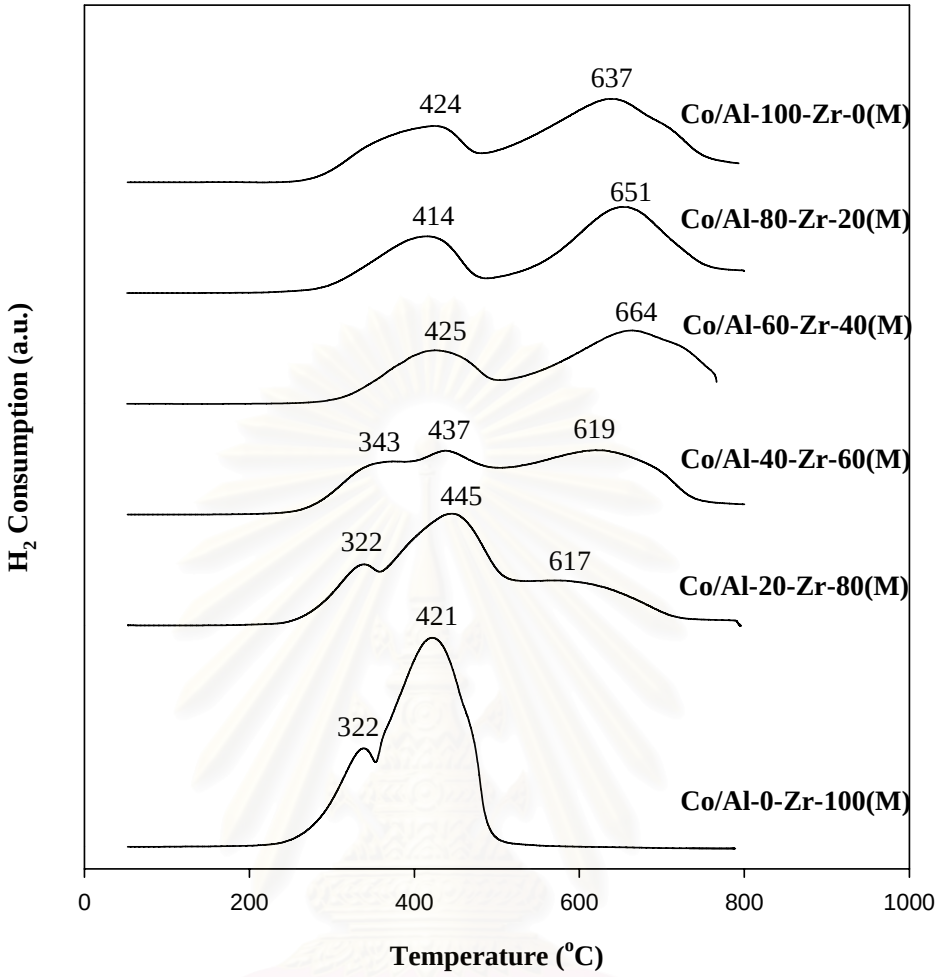

Figure 5.36 TPR profiles of cobalt oxide species dispersed on various mixed micron-Al_2O_3-ZrO_2 supports

Considering the TPR profiles of Co oxide species dispersed on the nanoscale supports as shown in Figure 5.18, there was only one major reduction peak located at ca. 440 to 460°C. Again this peak was also related to the reduction of Co_3O_4 to CoO, CoO to Co metal, and Co_XO_Y-support to Co metal as mentioned before. It should be noted that with using the nanoscale support, the interaction of Co oxide species was more homogeneous leading to only one reduction peak observed. In order to give a better understanding, the suggested reduction behaviors of Co oxide species on different micron- and nanoscale supports are shown in Figure 5.38.

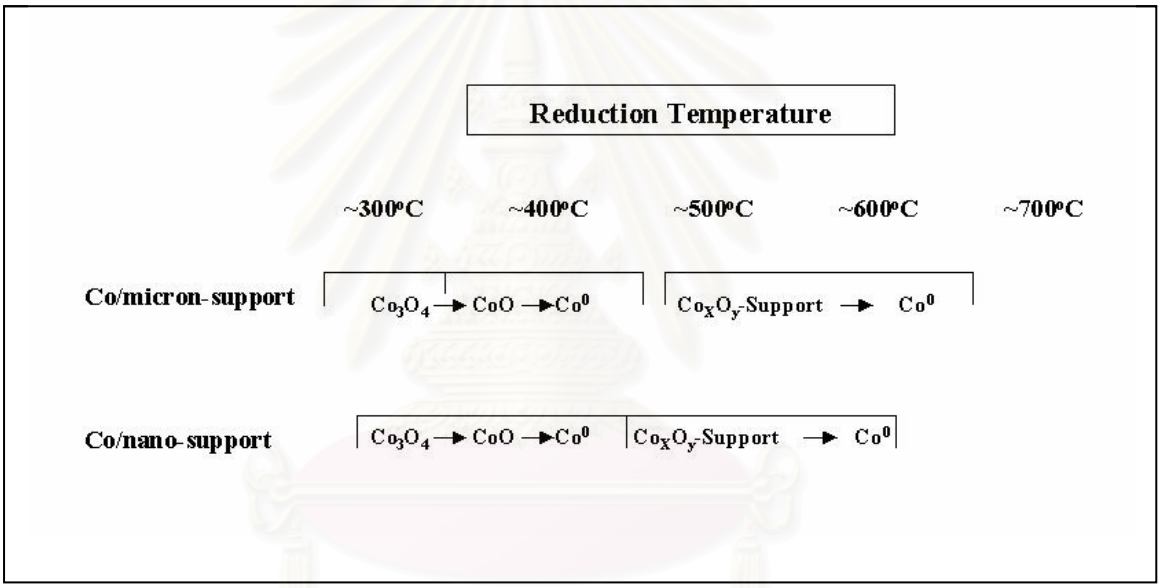

Figure 5.38 Suggested reduction behavior of Co catalysts on micron- and nanoscale Al_2O_3-ZrO_2 supports

5.3 Comparative study of cobalt catalysts supported on micron- and nanoscale mixed Al_2O_3-ZrO_2 in CO hydrogenation reaction.

CO hydrogenation was performed to measure the overall activity of the catalyst samples on various micron- and nanoscale mixed supports. The reaction rate and product selectivity during CO hydrogenation at steady-state are revealed in Table 5.1. For the Co catalysts on the pure micron- and nanoscale Al_2O_3, it can be observed that they exhibited the similar activity without any changes in the product selectivity. However, when the micronscale Al_2O_3 and ZrO_2 support were mixed, the catalytic performance of Co was identical with that of the sole micronscale Al_2O_3. It was suggested that the effect of Al_2O_3 was predominant compared to ZrO_2 regarding the micronscale supports. Differently, it can be also observed that with the use of nanoscale mixed supports, the activities decreased with the presence of ZrO_2. However, the selectivity of C_2-C_4 was found to increase with ZrO_2 present. Considering when the pure ZrO_2 support was used, the result was essentially different. It indicated that the catalyst on the nanoscale ZrO_2 exhibited higher activity than that on the micronscale ZrO_2 support. In addition, the selectivity to C_2-C_4 was slightly higher with the ZrO_2 support. These results based on the ZrO_2 support used were in accordance with those reported by Panpranot et al. [21]. The increased activity for the nanoscale ZrO_2 support can be attributed to the larger number of reduced Co metal surface atom [21]. In order to better understand effect of various micron- and nanoscale supports on the catalyst performance, the summarized results are illustrated in Table 5.2. Since CO hydrogenation is a structure insensitive reaction, thus, the catalytic activity depends only on the number of reduced Co metal surface atoms available for catalyzing the reaction. In particular, differences in the catalytic performance based on using the micron- and nanoscale Al_2O_3 and ZrO_2 supports can

be described by the reduction behaviors of the catalysts on various supports. TPR peak locations are affected by reduction kinetics. A wide range of variables including particle size, support interaction and the reduction gas composition [8] can affect the kinetics of reduction. The effects of particle size and support interaction can be superimposed on each other. Thus, while a decrease in metal oxide particle size can result in faster reduction due to a greater surface area/volume ratio, smaller particles may interact more with the support, slowing reduction. Based on the resulted activities, it can be concluded that no effect of support interaction and particle size was observed for the Al_2O_3 support. Conversely, for the Co oxide species on the ZrO_2 with weak interaction between the catalysts, the nanoscale ZrO_2 support gave higher activity of the catalyst than the micronscale one. This indicates that besides the support interaction and particle size, the nature of different supports is also the key to determine the catalytic performance.

Table 5.1 Reaction rates and product selectivity of samples during CO hydrogenation at steady-state

Sample	**Rate (x 10^2 gCH_2/g cat.h)**	**Product Selectivity (%)**		
		C_1	**C_2-C_3**	**C_4**
Co/Al-100-Zr-0(M)	36.12	99.3	0.7	-
Co/Al-80-Zr-20(M)	36.37	99.1	0.9	-
Co/Al-60-Zr-40(M)	35.56	99.5	0.5	-
Co/Al-40-Zr-60(M)	36.81	99.7	0.3	-
Co/Al-20-Zr-80(M)	35.81	99.5	0.5	-
Co/Al-0-Zr-100(M)	5.6	95.9	4.0	0.1
Co/Al-100-Zr-0(N)	37.50	99.4	0.6	-
Co/Al-80-Zr-20(N)	35.64	99.1	0.9	-
Co/Al-60-Zr-40(N)	20.30	90.8	6.5	2.7
Co/Al-40-Zr-60(N)	20.81	90.4	6.8	2.8
Co/Al-20-Zr-80(N)	19.09	91.4	5.4	3.2
Co/Al-0-Zr-100(N)	34.15	95.6	3.2	1.2

Table 5.2 Summarized results on effect of various micron- and nanoscale supports for the Co catalyst during CO hydrogenation

Catalyst Performance*	**Supports**					
	Al_2O_3		**Mixed Al_2O_3-ZrO_2**		**ZrO_2**	
	M	**N**	**M**	**N**	**M**	**N**
Activity	**0**	**0**	**0**	**-**	**-**	**0**
Selectivity to C_2-C_4	**0**	**0**	**0**	**+**	**+**	**+**

* Based on Al_2O_3 (both M, N)
+ = Positive effect
- = Negative effect
0 = No effect

CHAPTER VI

CONCLUSIONS AND RECOMMENDATIONS

6.1 Conclusions

Based on the present study, it can be concluded as follows:

1. The size of Co oxide species dispersed on a support was corresponding to the size of the support used.
2. Besides the support interaction and particle size, the nature of supports used was also the key to determine the number of active sites present.
3. For the Al_2O_3 support, the catalyst dispersed on both micron- and nanoscale Al_2O_3 exhibited similar activities and selectivity during CO hydrogenation.
4. For the ZrO_2 support, the catalyst dispersed on the nanoscale ZrO_2 was more active due to the weak interaction between ZrO_2 and the catalyst. Hence, the smaller particle can be reduced more easily.
5. Use of mixed micronscale Al_2O_3-ZrO_2 supports apparently resulted in similar properties with the sole micronscale Al_2O_3 support. However, when mixed nanoscale Al_2O_3-ZrO_2 supports were applied, it showed that the presence of nano-ZrO_2 resulted in decreased activities, but somehow increased selectivities to C_2-C_4.

6.2 Recommendations

1. In order investigation on different interaction, the amounts of Co loading should be varied
2. Besides Co metal, other metals such as Ni, Pd, Fe and etc. should be further investigated with various supports.

REFERENCES

1 Martinez, A.; Lopez, C.; Marquez, F.; Diaz, I. Fischer-Tropsch Synthesis of Hydrocarbons over Mesoporous Co/SBA-15 Catalysts: the Influence of Metal Loading, Cobalt Precursor, and Promoters. J. Catal. 200 (2003): 486.

2 Panpranot, J.; Goodwin, J.G., Jr.; Sayari, A. Synthesis and Characteristics of MCM-41 Supported Ru Catalysts. Catal. Today 77 (2002): 269.

3 Panpranot, J.; Goodwin, J.G., Jr.; Sayari, A. CO Hydrogenation on Ru-Promoted Co/MCM-41 Catalysts. J. Catal. 211 (2002): 530.

4 Sun, S.L.; Tsubaki, N.; Fujimoto, K. The Reaction Performances and Characteristics of Fischer-Tropsch Synthesis Co/SiO_2 Catalysts Prepared from Mixed Cobalt Salts. Appl. Catal. A. 202 (2000): 121.

5 Jongsomjit, B.; Panpranot, J; Goodwin, J.G., Jr. Effect of Zirconia-Modified Alumina on the Properties of Co/γ-Al_2O_3 Catalysts. J. Catal. 215 (2003): 66.

6 Das, T.; Jacobs, G.; Patterson, P.M.; Conner, W.A.; Li, J.L.; Davis, B.H. Fischer-Tropsch Synthesis: Characterization and Catalytic Properties of Rhenium Promoted Cobalt Alumina Catalysts. Fuel. 82 (2003): 805.

7 Jacobs, G.;Patterson, P.M.; Zhang, Y.Q.; Das, T.; Li, J.L; Davis, B.H. Fischer-Tropsch Synthesis: Deactivation of Noble Metal-Promoted Co/Al2O3 Catalysts. Appl. Catal. A. 233 (2002): 215.

8 Jongsomjit, B.; Goodwin, J.G., Jr. Co-Support Compound Formation in Co/Al2O3 Catalyst: Effect of Reduction Gas Containing CO. Catal. Today 77 (2002): 191.

9 Jongsomjit, B.; Panpranot, J.; Goodwin, J.G., Jr. Co-Support Compound Formation in Alumina-Supported Cobalt Catalyst. J. Catal. 204 (2001): 98.

10 Li, J.L.; Jacobs, G.; Das, T.; Davis, B.H. Fischer-Tropsch Synthesis: Effect of Water on the Catalytic Properties of a Rhuthenium Promoted Co/TiO2 Catalysts. Appl. Catal. A. 233 (2002): 255.

11 Jacobs, G.; Das, T.; Zhang, Y.Q.; Li, J.L.; Racoillet, G.; Davis, B.H. Fischer-Tropsch Synthesis: Loading and Promoter Effects on the Reducibility of Cobalt Catalysts. Appl. Catal. A. 233 (2002): 263.

12 Li, J.L.; Xu, L.G.; Keogh, R.; Davis, B.H. Fischer-Tropsch Synthesis: Effect of CO Pretreatment on a Ruthenium Promoted Co/TiO_2. Catal. Lett. 70 (2000): 127.

13 Jongsomjit, B.; Sakdamnuson, C.; Goodwin, J.G., Jr.; Praserthdam, P. Co-Support Compound Formation in Titania-Supported Cobalt Catalysts. Catal. Lett. 94 (2004): 209.

14 Jongsomjit, B.; Wongsalee, T.; Praserthdam, P. Study of Cobalt Dispersion on Titania Consisting Various Rutile:Anatase Ratios. Mater. Chem. Phys. 92 (2005): 572.

15 Jongsomjit, B.; Wongsalee, T.; Praserthdam, P. Characteristics and Catalytic Properties of Co/TiO2 for Various Rutile:Anatase Ratios. Catal. Comm. 6 (2005): 705.

16 Panpranot, J.; Taochaiyaphum, N.; Praserthdam, P. Glycothermal Synthesis of Nanocrystalline Zirconia and Their Application as Cobalt Catalyst Support. Mater. Chem. Phys. 94 (2005): 207.

17 Li, X.H.; Asami, K.; Luo, M.F.; Michiki, K.; Tsubaki, N.; Fujimoto, K. Direct Synthesis of Middle iso-Parafins from Synthesis Gas. Catal. Today. 84 (2003): 59.

18 Jongsomjit, B.; Ngamposri, S.; Praserthdam, P.; Role of titania in TiO_2– SiO_2 mixed oxides-supported metallocene catalyst during ethylene/1-octene copolymerization. Catal. Lett. 100 (2005): 139.

19 Jongsomjit, B.; Ngamposri, S.; Praserthdam, P.; Catalytic activity during copolymerization of ethylene and 1-hexene via mixed TiO_2/SiO_2-supported MAO with rac-Et[Ind] $2ZrCl_2$ metallocene catalyst Molecules 10 (2005): 672.

20 Jongsomjit, B.; Ngamposri, S.; Praserthdam, P.; Application of silica/titania mixed oxide-supported zirconocene catalyst for synthesis of linesr low-density polyethylene. Ind. Eng. Chem. Res. 44 (2005): 9059.

21 Panpranot, J.; Taochaiyaphum, N.; Praserthdam, P. Differences in characteristic and catalytic properties of Co catalysts supported on micron-and nano-sized zirconai. Catal. Comm. 7 (2006): 192.

22 Farrauto, R. J.; and Bartholomew, C. H.. Fundamentals of Industrial Catalytic Processes (1997).

23 Young, R.S. COBALT: Its Chemistry, Metallurgy, and Uses. New York: Reinhpld Publishing Corporation, 1960.

24 Othmer, K. Encyclopedia of chemical technology. Vol. 6. 4 th ed. New York: A Wiley-Interscience Publication, John Wiley&Son, 1991.

25 Kronberg M.L., Plastic deformation of Single crystals of sapphire. Acta Materialia. 5 (1957): 507-524.

26 Lippens, B. D. and J. H. De. Boer ., Study of phase transformations during calcination of aluminum hydroxides by selected area electron diffraction. Acta Crystallography. 17 (1964) :1312.

27 Wilson, S. J., Phase transformations and development of microstructure in-derived transition aluminas. Proceedings of the British Ceramic Society. 28 (1979) : 281-94.

28 Gitzen W.H., Alumina as a ceramic material. 1970.

29 Inoue, M., Kominami, H., and Inui, T., Novel Synthesis Method for The Catalytic Use of Thermally Stable Zirconia: Thermal Decomposition of Zirconium Alkoxide in Organic Media. Applied Catalyst. A 77 *(*1993): 25.

30 Gavalas, G. R.; Phichitkul, C.; and Voecks, G. E. Structure and activity of NiO alpha-Al_2O_3 and NiO/ZrO_2 calcined at high-temperatures.1. structure. J. Catal. 88 (1984): 54-64.

31 Tani, E.; Yoshimura, M.; and Somiya, S. Formation of Ultrafine tetragonal ZrO_2 powder under hydrothermal conditions. J. Am. Ceram. Soc. 66 (1982): 11-14.

32 Osendi, M. I.; et al. Metastability of tetragonal zirconia powders. J. Am. Ceram. Soc. 68 (1985): 135-39.

33 Livage, J.; Doi, K.; and Mazieres, C. Nature and thermal evolution of amorphous hydrated zirconium oxide. J. Am. Ceram. Soc. 51 (1968): 349-53.

34 West, A. R.; Solid State Chemistry and its Application, John Wiley&Sons, Brisbane, (1997): 232.

35 Heuer, A. H. Transformation Toughening in ZrO_2-containing Ceramics. J. Am. Ceram. Soc. 70 (1987): 689-98.

36 Rafeh Bechara, david, dominique, Appl. Catal. A: General. 207 (2001): 343-53.

37 Zhang, J.; Chen, J.; Ren, J.; Li, Y.; Sun, Y.; Support effect of Co/Al_2O_3 catalysts for Fischer-Tropsch synthesis. Fuel.82 (2003): 581-86

38 Haifeng, X.; Yuhua, Z.; Kongyong, L.; Catalytic performance of zirconium-modified Co/Al_2O_3 for Fischer-Tropsch synthesis. J. Mol. Catal. A: Chemical. 231, 145-151 (2005).

39 Kraum, M.; and Baerns, M. Fischer–Tropsch synthesis: the influence of various cobalt compounds applied in the preparation of supported cobalt catalysts on their performance. App. Catal. 186 (1999): 189-200.

40 Maruya, K.; et al. Active sites on ZrO for the formation of isobutene from 2CO and H_2. J. of Mol. Catal. A: Chemical 159 (2000): 97-102.

41 Enache, D. I.; et al. In SituXRD Study of the Influence of Thermal Treatment on the Characteristics and the Catalytic Properties of Cobalt-Based Fischer-Tropsch Catalysts. J. Catal. 205, (2002): 346-353.

42 Enache, D. I.; et al. Differences in the characteristics and catalytic properties of cobalt-based Fischer–Tropsch catalysts supported on zirconia and alumina. Appl. Catal. A: General 268 (2004): 51-60.

43 Shinoda, M.; et al. New bimodal pore catalysts for Fischer–Tropsch synthesis. Fuel Pro. Tech.(2004).

44 Rohra, F.; et al. Fischer–Tropsch synthesis over cobalt catalysts supported on zirconia-modified alumina. Catal. Today 58 (2000): 247-254.

45 Reuel, R. C.; and Bartholomew, C. H. The Stoichiometries of H_2 and CO Adsorption on cobalt : Effect of Support and Preparation. J. Catal. 85 (1984): 63-77.

46 Choi,. J.G. Reduction of supports cobalt catalysts by hydrogen. Catal Lett.35 (1995): 291-296.

47 Jacobs, G.; et al. Fischer–Tropsch synthesis: support, loading, and promoter effects on the reducibility of cobalt catalysts. Appl. Catal. A: General 233 (2002): 263-281.

48 Vob, M.; Borgmann, D.; Wedler, G. Characterizaton of alumina, silica, and titania supported cobalt catalysts. J Catal. 212 (2002): 10-21.

APPENDICES

APPENDIX A

CALCULATION FOR CATALYST PREPARATION

Preparation of 20%Co/Al_2O_3-ZrO_2 catalysts by the incipient wetness impregnation method are shown as follows:

Reagent: - Cobalt (II) nitrate hexahydrate [$Co(NO_3)_2 \cdot 6H_2O$]

Molecular weight = 291.03 g

- Nano-γ-Al_2O_3 support
- Nano-ZrO_2 support
- Micron-Al_2O_3 support
- Micron-ZrO_2 support

Example Calculation for the preparation of catalyst 20% Co/Al-0-Zr-100

Based on 100 g of catalyst used, the composition of the catalyst will be as follows:

Cobalt = 20 g

ZrO_2 = 100-20 = 80 g

For 1 g of catalyst

Cobalt required = 1×(20/100) = 0.2 g

Cobalt 0.2 g was prepared from $Co(NO_3)_2 \cdot 6H_2O$ and molecular weight of Co is 58.93

$$\text{the } Co(NO_3)_2 \cdot 6H_2O \text{ content} = \frac{\text{MW of } Co(NO_3)_2 \cdot 6H_2O \times \text{cobalt required}}{\text{MW of Co}}$$

$$= (291.03/58.93)\times 0.2 = 0.99 \text{ g}$$

Since the pore volume of the pure zirconia support is 0.402 ml/g for ZrO_2. Thus, the total volume of impregnation solution which must be used is 0.803 ml for ZrO_2 by the requirement of incipient wetness impregnation method, the de-ionised water is added until equal pore volume for dissolve Cobalt (II) nitrate hexahydrate.

APPENDIX B

CALCULATION FOR TOTAL H_2 CHEMISORPTION

Calculation of the total H_2 chemisorption of the catalyst, a stoischiometry of H/Co = 1, measured by H_2 chemisorption is as follows:

Let the weight of catalyst used	=	W	g
Integral area of H_2 peak after adsorption	=	A	unit
Integral area of 45 μl of standard H_2 peak	=	B	unit
Amounts of H_2 adsorbed on catalyst	=	B-A	unit
Concentration of Co (by AAS)	=	C	% wt
% reducibility (TPR)	=	D	%
Volume of H_2 adsorbed on catalyst	=	45×[(B-A)/B]	μl
Volume of 1 mole of H_2 at 100°C	=	28.038	μl
Mole of H_2 adsorbed on catalyst	=	[(B-A)/B]×[45/28.038]	μmole

Total hydrogen chemisorption = [(B-A)/B]×[45/28.038]×[1/W] μmole /g of catalyst

= N μmole /g of catalyst

APPENDIX C

CALIBRATION CURVES

This appendix shows the calibration curves for calculation of composition of reactant and products in CO hydrogenation reaction. The reactant is CO and the main product is methane. The other products are linear hydrocarbons of heavier molecular weight that are C_2-C_4 such as ethane, ethylene, propane, propylene and butane.

The thermal conductivity detector, gas chromatography Shimadzu model 8A was used to analyze the concentration of CO by using Molrcular sieve 5A column. The chromatograms of catalyst sample are shown in Figure C.1.

The VZ10 column are used with a gas chromatography equipped with a flame ionization detector, Shimadzu model 14B, to analyze the concentration of products including of methane, ethane, ethylene, propane, propylene and butane. The chromatograms of catalyst sample are shown in Figure C.2.

Mol of reagent in y-axis and area reported by gas chromatography in x-axis are shown in the curves. The calibration curves of CO, methane, ethane, ethylene, propane, propylene and butane are illustrated in the following figures.

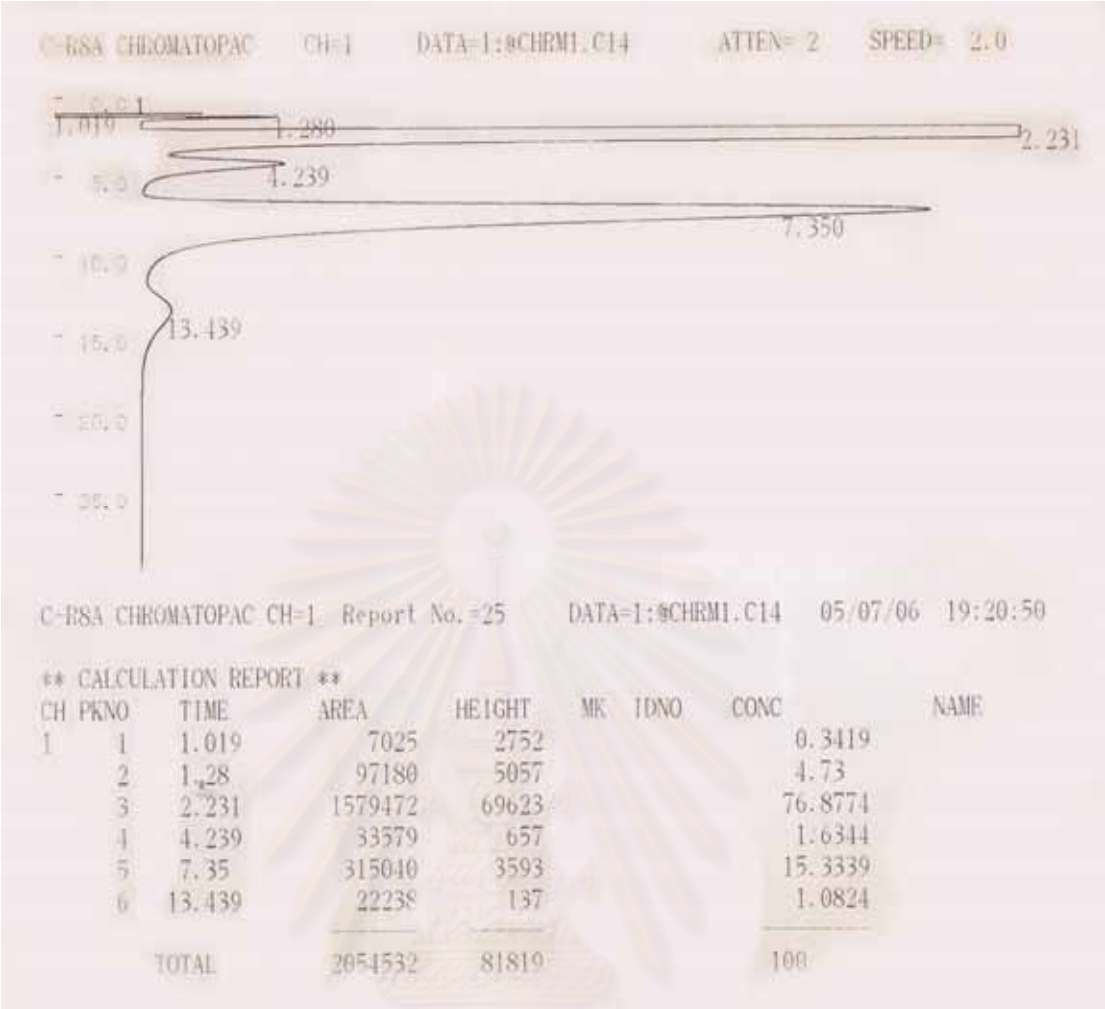

Figure C.1 The chromatograms of catalyst sample from thermal conductivity detector, gas chromatography Shimadzu model 8A (Molecular sieve 5A column).

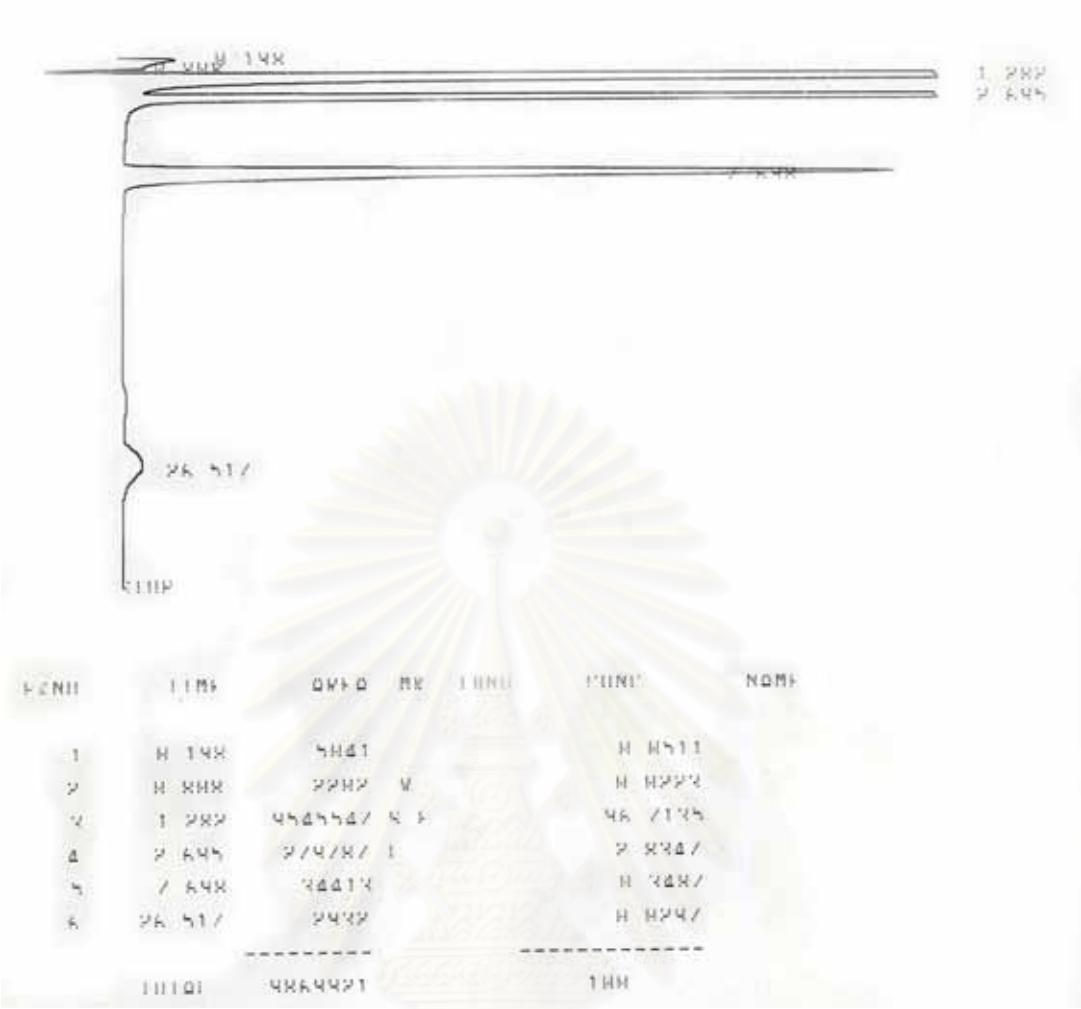

Figure C.2 The chromatograms of catalyst sample from flame ionization detector, gas chromatography Shimadzu modal 14B (VZ10 column).

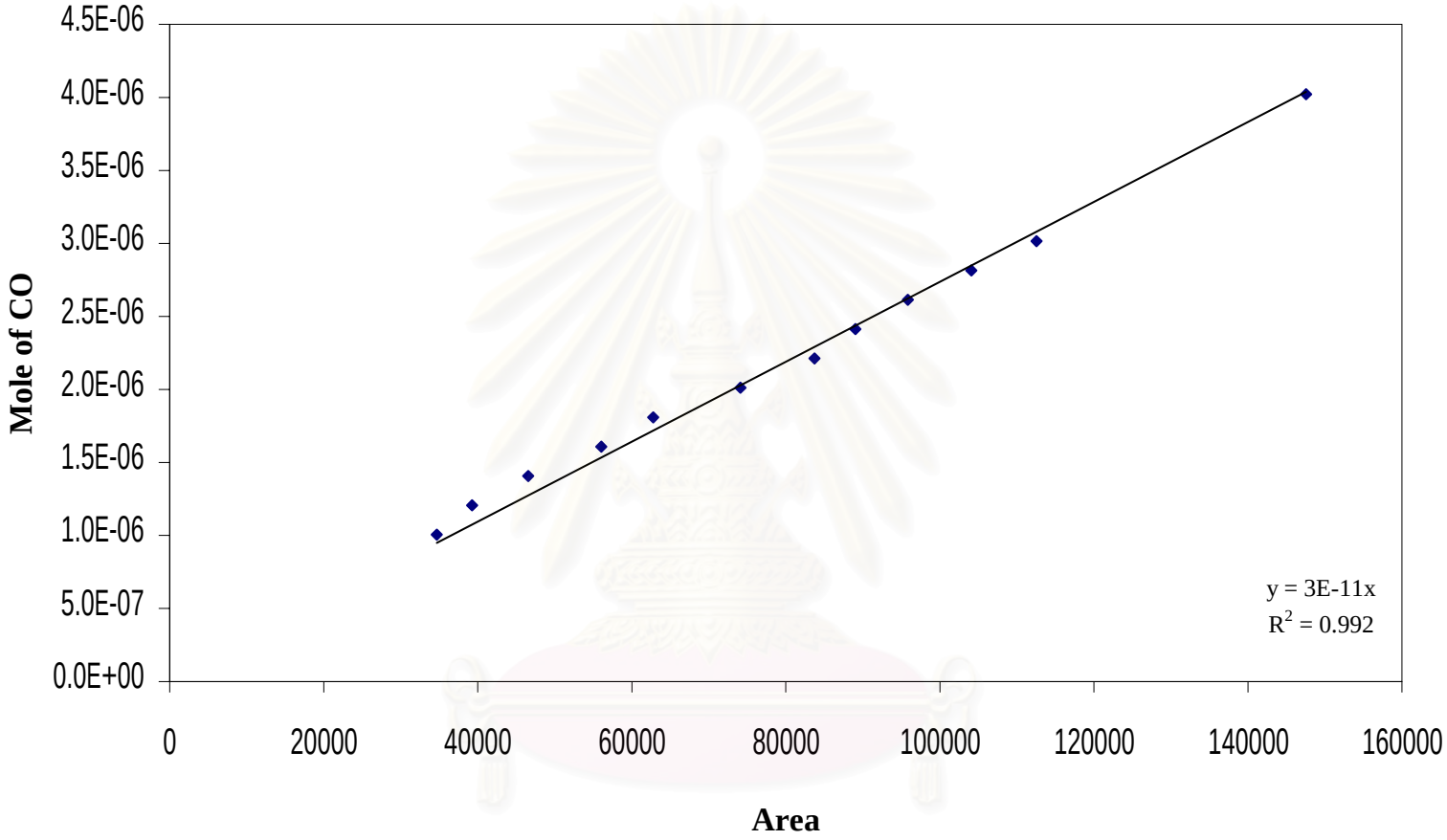

Figure C.3 Calibration curve of CO

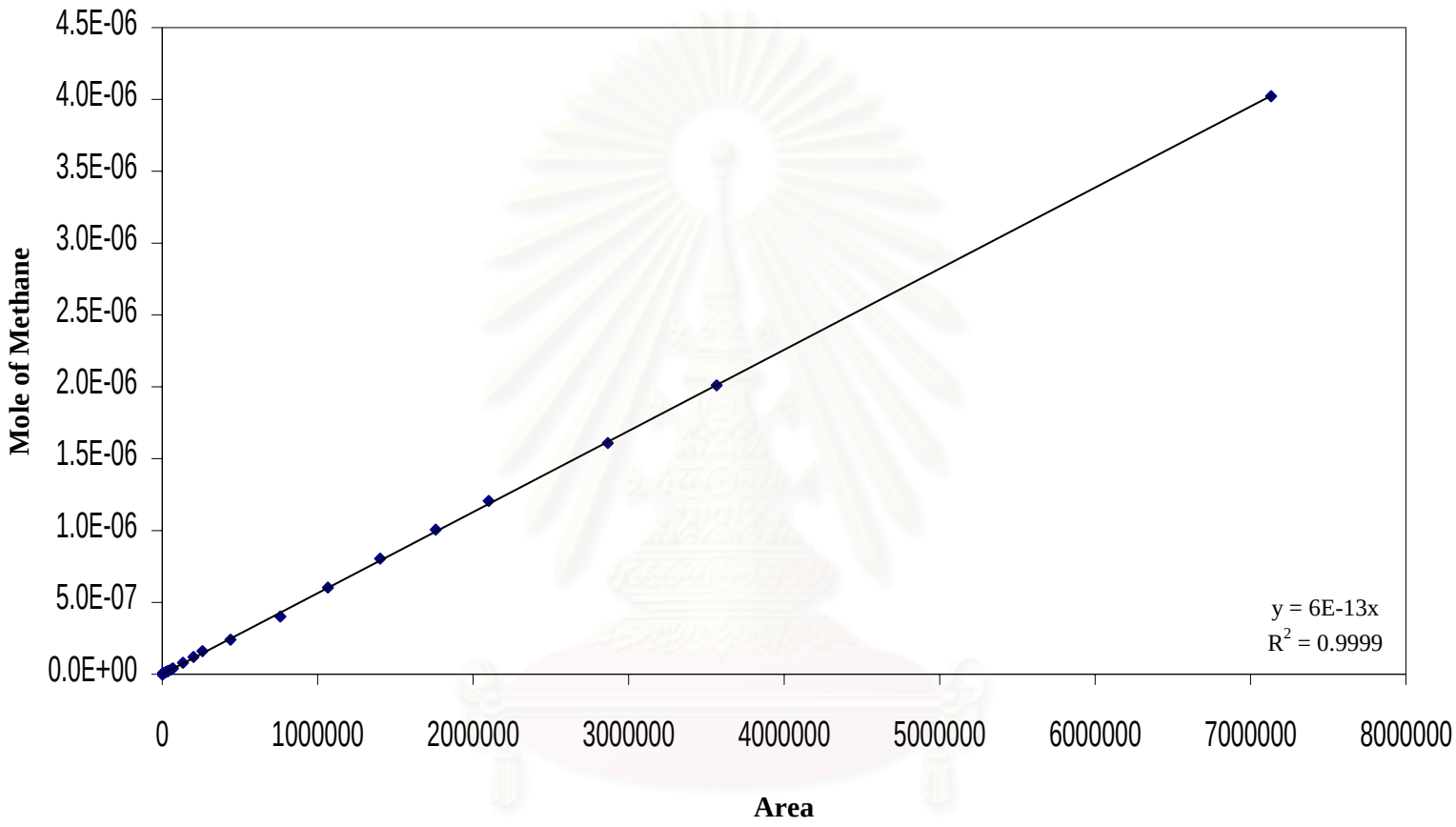

Figure C.4 Calibration curve of methane

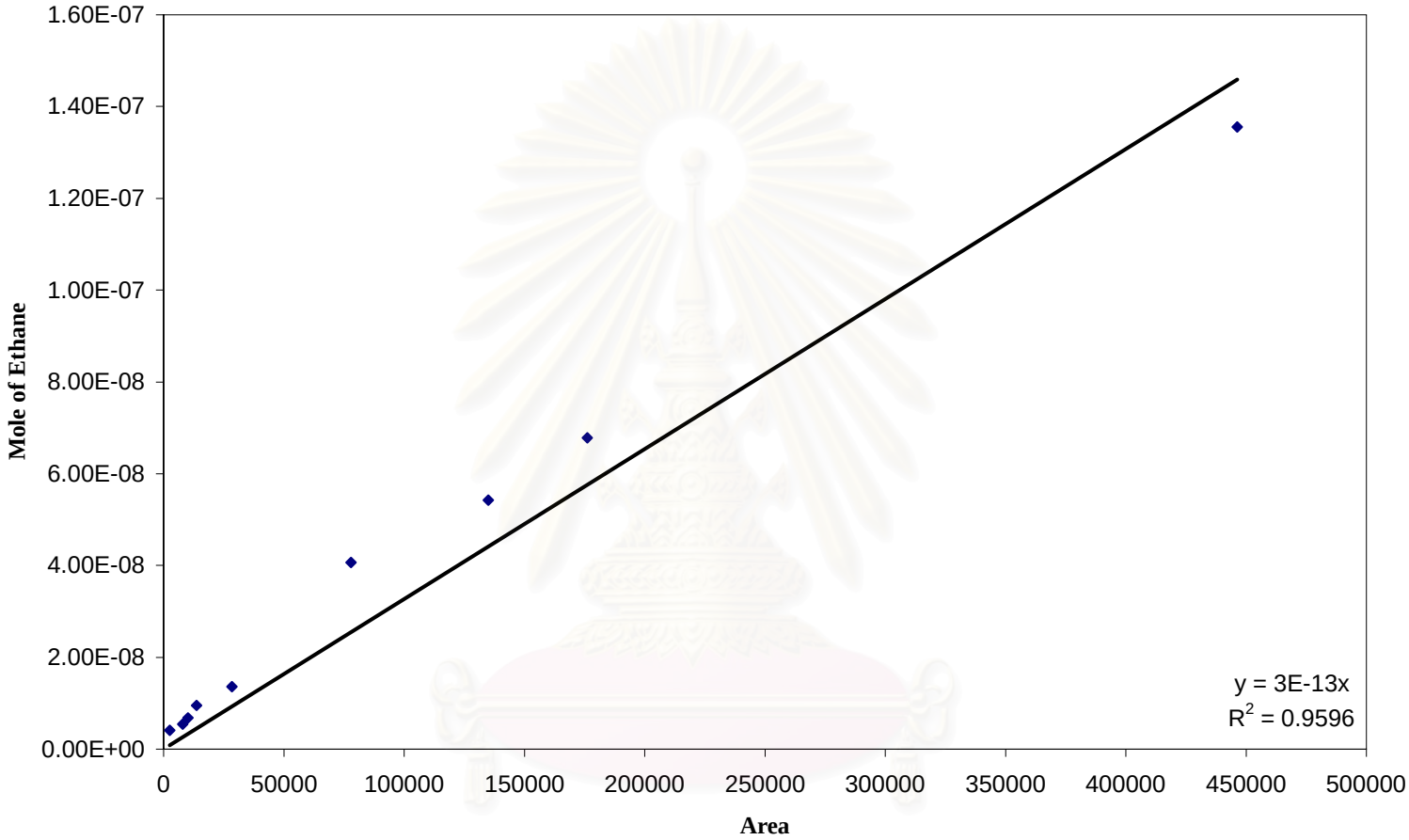

Figure C.5 Calibration curve of ethane

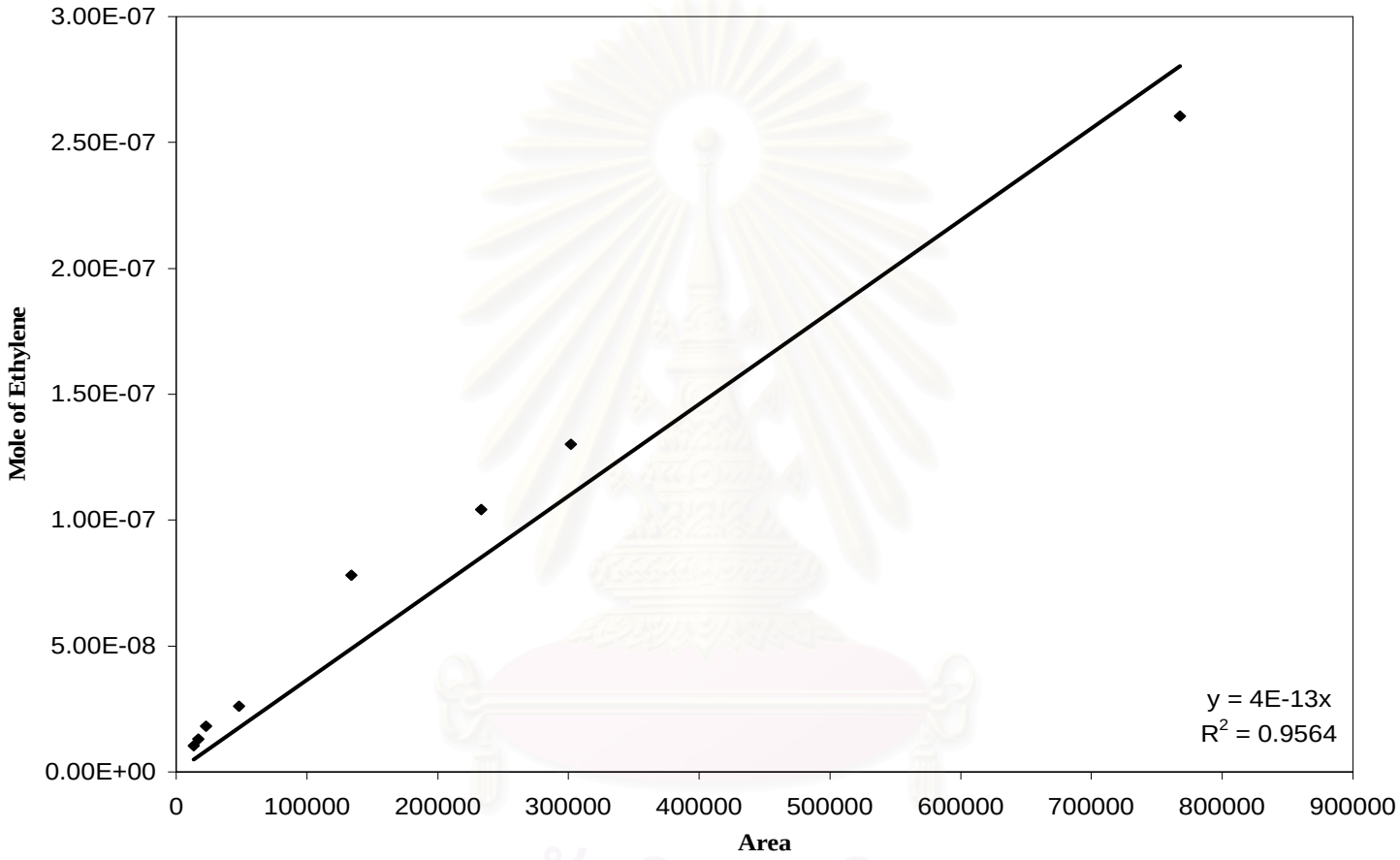

Figure C.6 Calibration curve of ethylene

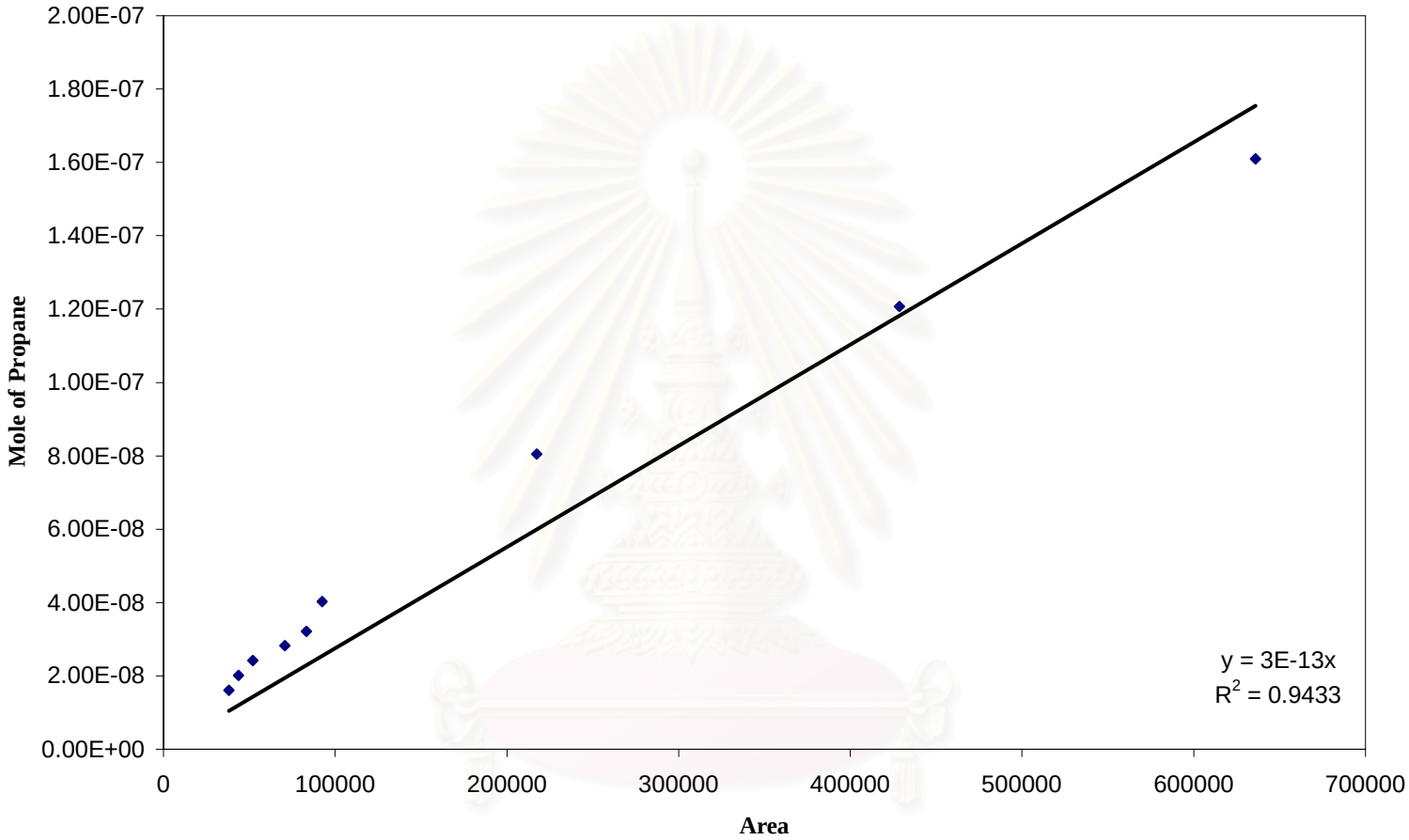

Figure C.7 Calibration curve of propane

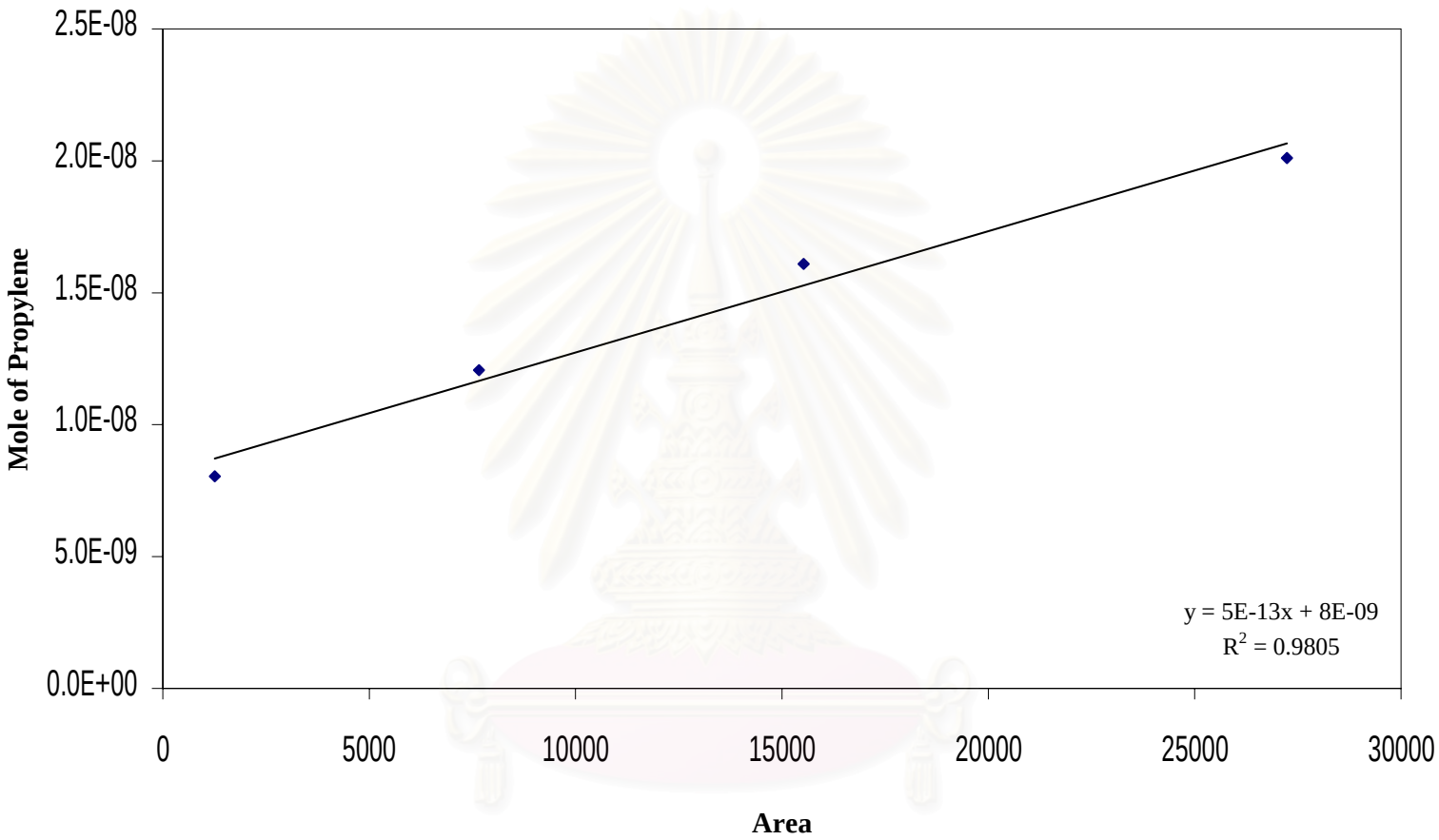

Figure C.8 Calibration curve of propylene

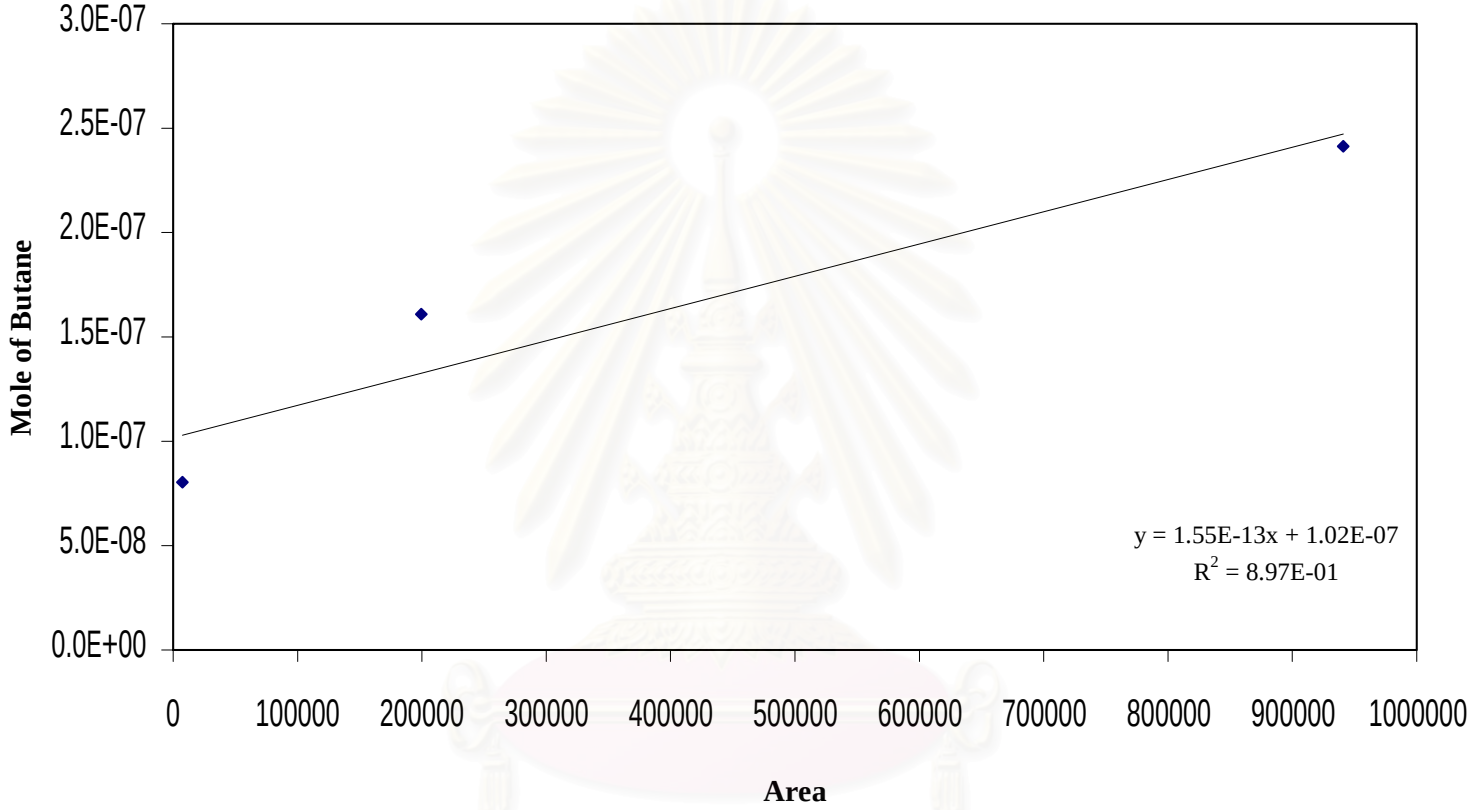

Figure C.9 Calibration curve of butane

APPENDIX D

CALCULATION OF CO CONVERSION, REACTION RATE AND SELECTIVITY

The catalyst performance for the CO hydrogenation was evaluated in terms of activity for CO conversion reaction rate and selectivity.

Activity of the catalyst performed in term of carbon monoxide conversion and reaction rate. Carbon monoxide conversion is defined as moles of CO converted with respect to CO in feed:

$$\text{CO conversion (\%)} = \frac{100 \times [\text{mole of CO in feed} - \text{mole of CO in product}]}{\text{mole of CO in feed}} \quad \text{(i)}$$

where mole of CO in feed can be measured employing the calibration curve of CO in Figure C.1, Appendix C., i.e.,

mole of CO in feed = (area of CO peak from integrator plot on GC-8A)× 3× 10^{-11}

mole of CO in product = mole of C(balance) in product from GC-14B

Reaction rate was calculated from CO conversion that is as follows:

Let the weight of catalyst used	=	W	g
Flow rate of CO	=	4	ml/min
Reaction time	=	60	min
Weight of CH_2	=	14	g
Volume of 1 mole of gas at 1 atm	=	22400	ml
Concentration of Co (by AAS)	=	C	% wt

$$\text{Reaction rate (g } CH_2\text{/g of catalyst/h)} = \frac{[\text{\% conversion of CO}/100]\times 60\times 14\times 4}{W\times 22400} \quad \text{(ii)}$$

$$= A \quad \text{(g } CH_2\text{/g of catalyst/h)}$$

Selectivity of product is defined as mole of product (B) form with respect to mole of CO converted:

Selectivity of B (%) = 100 × [mole of B form/mole of CO converted] (iii)

Where B is product, mole of B can be measured employing the calibration curve of products such as methane, ethane, ethylene, propane, propylene and butane

mole of CH_4 = (area of CH_4 peak from integrator plot on GC-14B)× 6×10^{-13} (v)

APPENDIX E

LIST OF PUBLICATION

1. Tanuchnun Burakorn, Bunjerd Jongsomjit, and Piyasan Praserthdam, "Properties of Cobalt Oxide Specice Dispersed on the Nano Al_2O_3-ZrO_2 Mixed Oxide supports", Proceedings of the Thai Institute of Chemical Engineering and Applied Chemical Conference 15th, Chonburi, Thailand, Oct., 27-28, 2005, Ref. No. NA-14.
2. Tanuchnun Burakorn, Bunjerd Jongsomjit, and Piyasan Praserthdam, "Physicochemical Properties of Cobalt Dispersed on the Mixed Nano-Al_2O_3-ZrO_2 Supports", Submitted to Industrial of Engineering Chemistry Research, Nov., 2005
3. Tanuchnun Burakorn, Bunjerd Jongsomjit, and Piyasan Praserthdam, "A Comparative Study on Physicochemical Properties of Cobalt Oxide Species Dispersion on Micron- and Nanoscale Mixed Al_2O_3-ZrO_2 Supports", Submitted to The Journal of Physical Chemistry B, Mar.,2006

Properties of Cobalt Oxide Species Dispersed on the Nano Al_2O_3-ZrO_2 Mixed Oxide Supports

Tanuchnun Burakorn, Bunjerd Jongsomjit* and Piyasan Praserthdam

Center of Excellence on Catalysis and Catalytic Reaction Engineering
Department of Chemical Engineering, Faculty of Engineering
Chulalongkorn University, Bangkok 10330, Thailand

* Presenter and corresponding author (Tel: +66-02-2186766, Fax: +6602-2186766)
E-mail: Tanuchnun@hotmail.com

ABSTRACT

In the present study, properties of cobalt (Co) oxide species dispersed on the nano Al_2O_3-ZrO_2 mixed oxide supports were investigated using different characterization techniques. XRD revealed that the Co oxide species were highly dispersed on the supports consisting of various weight ratios of the nano Al_2O_3-ZrO_2. However, there was no significant change in morphologies of samples upon the various support used. It was found that the number of active Co metals determined using the H_2 chemisorption technique on the nano Al_2O_3 support was the highest compared to any other samples.

Keywords: cobalt catalyst, Al_2O_3, ZrO_2, nanoparticle, chemisorption

1. Introduction

The cobalt-based catalysts are known to be commercially attractive for Fischer-Tropsch synthesis (FTS) due to their high activity, selectivity for linear hydrocarbons and lower price compared with noble metals. The active phase is generally deposited in the surface of support. The role of the support is to disperse strength and good thermal stability [1]. The types of support commonly used for this purpose are oxides such as Al_2O_3, SiO_2 and TiO_2.

It is known that Al_2O_3 is usually adopted as the support to prepare cobalt catalysts due to the excellent texture and thermal stability. However, the catalysts exhibited limited reducibility because of the strong interaction between the cobalt and the support. This can be improved to a certain extent by promotion with metal or metal oxide such as Pt, Re, ZrO_2 and etc[2]. and/or using the appropriated supports. Due to the significant development in nanoscience and nanotechnology, the nanoparticles have brought much attention and perhaps can be used as catalyst supports as well.

This research focused on investigation of properties of cobalt (Co) oxide species dispersed on the nano Al_2O_3-ZrO_2 mixed oxide supports. The mixed supports consisting of various ratios of nano Al_2O_3 and ZrO_2 were prepared, then impregnated with the Co precursor. After calcination, all samples were characterized using XRD, SEM/EDX, TPR and H_2 chemisorption. The properties of samples were further discussed.

2. Experimental

2.1 Materials

2.1.1 Raw Materials

1. Nano-γ-Al_2O_3 supports from Aldrich
2. Nano-ZrO_2 supports prepared by flame spray pyrolysis (FSP)
3. Cobalt (II) nitrate hexahydrate from Aldrich
4. Toluene from Fisher Scientific

2.1.2 Preparation of nano Al_2O_3-ZrO_2 mixed oxide support

The nano Al_2O_3-ZrO_2 mixed oxide supports consisting of various weight ratios of Al_2O_3-ZrO_2 were prepared by the solution mixing. The desired amounts containing 1 g of mixture of Al_2O_3-ZrO_2 were mixed and stirred in toluene (20 ml) with a magnetic stirrer for 30 min. The solvent was removed and the mixture was dried at 110 ^{o}C for 12 h and, then calcined in air at 350 ^{o}C for 2 h.

2.1.3 Preparation of catalyst samples

A 20 wt% of Co/nano Al_2O_3-ZrO_2 support was prepared by the incipient wetness impregnation. A designed amount of cobalt nitrate [$Co(NO_3)\bullet 6H_2O$] was dissolved in deionized water and then impregnated onto the mixed oxide supports obtained from 2.1.2. The catalyst precursor was dried at 110°C for 12 h and calcined in air at 500°C for 4 h.

2.2 Catalyst nomenclature

The nomenclature used for the catalyst samples in this study is following:

- **Co/Al-a-Zr-b** refers to the cobalt catalyst on the nano Al_2O_3-ZrO_2 mixed oxide support, where **a** = the weight ratio of nano-γ-Al_2O_3 and **b** = the weight ratio of nano-ZrO_2

2.3 Catalyst characterization

2.3.1 X-ray diffraction

XRD was performed to determine the bulk crystalline phases of catalyst. It was conducted using a SIEMENS D-5000 X-ray diffractometer with CuK_α (λ = 1.54439 Å). The spectra were scanned at a rate of 2.4 degree/min in the range 2θ = 20-80 degrees.

2.3.2 Scanning electron microscopy and energy dispersive X-ray spectroscopy

SEM and EDX were used to determine the catalyst morphologies and elemental distribution throughout the catalyst granules, respectively. The SEM of JEOL mode JSM-5800LV was applied. EDX was performed using Link Isis series 300 program.

2.3.3 Hydrogen chemisorption

Static H_2 chemisorption at 100°C on the reduced sample was used to determine the number of reduced surface cobalt metal atoms. This is related to the overall activity of the catalysts during CO hydrogenation. Gas volumetric chemisorption at 100°C was performed using the method described by Reuel and Bartholomew [3]. The experiment was performed in a Micromeritics ASAP 2010 using ASAP 2010C V3.00 software.

2.3.4 Temperature-programmed reduction

TPR was used to determine the reduction behaviors of the samples. It was carried out using 50 mg of a sample and a temperature ramp from 35 to 800°C at 5°C/min. The carrier gas was 5% H_2 in Ar. A cold trap was placed before the detector to remove water produced during the reaction.

3 Results and discussion

XRD patterns of the nano Al_2O_3-ZrO_2 mixed oxide supports consisting of various weight ratios of Al_2O_3-ZrO_2 prior to impregnation are shown in **Figure 1**. Apparently, the pure Al_2O_3 support exhibited the XRD

peaks at 32.5°, 37°, 46° and 67.5° indicating the gamma alumina [4]. It was observed that the pure ZrO_2 exhibited XRD peaks at 29.8°, 34.2°, 49.6°, and 59.5° assigning to the ZrO_2 in tetragonal phase. Besides, the XRD peaks at 24°, 28.2°, 31.5°, 41°, 45° and 55.8° were also detected indicating the ZrO_2 in monoclinic phase [5]. XRD patterns of the nano Al_2O_3-ZrO_2 mixed oxide supports consisting of various weight ratios of Al_2O_3-ZrO_2 revealed the combination of Al_2O_3-ZrO_2 supports based on their contents. After impregnation with the cobalt precursor, the catalyst samples were dried and calcined. The XRD patterns for the Co catalysts on various supports are shown in **Figure 2**. Besides the observation of the characteristic peaks of the supports as shown in **Figure 1**, all calcined samples exhibited XRD peaks at 31° (weak), 36° (strong), and 65° (weak) [6], which were assigned to the presence of Co_3O_4. This indicated that the Co_3O_4 formed was highly dispersed.

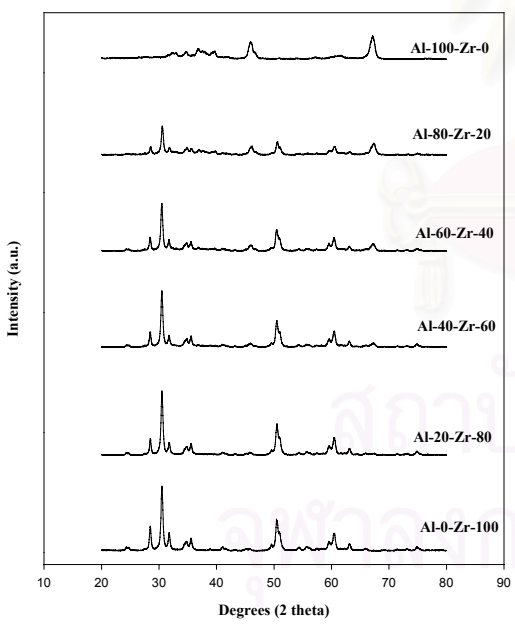

Fig. 1. The XRD patterns of various weight ratios of nano Al_2O_3-ZrO_2 mixed oxide support

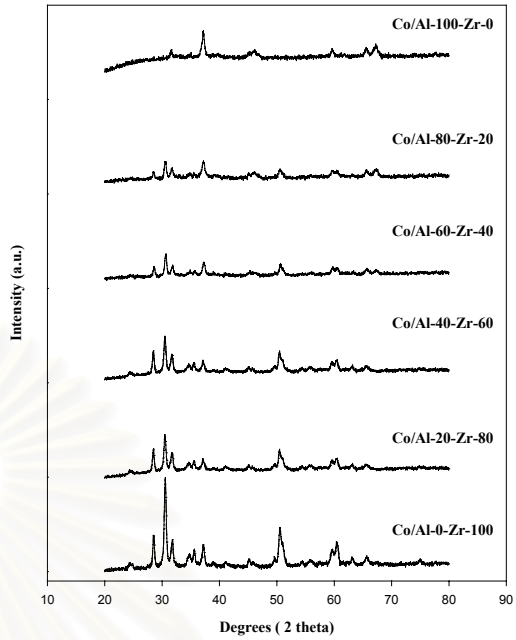

Fig. 2. The XRD patterns of various Co/nano Al_2O_3-ZrO_2 catalysts

SEM and EDX were also conducted in order to study the morphologies and elemental distribution of the samples, respectively. In general, there was no significant change in morphologies and elemental distribution of all catalyst samples after calcination. A typical SEM micrograph and EDX mapping for Co/Al-60-Zr-40 sample are illustrated in **Figure 3**. It can be seen that ZrO_2 was located on the outer surface of Al_2O_3. It appeared that the distribution of Co was well on the surface of the support.

TPR was performed in order to determine the reduction behaviors of samples. The TPR profiles for all samples are shown in **Figure 4**. It was found that there was only one reduction peak, however, at different reduction temperatures for all calcined samples. The one reduction peak can be assigned to the overlap of two-step reduction of Co_3O_4 to CoO and then to Co metal. Upon the TPR conditions, the two-step reduction may or may not be observed.

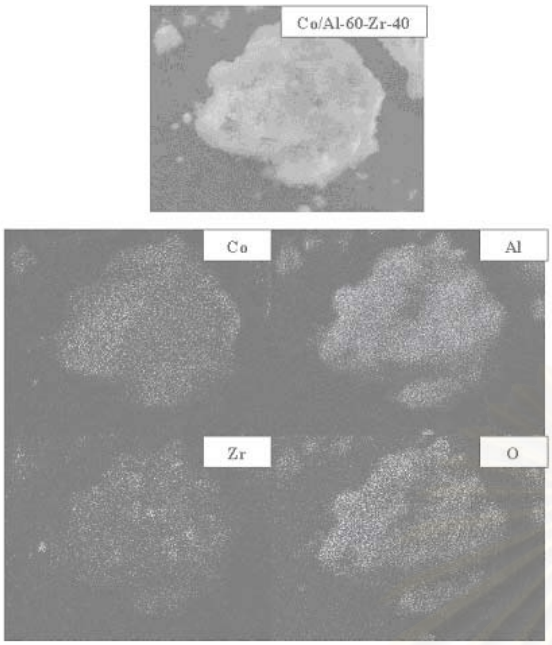

Fig. 3. SEM micrograph and EDX mapping for Co/Al-60-Zr-40 catalyst

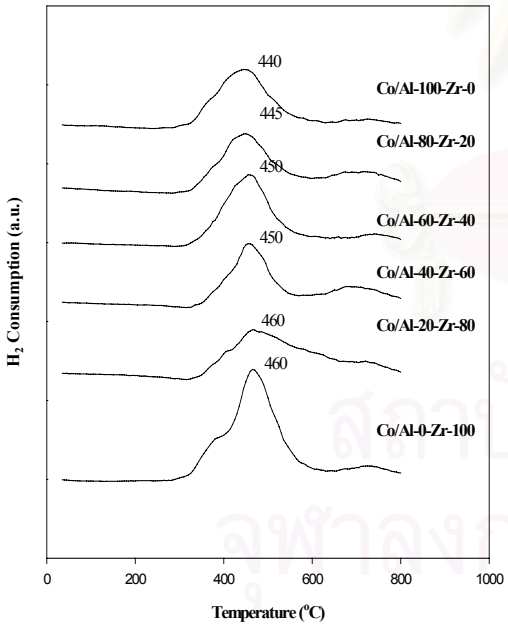

Fig. 4. TPR profiles of various Co/nano Al_2O_3-ZrO_2 catalysts

Based on the TPR profiles, it indicated that Co oxides dispersed on the pure Al_2O_3 exhibited the lowest maximum reduction temperature than those on the mixed Al_2O_3-ZrO_2 supports. It was suggested that using the mixed Al_2O_3-ZrO_2 supports could result in increasing the reduction temperature of Co oxides due to the stronger metal-support interaction. The resulted H_2 chemisorption is illustrated in **Table 1**. It was found that the number of the reduced cobalt metal surface atoms was the largest for Co supported on the pure Al_2O_3. It seemed that the presence of ZrO_2 in the mixed supports could result in less number of active Co metal atoms. However, the reaction study needs to be further investigated in the near future.

Table 1 Results of H_2 chemisorption for various samples

Sample	**Total H_2 Chemisorption (μmole/g. cat.)**
Co/Al-100-Zr-0	6.59
Co/Al-80-Zr-20	2.94
Co/Al-60-Zr-40	3.48
Co/Al-40-Zr-60	1.75
Co/Al-20-Zr-80	1.25
Co/Al-0-Zr-100	2.01

4 Conclusions

The present study revealed properties of Co oxides on various nano Al_2O_3-ZrO_2 mixed oxide supports. It indicated that Co oxide species were in the highly dispersed form on the various supports. There was no significant change in morphologies and elemental distributions of samples as seen from SEM/EDX. The presence of ZrO_2 in the mixed supports could result in the low number of active Co metal atoms as detected using H_2 chemisorption technique. However, in order to determine the activity and selectivity, reaction study needs to be further investigated in more details.

Acknowledgements

We gratefully acknowledge the financial support by the National Research Council of Thailand (NRCT), the Thailand Research Fund (TRF) and Thailand-Japan Technology Transfer Project (TJTTP-JBIC). We would like to thank Prof. James G. Goodwin, Jr. at Clemson University for initiating this kind of project.

References

1. Ducreux O., Ecole Nationale Supérieure du Pétrole et des Moteurs, (1999).
2. Haifeng, Yuhua, Kongyong, Liew, J. Mol. Catal. A: Chemical. 231, 145-151 (2005).
3. Reuel, R. C.; and Bartholomew, C. H. J. Catal. 85, 63-77 (1984).
4. Mekasuwandumorong, O. Department of Chemical Engineering Chulalongkorn University. 46-48 (2003).
5. Mueller R., Joseen R., Soyiris E. Pratsinis. J.Am. Ceram. Soc. 87 [2] 197-202 (2004).
6. Jongsomjit, B.;Panpranot, J.;Goodwin, J.G. J. of Catal. 215, 66-77 (2003).

VITA

Mr. Tanuchnun Burakorn was born in June 4th, 1981 in Ubonratchatani, Thailand. He finished high school from Benjamamaharat School, Ubonratchatani in 1999, and received bachelor's degree in Chemical Engineering from the department of Chemical Engineering, Faculty of Engineering, King Mongkut's Institute of Technology Ladkrabang, Bangkok, Thailand in 2003.